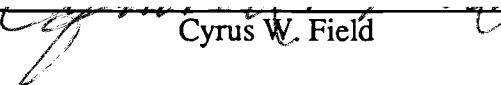


AN ABSTRACT OF THE THESIS OF

John M. Curless for the degree of Master of Science
in Geology presented on May 30, 1991

Title: Geology and Hydrothermal Mineralization in the Vicinity of Rocky Top, Marion
County, Oregon

Redacted for Privacy

Abstract approved:  Cyrus W. Field

The Rocky Top area is located within the Western Cascades subprovince of Oregon, approximately 65 km east-southeast of Salem. Late Oligocene to late Miocene age volcanic rocks exposed within the area form an impressive 3000 meter thick stack of calc-alkaline volcanic rocks which locally records subsequent events of tectonic deformation, magmatic intrusion, and hydrothermal mineralization. Pliocene to Pleistocene volcanic rocks in the Rocky Top area are unaltered, chemically distinct, and found as intracanyon flows into the older rocks.

Plutonic rocks of late Miocene age have been hydrothermally mineralized and are exposed as northwest-trending dikes and small stocks. Their spatial distribution as well as mineralogical, textural, and chemical features indicate that they are related to the nearby Detroit Stock. Early formed quartz diorites at Sardine Creek and Rocky Top are exposed as dikes with sharp to slightly brecciated contacts, and were emplaced along pre-existing northwest-trending structures. Later hornblende granodiorites, with contacts defined by well-developed intrusive breccias, are exposed as irregularly-shaped

northwest-elongate dikes and small stocks. Stratigraphic reconstruction from Sardine Creek to Rocky Top suggests that the later hornblende granodiorites were emplaced at a minimum depth of roughly 1 km, with the earlier quartz diorites intruding to shallower levels.

Propylitic alteration is widespread throughout the Rocky Top area and intensifies with proximity to northwest-trending structures. Potassic alteration is limited to within the Detroit Stock, where several samples contain incipient veinlets and diffuse replacement zones of hydrothermal biotite. Late-stage sericitic (sericite-quartz) and argillic (clay-quartz±barite) alteration is characterized by the replacement of groundmass and phenocrysts by sericite or clay minerals, quartz, and pyrite, along with a loss of primary textures, which accompanies mild to strong bleaching of the wall rocks. Late-stage alteration is structurally controlled, and overprints earlier propylitic and potassic alteration.

Zones of hydrothermal metallization are narrow, weakly developed, and lack evidence of past exploration activity. Sulfide minerals occur as open-space fillings and as disseminations in the volcanic and plutonic rocks. The principal sulfide is pyrite, although sphalerite, chalcopyrite, and galena are locally abundant in small veins and disseminations associated with sericitic alteration. Sulfur isotopic compositions of these minerals range from +2.8 permil to -3.3 permil and average about -0.5 permil. This relatively narrow range of $\delta^{34}\text{S}$ values, near 0 permil, is suggestive of a magmatic origin of sulfur and is consistent with data obtained elsewhere from the Western Cascades. Isotopic temperature estimates from coexisting sphalerite and galena indicate sulfide deposition occurred at 200-220°C.

More than 80 rock-chip samples from the Rocky Top, Sardine Creek, and Detroit Stock areas have been analyzed for Cu, Pb, Zn, and other trace metals. Concentrations of these metals in samples from the Rocky Top area range up to 16 ppm Ag, 16 ppb Au,

830 ppm Cu, 75 ppm Mo, 1330 ppm Pb, and 3570 ppm Zn. Threshold values dividing background and mineralized samples were determined to be 60 ppm Cu, 30 ppm Pb, and 100 ppm Zn. The relative proportions of these metals in mineralized samples depict a progressive change with increasing horizontal and vertical distance from more Cu (Zn) rich at the Detroit Stock, through Zn (Cu) at Sardine Creek, to Pb (Zn) at Rocky Top.

Investigation of the interrelationships between mineralization and associated plutonic rocks combined with volcanic stratigraphy, structure, and topography suggest that Rocky Top may be one of the youngest and highest level hydrothermal systems recognized in the Western Cascades. Although plutonism and hydrothermal mineralization in this area has many features in common with nearby mining districts of the Western Cascades, the absence of well-developed breccia pipes, through-going veins, and zones of intense pervasive alteration are consistent with the lack of previous mining activity or extensive exploration.

© Copyright by John M. Curless

May 30, 1991

All Rights Reserved

**Geology and Hydrothermal Mineralization in the Vicinity
of Rocky Top, Marion County, Oregon**

by

John M. Curless

A THESIS

submitted to

Oregon State University

in partial fulfillment of
the requirements for the
degree of

Master of Science

Completed May 30, 1991

Commencement June 1992

APPROVED:

Redacted for Privacy

Professor of Geology in charge of major

Redacted for Privacy

Chair of Department of Geosciences

Redacted for Privacy

Dean of Graduate School

Date thesis is presented _____ May 30, 1991

Typed by _____ John M. Curless

ACKNOWLEDGEMENTS

Special thanks goes to Dr. Cyrus Field for his support, and advice which ranged far beyond matters related to geology. Thanks also to committee members Dr. Edward Taylor, Dr. John Dilles, and Dr. Martin Fisk for their help and encouragement.

Partial financial support for this project was provided by the Geology Mineral Research Group, and the Geological Society of America. Reactor time and facilities for INAA were provided thanks to the OSU Radiation Center staff, especially Dr. Bob Walker. Microprobe analyses were provided by the Department of Geoscience thanks to Dr. Roger Nielsen.

Critical reviews and helpful suggestions by Dr. Reed Lewis, Britt Hill, and Dave Nicholson are gratefully acknowledged. In addition, I appreciate the advice of former office-mates Dana Willis, and Allyson Mathis.

In closing, I would like to thank the members of my family for their support and understanding over the years. Sincere thanks (and the coveted geo-spouse award) goes to my wife, Valerie Hipkins, for her patience, love, and motivation. When the going got long, she got me going.

TABLE OF CONTENTS

	<u>Page</u>
INTRODUCTION.....	1
GEOLOGIC SETTING	5
VOLCANIC ROCKS.....	13
DESCRIPTION OF VOLCANIC UNITS	18
Sardine sequence.....	18
Pyroclastic sequence of Elkhorn Creek	23
Elk Lake sequence	25
Andesite sequence of Rocky Top	27
Northern basalts	28
Southern basalts	29
CHEMICAL CHARACTERISTICS	29
DISCUSSION	33
PLUTONIC ROCKS	37
DESCRIPTION OF PLUTONIC UNITS	39
Quartz diorite	39
Granodiorite	42
CHEMICAL CHARACTERISTICS	44
DISCUSSION	49
SURFICIAL DEPOSITS.....	51
DESCRIPTION OF SURFICIAL DEPOSITS	51
Terrace deposits	51
Glacial drift	51
Colluvium	52
Alluvium	52
DISCUSSION	52
STRUCTURAL GEOLOGY	54
BEDDING ATTITUDES AND UNCONFORMITIES.....	54
FAULTS AND DIKE ORIENTATIONS	57
UPLIFT	60
DISCUSSION	62
HYDROTHERMAL MINERALIZATION	65
HYDROTHERMAL ALTERATION.....	65
VEIN MINERALOGY AND TEXTURES	69
SULFUR ISOTOPES.....	73
FLUID INCLUSIONS	74
TRACE METALS	77
DISCUSSION	82
SUMMARY AND CONCLUSIONS	88
BIBLIOGRAPHY	93

APPENDICES

APPENDIX 1: Locations of samples from Rocky Top	99
APPENDIX 2: Chemical analyses of volcanic rocks from Rocky Top.....	100
APPENDIX 3: Chemical analyses of plutonic rocks from Rocky Top	102
APPENDIX 4: Chemical analyses of plutonic rocks from Detroit Dam.....	103
APPENDIX 5: Chemical analyses of altered rocks from Rocky Top	104
APPENDIX 6: Sulfide mineral analyses	105
APPENDIX 7: Fluid inclusion data.....	107
APPENDIX 8: Trace metal concentrations for samples from Rocky Top	108
APPENDIX 9: Trace metal concentrations for samples from Sardine Creek	109
APPENDIX 10: Trace metal concentrations for samples from Detroit Dam.	110
APPENDIX 11: List of abbreviations.....	111

LIST OF FIGURES

<u>Figure</u>	<u>Page</u>
1. Location map of Rocky Top and surrounding areas.....	2
2. Current land status and road network.....	3
3. Western and High Cascades Boundaries	6
4. Location of Rocky Top with respect to the folds of Thayer.....	9
5. Summary of regional fault trends.....	10
6. Composite stratigraphic column.	15
7. Classification of volcanic rocks using the TAS (total alkalis vs. silica) diagram.	16
8. Silica variation diagrams of major oxide components.....	30
9. Ternary AFM diagram.	32
10. Chondrite-normalized trace element plots for volcanic rocks.....	34
11. Th-Hf-Ta discrimination diagram for volcanic rocks.....	35
12. Distribution of Plutonic rocks.....	38
13. IUGS classification of intrusive rocks based on modal mineralogy.....	40
14. Silica variation diagrams of major oxide components for plutonic rocks.	45
15. Chondrite-normalized trace element plots for plutonic rocks.....	47
16. Bedding attitudes for volcanic rocks of three age groups from Rocky Top. ...	55
17. Contoured poles to planes for faults and dikes at Rocky Top.....	56
18. Northwest trend of depleted $\delta^{18}\text{O}$ values.	59
19. Chemical changes with respect to alteration assemblage.....	70
20. Paragenetic sequence of hydrothermal mineralization at Rocky Top.	72
21. Homogenization temperatures and salinities of fluid inclusions.	76
22. Log-probability plots for Cu, Pb, and Zn.	78
23. Ternary Cu-Pb-Zn diagrams.	80
24. Log $f\text{O}_2$ -pH diagram at 250°C for the system Fe-S-O-Cu-Ba-K-Al-HCl-KCl. 84	84
25. Isotopic relationship between coexisting sulfide and sulfate species.	86
26. Summary of pre- to post-mineralization events.....	89

LIST OF TABLES

<u>Table</u>	<u>Page</u>
1. General character of the volcanic rock units exposed at Rocky Top.....	14
2. General character and modal mineralogy of plutonic rock units exposed at Rocky Top.....	41
3. Mineralogy of pervasive hydrothermal alteration assemblages.....	66

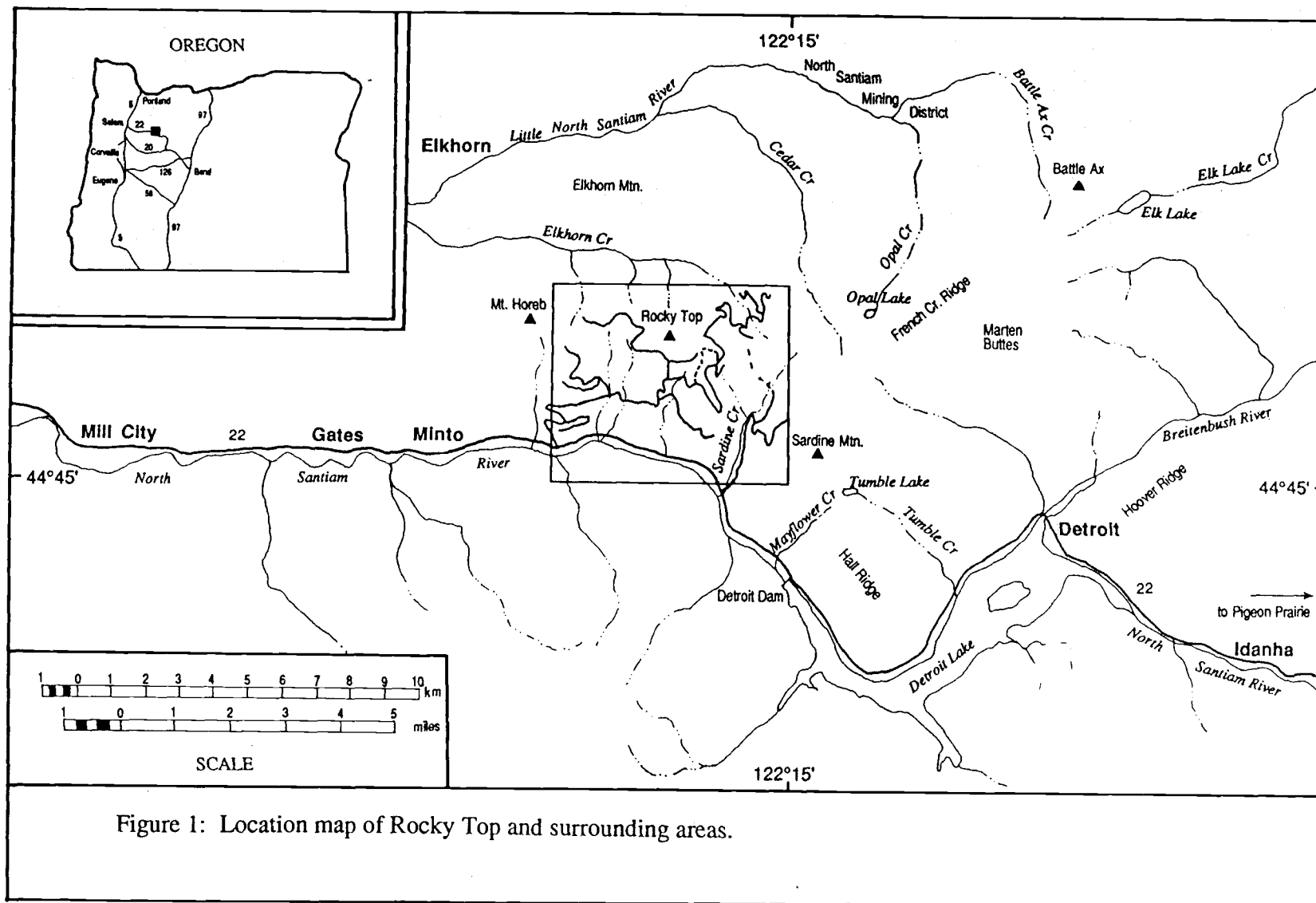
Geology and Hydrothermal Mineralization in the Vicinity of Rocky Top,
Marion County, Oregon

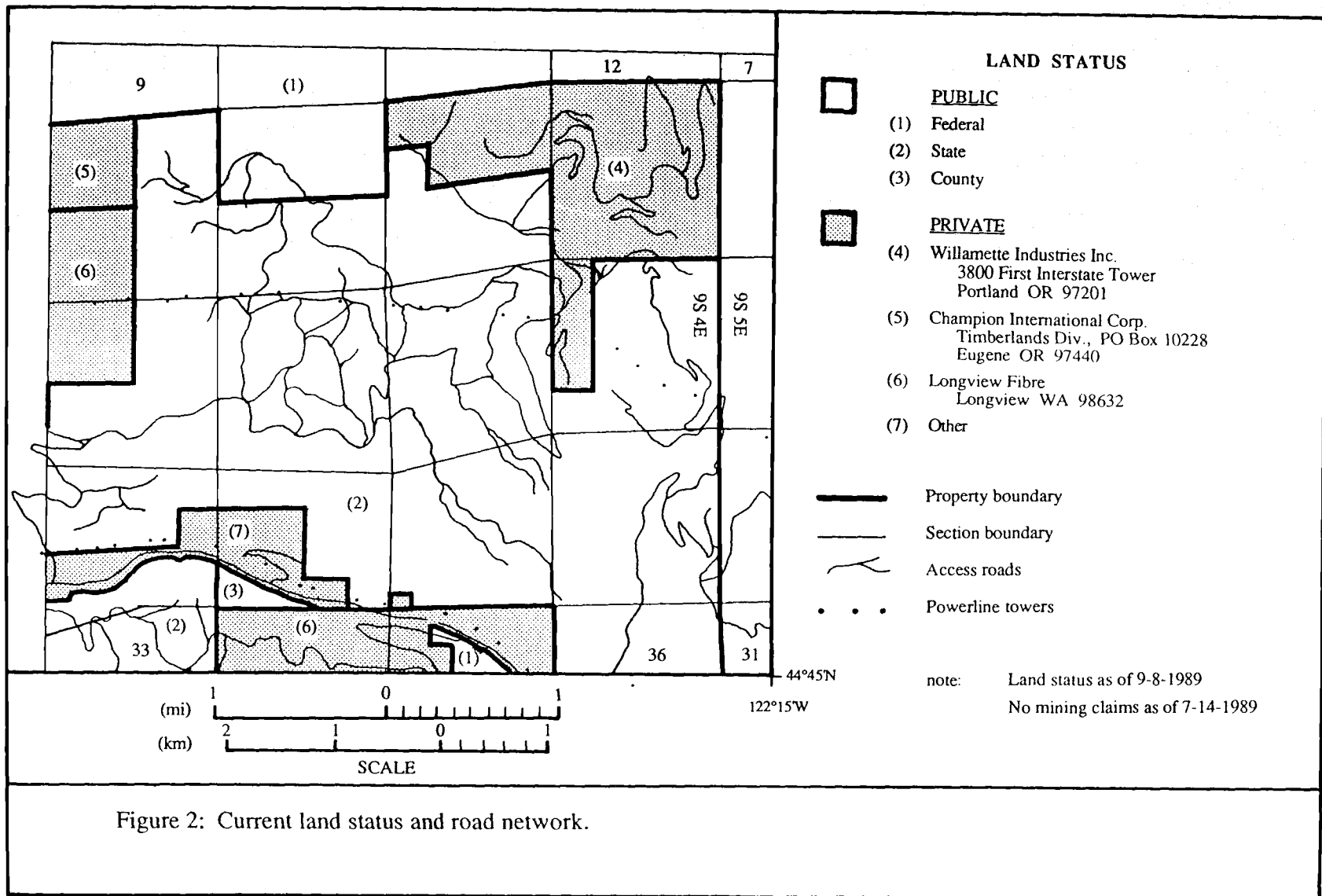
INTRODUCTION

The Rocky Top area, as illustrated in Figure 1, is located within the Western Cascades subprovince of Oregon, approximately 65 km east-southeast of Salem. The area consists of a thick, well-exposed sequence of mid-Tertiary calc-alkaline volcanic rocks which record subsequent events of tectonic deformation, magmatic intrusion, and hydrothermal mineralization. The Rocky Top area was chosen for study because of its complex structural and intrusive history, as well as the presence of extensive and previously undocumented zones of hydrothermal alteration. Mineralized zones at Rocky Top that contain anomalous concentrations of trace metals are in general structurally controlled, narrow, weakly developed, and lack evidence of past exploration activity. Nevertheless, chemical and spatial relationships of intrusive magmatism and hydrothermal mineralization resemble those of historically productive districts elsewhere in the Western Cascades.

Recent logging of Rocky Top and adjacent areas has provided good access to the study area. The current land status and road network is detailed in Figure 2. Slope gradients range from moderately steep with occasional cliffs to nearly flat, and total relief exceeds 1200 meters (4000 ft). Soils are generally thin, well drained, and locally derived. Bedrock outcrops amount to roughly 10 percent of the landscape, which is relatively high compared to other areas of the Western Cascades.

Field work included mapping within the southeast quarter of the 7.5 minute Elkhorn quadrangle where the relationships between structure, emplacement of plutonic rocks, and development of hydrothermal mineralization were established.





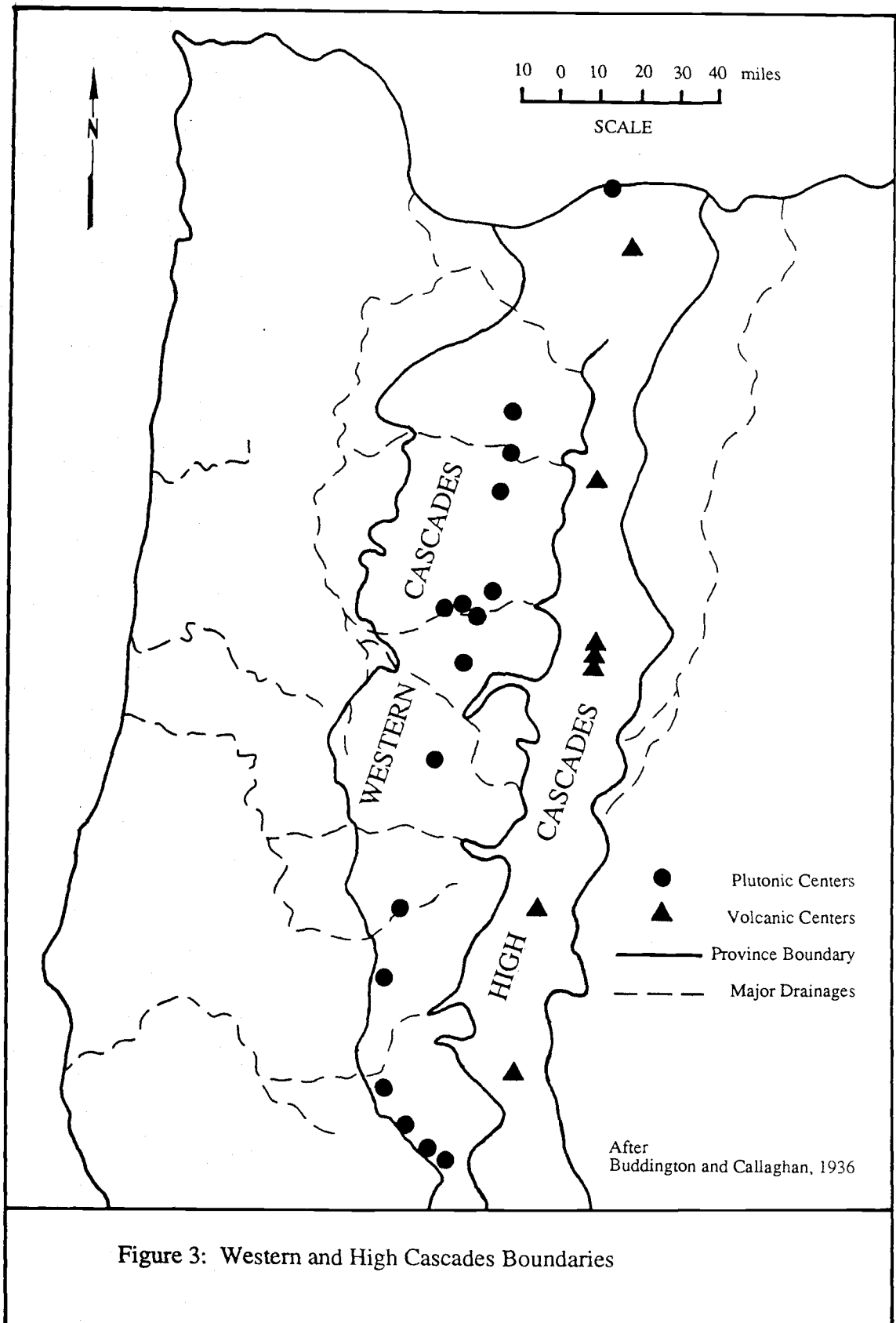
Approximately 150 rock-chip samples were collected from road cuts and natural exposures. A representative group of 35 samples was selected for petrographic study and chemical analysis of the trace metals Cu, Mo, Pb, Zn, and Ag. A subset of 21 samples was analyzed for major oxide concentrations by using inductively coupled plasma spectrometry. Minor and trace element concentrations were obtained on 22 samples by instrumental neutron activation analysis. Isotopic compositions of sulfur in pyrite, chalcopyrite, sphalerite, galena and barite were determined to better constrain possible sources of sulfur and to establish temperatures of hydrothermal mineralization.

GEOLOGIC SETTING

The Cascade Range consists of a north-trending magmatic arc which began to develop about 40 million years ago in response to subduction of the Juan de Fuca Plate beneath the Pacific Northwest margin of North America (McBirney and others, 1974; Lux, 1981; Verplanck and Duncan, 1987). This arc extends approximately 1100 km from Northern California to Southern British Columbia, and is underlain by crust which varies widely in age, composition, and thickness. Although this margin lacks an active Benioff zone and a well defined trench, the Cascade Range has most of the features of continental arcs associated with convergent plate boundaries (McBirney and White, 1982).

Paleomagnetic studies by Simpson and Cox (1977), Magill and Cox (1981), and Bates and others (1981) indicate that sections of the Western Cascades may have rotated clockwise 30° since Oligocene time and possibly as much as 75° since Eocene time. The paleomagnetic evidence is supported by the apparent convergent linear trends defined by Tertiary plutons of the Western Cascades with Quaternary stratovolcanoes of the High Cascades, which implies a clockwise rotation of roughly 15° over the past 20 million years (Power, 1984).

The central Cascade Range of Oregon has been subdivided into two, roughly parallel north-south trending subprovinces on the basis of age, lithology, degree of deformation, and topographic expression (Callaghan, 1933; Thayer, 1934; Buddington and Callaghan, 1936; Peck and others, 1964; Priest and Vogt, 1983). These subprovinces, as illustrated in Figure 3, are designated the Western Cascades and High Cascades (Callaghan, 1933). The majority of the Western Cascades subprovince is composed of late Eocene to late Miocene lava and pyroclastic flows, and epiclastic rocks which range in composition from basalt to rhyolite. Peck and others (1964) contend



that these rocks were produced from numerous eruptive centers within the subprovince and have an estimated volume of roughly 100,000 km³. These volcanic rocks have been structurally deformed, locally intruded by Tertiary plutons, and hydrothermally altered in discontinuous areas associated with intrusions.

In contrast, the High Cascades subprovince consists of relatively undeformed late Miocene to Holocene volcanic rocks which occupy a discontinuous fault-bounded graben and partially cover the older rocks of the Western Cascades (Allen, 1966; Taylor, 1968, 1980). The High Cascades are composed of a broad platform of mafic rocks which are occasionally capped by intermediate to silicic stratovolcanoes (McBirney and others, 1974; Hughes and Taylor, 1986).

A small number of formational names have been assigned to a wide range of complexly associated volcanic rocks in the Western Cascades. However, rather than using the rock-stratigraphic units of previous workers, Priest and others (1983) divided the volcanic rocks of the Western Cascades into time-stratigraphic groups which have been termed the early and late Western Cascade episodes. Based on a regional unconformity, Priest and others (1983) placed the time boundary separating these episodes at 18 million years ago.

The late Eocene to early Miocene rocks of the early Western Cascade episode are chiefly dacitic to rhyodacitic lavas and tuffs, with lesser amounts of basalt and basaltic andesite flows and minor volcanoclastic interbeds. Priest and others (1983) correlated these rocks with the Breitenbush Series and much of the Sardine Series of Thayer (1936, 1939), and the Breitenbush Formation and Scorpion Mountain lavas as described by White (1980a, 1980b).

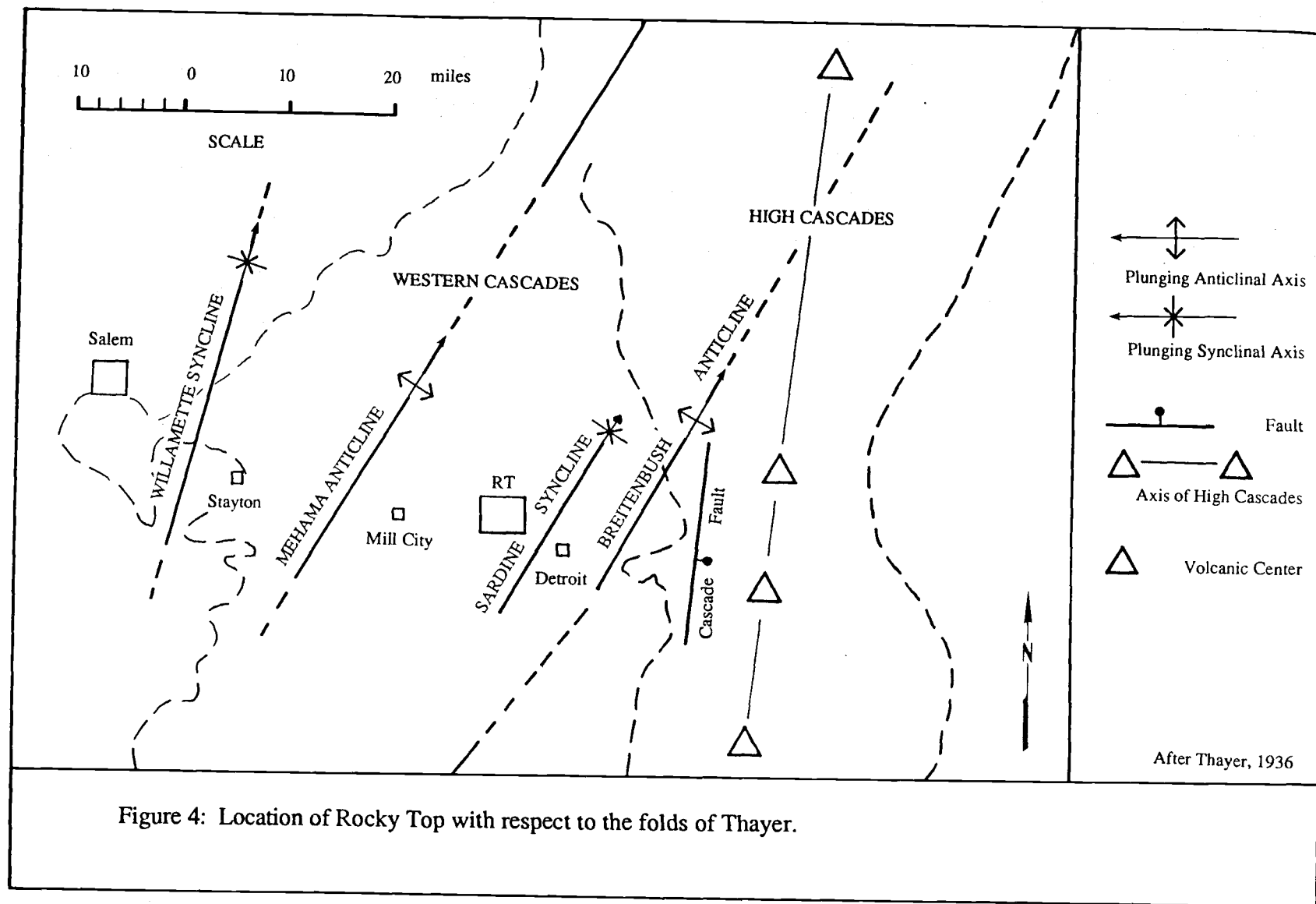
The older units are overlain by the predominantly middle Miocene volcanic rocks of the late Western Cascade episode, which are chiefly lava flows of pyroxene andesite and aphyric basalt and basaltic andesite. Priest and others (1983) correlated these rocks

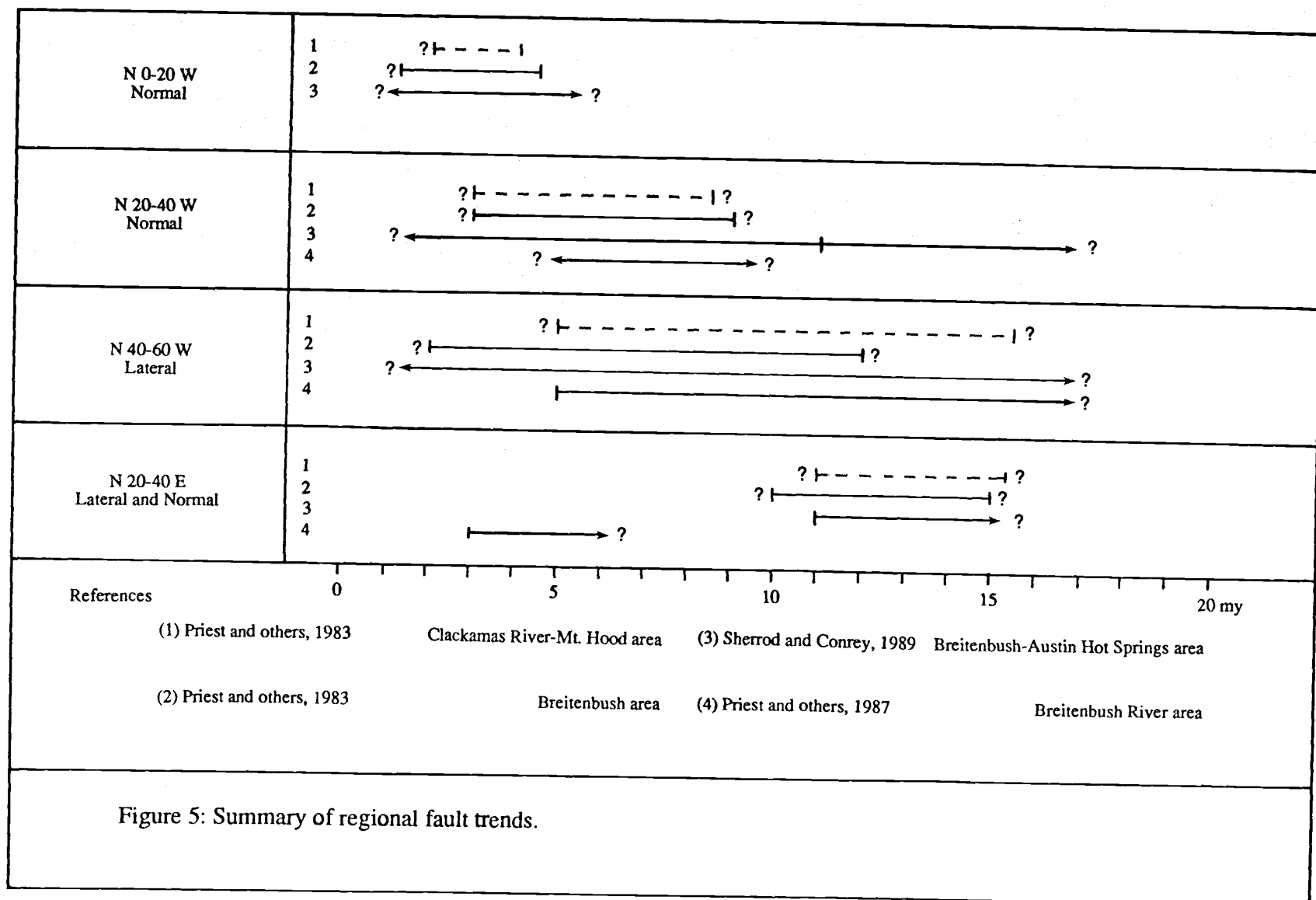
with the uppermost Sardine Series of Thayer (1936, 1939), the Sardine Formation of Peck and others (1964), and the Sardine and Elk Lake Formations of White (1980a, 1980b).

The rocks of the Western Cascades have been interpreted to be gently folded into a series of northeast-trending anticlines and synclines (Thayer, 1934, 1936; Peck and others, 1964). The Rocky Top area, as illustrated in Figure 4, is located between extensions of the Mehama Anticline and Sardine Syncline as defined by Thayer (1936). White (1980a, 1980b) has estimated the time of deformation to have occurred between 15 to 11 million years ago on the basis of K-Ar dates of samples collected from the Sardine and Elk Lake Formations. Although folding in the North Santiam drainage near Detroit is well-documented, the gentle dips that Peck and others (1964) interpreted as folds in areas as far south as the town of Oakridge could be explained by local deformation associated with faulting. In some cases, these dips may represent primary depositional attitudes (Priest and others, 1983).

The regional study of the central Cascade Range of Oregon by Priest and others (1983) detailed four fault orientations, which are summarized in Figure 5. The most notable are northwest-trending faults and fractures which are present throughout mineralized areas of the Western Cascades and served as channels for hydrothermal fluids (Callaghan and Buddington, 1938). Where exposed, most of the northwest-trending faults dip steeply and displacement rarely exceeds 20 meters. Lack of recognizable marker units and large amounts of cover make delineation of these small-scale structures difficult. Callaghan and Buddington (1938) noted that intrusive rocks and mineralized veins in the Western Cascades tend to preferentially follow these northwest-trending structures.

Buddington and Callaghan (1936) were the first to describe in detail the dioritic plutonic bodies that intrude Tertiary volcanic rocks of the Western Cascades. These





intrusive rocks have a north-south distribution and were emplaced as small monolithologic dikes, plugs, and sills, and as larger composite stocks, which broadly exhibit a south to north increase in size and number of intrusive events. They commonly have steep contacts that are sharply defined by chill zones, or intrusive breccias. The intrusions range in size from isolated dikes a few meters wide to the Nimrod Stock which is roughly 4 km by 2.5 km in surface dimension. Most of the intrusions are porphyritic and contain fine- to medium-sized phenocrysts, but equigranular textures are also common (Callaghan and Buddington, 1938; Power, 1984; and references cited therein). Modal mineralogy indicates that quartz diorite and granodiorite are the most common rock types, but diorite, quartz monzodiorite, tonalite, and granite are also present. The K-Ar age determinations of intrusions in the Western Cascades of Oregon range from 7 to 22 million years, and do not display any apparent correlations between age and location, size, or composition (Power, 1984).

Hydrothermal mineralization in the Western Cascades is temporally and spatially related to the dioritic intrusions (Callaghan and Buddington, 1938). Intrusive rocks are abundant within all of the larger mineralized areas in this subprovince, and may represent sub-volcanic stocks. Regional crosscutting fault and fracture systems may have provided a favorable environment for hydrothermal mineralization. Field and others (1987) have noted that emplacement of breccia pipes into plutons and volcanic country rocks of the Western Cascades marked the waning stages of intrusive magmatism and the onset of hydrothermal activity. Standard method K-Ar age determinations from the North Santiam and Washougal districts of the Western Cascades suggest, as in other mining districts, that hydrothermal mineralization dates are consistently 1-2 million years younger than the crystallization ages of the plutons (Power, 1984).

Large areas of propylitic alteration surround the exposed intrusions of the Western Cascades and have been documented on a district scale by Callaghan and Buddington (1938), and a regional scale by Peck and others (1964). Oxygen isotope studies by Taylor (1971) indicate that large convective systems of meteoric-hydrothermal origin produced the broad zones of propylitic alteration. Potassic alteration is well documented in the hydrothermal deposits of Northern Washington, but is only locally and weakly developed in parts of the Bohemia, North Santiam, and Washougal districts (Field and others, 1987). In addition, several samples from the Detroit Stock contain incipient veinlets and diffuse replacement zones of hydrothermal biotite (Curless and others, 1990). Late-stage phyllic and argillic alteration are localized along structural zones and overprint earlier hydrothermal alteration assemblages.

Mineral deposits within the Western Cascades consist primarily of fault- and fracture-controlled epithermal to mesothermal polymetallic (Cu-Pb-Zn) veins, and to a lesser extent include breccia pipe (Cu-Zn-Mo) and disseminated porphyry (Cu-Mo) types. Anomalously high concentrations of precious metals are present in all types of deposits, and are usually associated with high contents of Cu and total metals. Field and Power (1985) documented systematic latitudinal changes in the hydrothermal deposits within the Western Cascades. The interpretation of progressively deeper levels of exposure from south to north within these mineral deposits is supported by an increase in size and complexity of intrusions; a northward increase in the number of breccia pipes; larger concentrations of disseminated Cu and Mo relative to Pb and Zn in the volcanic and plutonic country rocks; an increase in widespread and pervasive phyllic, argillic, and local potassic alteration; a northward change from through-going veins to veinlets, disseminations, and breccia hosted mineralization; and an increase in salinities, homogenization temperatures, and amounts of daughter minerals of fluid inclusions.

VOLCANIC ROCKS

The volcanic stratigraphy of the Western Cascades is characterized by a complex assemblage of extrusive rocks which records episodes of tectonic deformation, magmatic intrusion, and hydrothermal mineralization. The complexity results from magmatic and tectonic features commonly associated with continental arc volcanism, and is further complicated by the poor quality of exposure which obscures lateral changes and structural relationships between rock units. In addition, destruction of primary rock textures and mineralogy has occurred in areas of moderate to intense hydrothermal alteration. Further complications have arisen in the Detroit region because previous workers have given the same rock units different names and have assigned them to a variety of stratigraphic and chronologic positions.

Previous workers conducting regional studies in the Western Cascades have mapped the Rocky Top area as an undifferentiated andesite sequence of Miocene age (Thayer, 1934; Peck and others, 1964; Walker and Duncan, 1989; Sherrod and Smith, 1989). The detailed mapping of this study in the vicinity of Rocky Top has revealed the presence of other types of volcanic units. The assemblage of volcanic rocks exposed in the Rocky Top area is inferred to range in age from late Oligocene to Pleistocene and has been divided into eight map units as indicated on Plate 1. The general character of each volcanic map unit is detailed in Table 1, and a composite stratigraphic column is presented in Figure 6. Volcanic rock names of fresh samples have been assigned, as illustrated in Figure 7, using the total alkalis versus silica subdivisions proposed by LeMaitre (1984). Pyroclastic rocks have been named following the recommendations of Schmid (1981). Chemical analyses of major and trace elements, specific gravities, and analytical techniques are presented in Appendix 2. Details of the chemical compositions of the units will be discussed at the end of this chapter.

TABLE 1: General character of the volcanic rock units exposed at Rocky Top.

VOLCANIC UNITS	LOWER SARDINE SEQUENCE	UPPER SARDINE SEQUENCE	PYROCLASTIC SEQUENCE OF ELKHORN CREEK	LOWER ELK LAKE SEQUENCE	UPPER ELK LAKE SEQUENCE	ANDESITE SEQUENCE OF ROCKY TOP	NORTHERN BASALTS	SOUTHERN BASALTS
AGE	late Oligocene early Miocene	late Oligocene early Miocene	early-middle Miocene	middle Miocene	middle Miocene	late Miocene	Pliocene Pleistocene	Pleistocene
DEGREE OF ALTERATION	weak-intense propylitic quartz-sericite argillic	weak-intense propylitic quartz-sericite argillic	weak-intense propylitic quartz-sericite argillic	weak-intense propylitic quartz-sericite argillic	weak-intense propylitic quartz-sericite argillic	weak-moderate propylitic	none	none
PLUTONIC ROCKS	yes Tid-Tig	yes Tid-Tig	yes Tid	yes Tid	yes Tid	none observed	no	no
STRIKE AND DIPS	variable with dips to 45°	variable with dips to 45°	variable with dips to 25°	variable with shallow dips	variable with shallow dips	horizontal	horizontal	horizontal
COMPOSITION	intermediate	intermediate	silicic	silicic	intermediate	intermediate	mafic	mafic
PRINCIPAL ROCK TYPE	fragmental minor flow	flow	fragmental	flow minor fragmental	flow	flow	flow	flow
DISTRIBUTION	lower Sardine Creek North Santiam River	upper Sardine Creek lower Rocky Top	Elkhorn Creek Rocky Top	head of Elkhorn Creek	head of Elkhorn Creek	capping Rocky Top	perched north of Rocky Top	high terrace south of Rocky Top
THICKNESS (m)	>600	>1500	≈300	≈150	>200	>200	>30	5-10
EXPOSURE	extensive poor	extensive good	limited poor-fair	limited good	limited good	very limited good	very limited fair-good	very limited good
CORRELATIVE UNITS	Sardine Series Sardine Formation	Sardine Series Sardine Formation	Breitenbush Formation	Elk Lake Formation	Elk Lake Formation	?	Battle Ax lavas	Pigeon Prairie lavas Santiam basalts

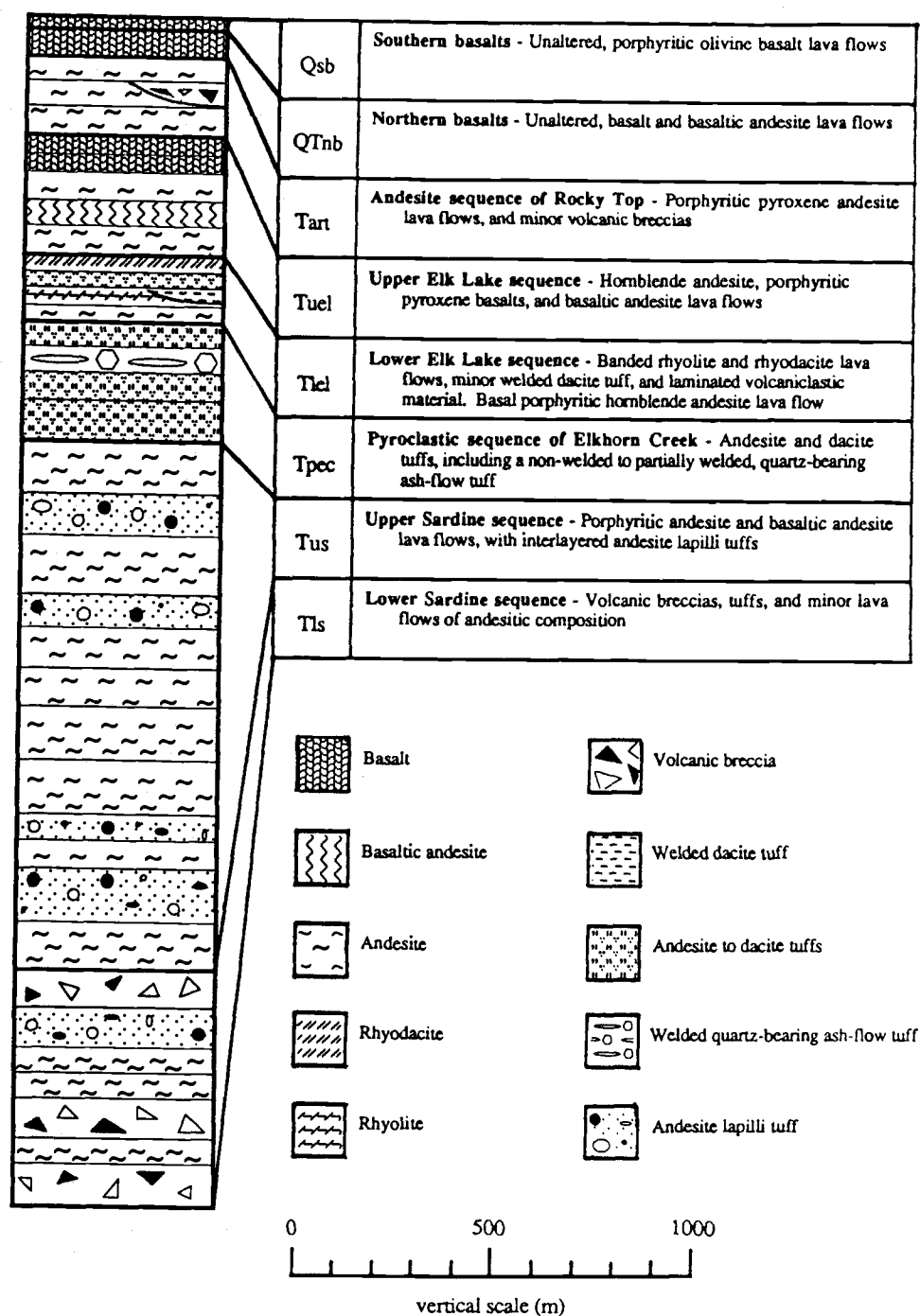
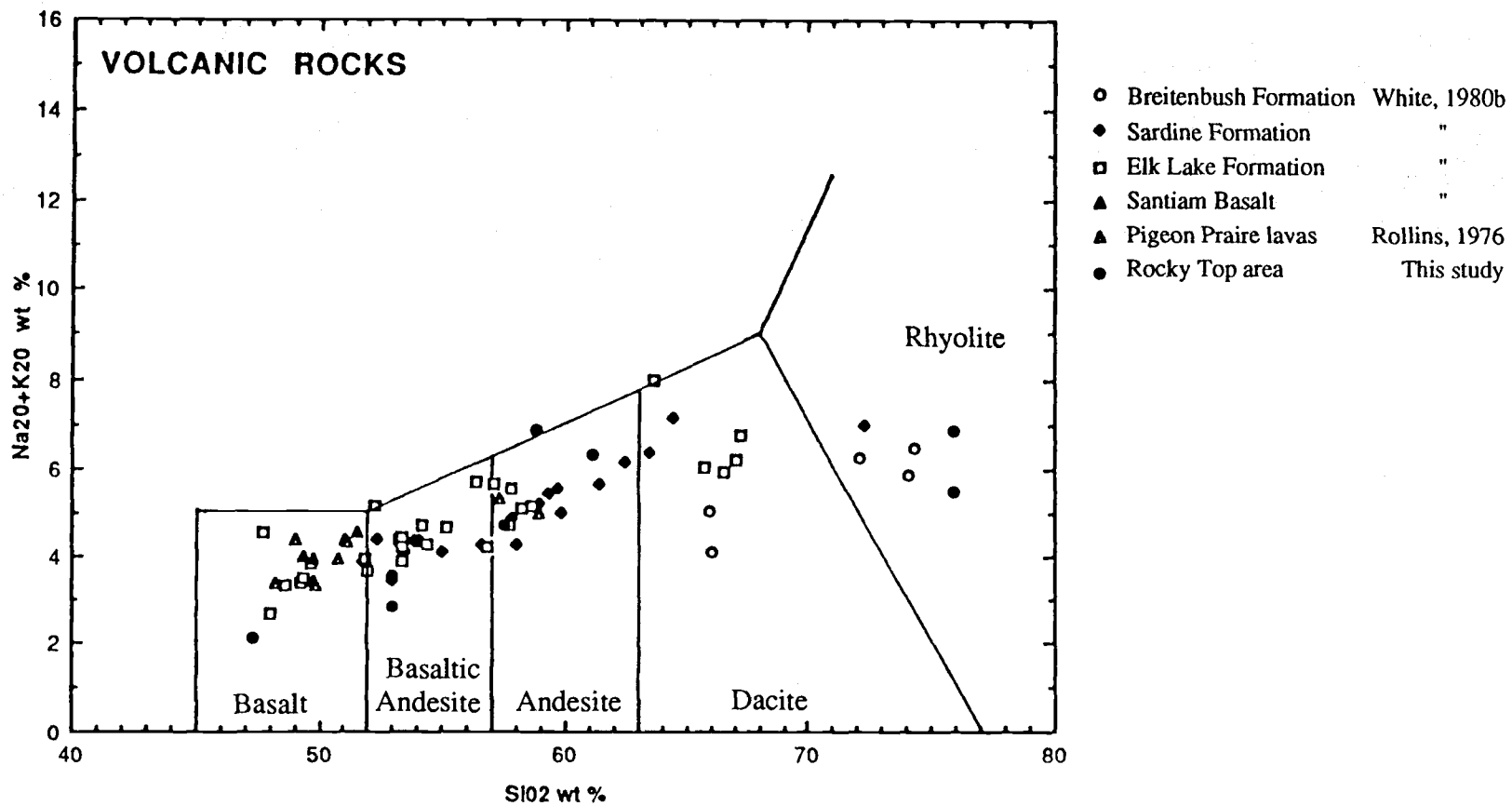


Figure 6: Composite stratigraphic column.



After LeMaitre (1984)

Figure 7: Classification of volcanic rocks using the TAS (total alkalis vs. silica) diagram

The majority of the late Oligocene to middle Miocene volcanic units in the Rocky Top area display the general characteristics of the Sardine Series as defined by Thayer (1934), or the Elk Lake formation as informally proposed by McBirney and others (1974), and are assigned to the Sardine and Elk Lake sequences, respectively. Each of these sequences are locally tilted, intruded by dikes, and hydrothermally altered. These map units represent characteristic assemblages of volcanic rocks that are individually distinct and which follow, for the most part, the divisions and descriptions as defined by previous detailed mapping in the region (Pungrassami, 1970; Olson, 1978; White, 1980a, 1980b; Pollock, 1985).

Notable additions to the previously recognized Tertiary assemblage of volcanic rocks in the vicinity of Rocky Top are limited exposures of the pyroclastic sequence of Elkhorn Creek and the andesite sequence of Rocky Top. These units are well constrained in the stratigraphic sequence and have undergone varying intensities of hydrothermal alteration. The upper and lower contacts of the pyroclastic sequence of Elkhorn Creek are delineated by angular unconformities with the underlying Sardine and overlying Elk Lake sequences. The pyroclastic sequence of Elkhorn Creek is locally tilted up to 25 degrees and intruded by dikes. In contrast, the andesite sequence of Rocky Top is stratigraphically above the Elk Lake sequence and is not deformed or cut by dikes.

Isolated exposures of post-Miocene intracanyon basalts have been named the Northern basalts and Southern basalts because of their geographic locations with respect to Rocky Top. Both basaltic units are flat lying, and are not hydrothermally altered. The Northern basalts are inferred to be Pliocene to Pleistocene in age and crop out exclusively in the Elkhorn Creek drainage above 1350 meters (4400 ft). This unit is probably correlative with the Battle Ax lavas as defined by White (1980a, 1980b) based on composition and location. In comparison, the Southern basalts are most likely

Pleistocene in age based on exposures which are restricted to an altitude of roughly 1000 meters (3200 ft) on a terrace-like surface in the North Santiam River drainage, immediately south of Rocky Top. This unit is probably correlative with the Santiam basalts of Pleistocene age as described by Thayer (1934, 1936, 1937) and White (1980a, 1980b), and the Pigeon Prairie lavas of Rollins (1976).

DESCRIPTION OF VOLCANIC UNITS

Sardine sequence

Outcrops of the Sardine sequence represent the oldest rocks exposed in the Rocky Top area. This assemblage of volcanic rocks is further subdivided into lower and upper members, which are distinguished from each other by the relative proportions of slope-forming pyroclastic rocks and cliff-forming lava flows. The upper member is dominated by lava flows, whereas the lower member contains a larger quantity of pyroclastic rocks.

The type locality of the Sardine Series was designated by Thayer (1934) at Sardine Mountain, two kilometers east of Rocky Top. In most areas, the Sardine consists predominantly of pyroxene-bearing andesite lava flows, breccias, and tuffs. Peck and others (1964) have reported that the Sardine Formation is generally less than 1,000 meters thick, but reaches a maximum thickness of 3,000 meters near Detroit.

Based on plant fossils discovered near Detroit, Peck and others (1964) suggested a middle Miocene age for the Sardine Formation. Priest and others (1987) published two age determinations on a plagioclase feldspar separate from a sample collected from the Sardine Formation on Hall Ridge, five kilometers southeast of Rocky Top. The standard K-Ar method provided a date of 22.1 ± 0.5 million years while a total fusion age using the ^{40}Ar - ^{39}Ar method was reported as 26.5 ± 0.5 million years. The sample

employed in the latter method, however, displayed a U-shaped age spectrum, which implies the presence of excess argon. Verplanck (1985) reported whole-rock K-Ar age determinations of 23.5 ± 0.3 million years on a sample from the Sardine taken near Mill City and 12.5 ± 0.2 million years on a sample from the Sardine in Rocky Top Area. In addition, whole-rock K-Ar age determinations of three samples collected by Sutter (1978) from the Sardine lavas at Hall Ridge are 16.7 ± 0.2 , 15.9 ± 0.2 , and 15.5 ± 0.2 million years in age.

Dates greater than 22 million years from Priest and others (1987) and Verplanck (1985) are interpreted here to represent the crystallization age of the volcanic rocks for the Sardine sequence, whereas dates younger than 17 million years from Sutter (1978) and Verplanck (1985) most likely have been modified as a result of subsequent hydrothermal alteration, as suggested by the oxygen isotope work of Taylor (1971).

Recent work by Priest (1989, 1990) has detailed a period of widespread erosion, or non-deposition, combined with deformation that occurred roughly 18 to 14 million years ago in the Western Cascades. This event is expressed in the Rocky Top area at the contact between the pyroclastic sequence of Elkhorn Creek and the upper member of the Sardine sequence. Therefore, it may be assumed that the Sardine sequence as mapped at Rocky Top ranges from greater than 26 to possibly as young as 18 million years in age.

Lower Sardine member

The lower member of the Sardine sequence of late Oligocene to early Miocene age consists primarily of volcanoclastic rocks and subordinate amounts of interbedded andesitic lava flows. The lower Sardine constitutes the base of the local stratigraphic sequence, and a minimum thickness of 600 meters is inferred from exposures in the western slopes of the Sardine Creek drainage. The lower Sardine member is poorly

exposed in the Rocky Top area and limited to lower elevations along the North Santiam River and Sardine Creek. The observed lateral variations in thickness and lithology at Rocky Top are characteristic of the lower Sardine (cf. Pungrassami, 1970). While most individual rock units can not be followed for more than 100 meters, the overall thickness and general lithology of the lower Sardine remains essentially constant from the North Santiam River to Sardine Creek. The rocks of this sequence display moderate to intense hydrothermal alteration, and locally contain high concentrations of trace metals. This unit, based on composition and stratigraphic position, is correlative with the Sardine as mapped by Thayer (1934), Pungrassami (1970), and Olson (1978), and unit A of Pollock (1985).

Pyroclastic breccias and lapilli tuffs are the most abundant rock types in the lower Sardine. These rocks are generally supported by a matrix consisting of coarse ash. They are well-indurated, poorly sorted, and form crudely bedded to massive outcrops. These deposits range in thickness from around 20 to more than 100 centimeters and may contain 10 to 20 centimeter thick interbeds of well sorted, thinly bedded fine ash tuff.

The clasts in pyroclastic breccias are angular to subangular and consist of rock fragments of nearly equal proportions of older tuff and lava flows. Clast size varies from less than one to greater than 20 centimeters, with an average of six centimeters. Clasts rarely exhibit preferred orientation and constitute anywhere from 25 to 60 percent of the rock with the remaining portion consisting of ash-sized constituents.

The rest of the lower Sardine is made up of lapilli to fine ash tuffs which dominate several horizons within the unit. Pungrassami (1970) described them as a major constituent of the lower Sardine exposed at Detroit Dam. Bedding is apparent on a small scale in some fine to coarse ash tuffs, but becomes less distinct with increasing clast size.

The bulk of these tuffs contain greater than 50 percent ash, with decreasing amounts of crystal fragments, subordinate pumice, and lithic clasts. The lapilli-sized clasts average one centimeter in diameter, are angular to subangular in shape, and are variably sorted. Broken feldspars make up most of the crystal fragments and are generally less than two millimeters in length. Trace amounts of quartz and pyroxene may also be present. Pumice varies in size up to two centimeters, and accounts for less than 10 volume percent of the rock. Lithic fragments rarely exceed five percent by volume.

Hydrothermal alteration of the volcanoclastic rocks tends to be more intense than in adjacent lava flows, presumably as a result of greater permeability and high reactivity of metastable glass. The color of altered samples depends upon the secondary mineral assemblage which generally ranges from characteristic epidote and chlorite greens to bleached white grays and yellows associated with hydrothermal quartz, sericite, and clay minerals. Unaltered samples generally have a gray colored matrix with clasts ranging in color from browns through grays to purple.

Upper Sardine member

The upper member of the Sardine sequence of late Oligocene to early Miocene age consists predominantly of porphyritic andesite and basaltic andesite lava flows which are occasionally interbedded with minor amounts of volcanic breccias and tuffs. The contact with the lower Sardine is based upon a gradational change from the volcanoclastic-dominated lower Sardine to the flow-dominated upper Sardine. On the basis of composition and stratigraphic position, this unit is correlative with the Sardine as mapped by Thayer (1934), Pungrassami (1970), and Olson (1978), and unit B of Pollock (1985).

The rocks of the upper Sardine are generally well-exposed, display moderate to intense hydrothermal alteration, and locally contain anomalously high concentrations of trace metals. These rocks crop out at the lowest elevations along Elkhorn Creek, intermediate elevations along Sardine Creek and at Rocky Top, and the highest elevations in the northwest quadrant of the map area. The lava flows of the upper Sardine are resistant to weathering and form prominent outcrops. Locally continuous exposures range in thickness from 300 to 500 meters, and combine for a total thickness in excess of 1500 meters. The best exposures of upper Sardine rocks in the map area are found in sections 15, 16, and 21 (T9S, R4E). The upper Sardine is generally flat-lying in the southwest and northeast quadrants of the Rocky Top area. In contrast, exposures strike northwest and may dip up to 45 degrees northeast along a three kilometer wide northwest-trending zone extending through the central part of the map area.

Unaltered lava flows of the upper Sardine member range in color from medium to dark gray, but where altered or weathered they are various shades of greens and bleached tans. They display platy to blocky jointing, and are chiefly porphyritic. Phenocrysts of plagioclase feldspar and clinopyroxene are set in an intergranular groundmass containing randomly oriented plagioclase microlites, subophitic clinopyroxene, minor magnetite, and trace amounts of apatite. Flow textures are indicated in a few samples by the presence of oriented plagioclase microlites.

Plagioclase feldspar constitutes from 50 to 70 percent of the phenocryst population and dominates the groundmass assemblage. Phenocrysts of plagioclase feldspar are complexly zoned, and highly variable in composition. They range from cores of An 70-50 to rims of An 50-40, and constitute anywhere from 15 to 30 volume percent of the rock. These phenocrysts are elongate, euhedral to subhedral, and occur separately or in glomeroporphyritic aggregates. They average five millimeters, and range up to one

centimeter in length. The maximum anorthite content for groundmass plagioclase feldspar is roughly An 40.

The primary mafic mineral in the upper Sardine is clinopyroxene, with trace amounts of orthopyroxene, magnetite, and rarely olivine. Augite is the dominant pyroxene phenocryst, with minor amounts of hypersthene. Olivine has been pseudomorphically replaced by chlorite, and is surrounded by granular rims of clinopyroxene. The groundmass pyroxene is nearly all granular or prismatic clinopyroxene. Mafic minerals comprise less than 20 volume percent of the rock.

Hydrothermal alteration of these rocks tends to be most intense near structures and intrusive rocks. Feldspars are commonly altered to sericite, clay minerals, or epidote and carbonate. Mafic minerals are almost without exception altered to chlorite, with traces of iron oxides, rutile, and pyrite.

Pyroclastic sequence of Elkhorn Creek

The pyroclastic sequence of Elkhorn Creek is inferred to be of early to middle Miocene age based on stratigraphic position. This unit consists of poorly exposed fine ash to lapilli tuffs, which range in composition from andesite to dacite, with minor rhyolite. The total thickness of this sequence is roughly 300 meters. These rocks exhibit moderate to intense hydrothermal alteration, and contain some of the highest concentrations of trace metals in the area. This sequence is best exposed immediately northeast of Rocky Top where it rests upon the upper Sardine with an angular unconformity of less than 10 to greater than 30 degrees. Work by Priest (1989, 1990) has documented a period of widespread erosion and deformation that occurred roughly 18 to 14 million years ago. Based on contact relationships with the upper Sardine, the pyroclastic sequence of Elkhorn Creek is inferred to be less than approximately 18 to 14 million years in age.

Fine ash to lapilli tuffs are exposed immediately north and east of Rocky Top in the Elkhorn Creek drainage. Outcrops of welded dacite ash-flow tuff are located in the eastern half of section 14 (T9S R4E), and a quartz-bearing ash-flow tuff is present in the center of section 13 (T9S R4E). Small exposures of the pyroclastic sequence of Elkhorn Creek are also located near the center of section 16 (T9S R4E). This unit ranges in color from brown and yellow to green where altered or weathered but may be various shades of gray where unaltered.

Coarse ash tuffs of this unit tend to be massive, while fine ash tuffs are frequently thinly bedded, with individual layers one to five centimeters in thickness. Welded tuffs have well-developed eutaxitic texture, with flattened pumice usually less than five millimeters in thickness.

Ash tuffs represent the majority of the pyroclastic rocks of this unit. They contain greater than 50 percent ash matrix combined with lapilli sized clasts consisting of crystal fragments, pumice and lithic clasts. Crystal fragments are dominated by plagioclase feldspar ranging up to five millimeters in length, and accompanied by trace amounts of pyroxene up to two millimeters in diameter. Rock fragments consist of angular to subangular clasts of porphyritic andesite, with subordinate amounts of basalt, and they account for less than 10 percent of the tuff. A distinctive ash-flow tuff located in the center of section 13 is characterized by up to 10 percent by volume embayed quartz crystals which reach two millimeters in diameter.

The rocks of the pyroclastic sequence of Elkhorn Creek exposed on Rocky Top appear to have been deposited after the Sardine sequence was faulted, flexed in a northwest-striking, northeast-dipping tilt-block, and eroded. Similarities in lithology, chemical composition, and stratigraphic position suggest that the pyroclastic sequence of Elkhorn Creek is correlative with the Breitenbush Formation of previous workers (cf. Thayer, 1934, 1939; White, 1980a, 1980b; Priest, 1987).

Elk Lake sequence

The Elk Lake sequence is divided into two map units based upon different lithologies. Rocks of the lower member are chiefly rhyolite and rhyodacite flows and interbedded pyroclastic rocks. In contrast, rocks of the upper member consist of lava flows of hornblende andesite, pyroxene andesite, and basaltic andesite.

The Elk Lake sequence as mapped at Rocky Top can be correlated with units C and D of Pollock (1985) and the Elk Lake Formation of White (1980a, 1980b). McBirney and others (1974) informally named the Elk Lake formation on the basis of radiometric age determinations and stratigraphic relations at its type locality about 10 kilometers north of Detroit. Whole-rock K-Ar age determinations of samples collected by Sutter (1978) from the Elk Lake formation in the vicinity of French Creek Ridge are 11.0 ± 0.4 and 11.0 ± 0.8 million years in age. According to White (1980a, 1980b) and Cummings and others (1989, 1990) the rocks of the Elk Lake formation were erupted from a volcanic center located in the French Creek Ridge area, less than six kilometers east of Rocky Top. Cummings and others (1989, 1990) have documented hydrothermal alteration within the Elk Lake formation at French Creek Ridge. If the age determinations presented by Sutter (1978) record this event, then the dates should be interpreted as minimum ages. The Elk Lake is stratigraphically above the 18 to 14 million year old unconformity of Priest (1989, 1990). Accordingly, the Elk Lake sequence at Rocky Top ranges from younger than about 14 to probably older than 11 million years old, and is therefore inferred to be middle Miocene in age.

Lower Elk Lake member

The lower member of the middle Miocene Elk Lake sequence consists primarily of moderately well-exposed, subhorizontally banded rhyolite and rhyodacite flows, a small

welded dacitic ash-flow tuff, and thinly bedded volcanoclastic rocks. The lower Elk Lake overlies the pyroclastic sequence of Elkhorn Creek across an angular unconformity of up to 15 degrees. The thickness of this unit is roughly 150 meters based on exposures in the headwaters of Elkhorn Creek. The rocks of this unit have been subjected to moderate to intense hydrothermal alteration. They have well developed liesegang banding, and locally contain anomalously high concentrations of trace metals. This unit is correlative with the lower member of the Elk Lake Formation as defined by White (1980a, 1980b), and unit C of Pollock (1985) based on stratigraphic position, similarities in lithology, and chemical composition.

The silicic lava flows of the lower Elk Lake member are generally light gray in color, flow banded, and their thickness often exceeds 10 meters. They contain less than 10 percent phenocrysts primarily of feldspar and quartz, in a devitrified and highly altered groundmass. Feldspar is represented by euhedral lath-shaped crystals which are entirely altered to an assemblage of quartz, sericite, and trace calcite. Phenocrysts of quartz up to two millimeters in diameter are subhedral and often embayed.

Upper Elk Lake member

The upper member of the middle Miocene Elk Lake sequence directly overlies the lower Elk Lake. The upper Elk Lake consists predominantly of well-exposed, subhorizontal lava flows of hornblende andesite, pyroxene andesite, and basaltic andesite. These rocks exhibit moderate to intense propylitic alteration. The total thickness of this unit exceeds 200 meters in the headwaters of Elkhorn Creek where colonnades of hornblende andesite up to 20 meters high are exposed. This unit is correlative with the upper member of the Elk Lake Formation as defined by White (1980a, 1980b), and unit D of Pollock (1985).

The rocks of the upper Elk Lake member contain abundant phenocrysts of plagioclase feldspar and about five volume percent hornblende. Phenocrysts of clinopyroxene are, in some flows, the dominant mafic mineral phase and hornblende is absent. Phenocrysts constitute 20 to 40 volume percent of the rock, and occur in a pilotaxitic groundmass consisting predominantly of microlites of plagioclase feldspar, minor pyroxene, and disseminated magnetite. Apatite is a common accessory mineral.

Andesite sequence of Rocky Top

The andesite sequence of Rocky Top is inferred to be late Miocene in age based on composition, and stratigraphic position. This unit consists primarily of horizontal lava flows of pyroxene andesite and minor debris flow deposits. The andesite sequence of Rocky Top is well-exposed as a ridge-capping unit about 200 meters thick that forms the summit of Rocky Top. The rocks of this unit have been subjected to mild propylitic alteration, and contain background trace metal concentrations. The andesite sequence of Rocky Top overlies the pyroclastic sequence of Elkhorn Creek with a slight angular unconformity of less than 10 degrees. Exposures of the andesite sequence are present as medium to dark gray ledgy outcrops which contrast with the lighter colored, slope-forming pyroclastic sequence of Elkhorn Creek.

Cliff-forming lava flows of pyroxene andesite make up the bulk of this unit. Fresh surfaces are dark gray, very finely crystalline, and contain phenocrysts of plagioclase feldspar, and clinopyroxene. Phenocrysts account for 15 to 30 volume percent of the rock. The dominant phenocryst is plagioclase (An 55) which make up to 25 volume percent of the rock. These phenocrysts are present as elongate, euhedral to subhedral laths which range from 0.1 to five millimeters in length. Clinopyroxene is an additional phenocryst component that constitutes five to 10 volume percent of the rock, and is present as euhedral to subhedral crystals 0.1 to two millimeters in diameter.

Groundmass phases consist of randomly oriented plagioclase feldspar and lesser amounts of granular pyroxene associated with trace amounts of magnetite and apatite.

The andesite sequence of Rocky Top is only mildly propylitically altered. Mafic minerals have been converted to chlorite, with trace amounts of iron oxides. Plagioclase feldspar is incompletely replaced by sericite and clay minerals.

Northern basalts

The Northern basalts are made up of horizontal intracanyon lava flows of basalt and basaltic andesite which are inferred to be Pliocene to Pleistocene in age based on stratigraphic and compositional similarities with the Battle Ax lavas described by White (1980a, 1980b). This is the oldest volcanic unit in the area that clearly post-dates hydrothermal mineralization. The Northern basalts overlie the upper member of the Elk Lake sequence and the andesite sequence of Rocky Top as paleo-intracanyon lava flows. These isolated exposures exceed 30 meters in thickness and crop out exclusively in the Elkhorn Creek watershed at elevations greater than 1350 meters (4400 ft). These lava flows are generally less than five meters thick, and consist of nearly equal proportions of basalt and basaltic andesite.

Plagioclase feldspar constitutes 40 volume percent of the rock. It is present as phenocrysts up to five millimeters in length, and is elongate and euhedral to subhedral in shape. Mole percent anorthite compositions of phenocrysts range from An 75 to An 60 and are normally zoned. Groundmass plagioclase feldspar compositions are less than An 65. Clinopyroxene is present as small, subophitic groundmass crystals and less commonly as phenocrysts. Less than five volume percent olivine is present in some flows as subhedral crystals about one millimeter in diameter. Magnetite occurs as disseminated intergranular groundmass crystals.

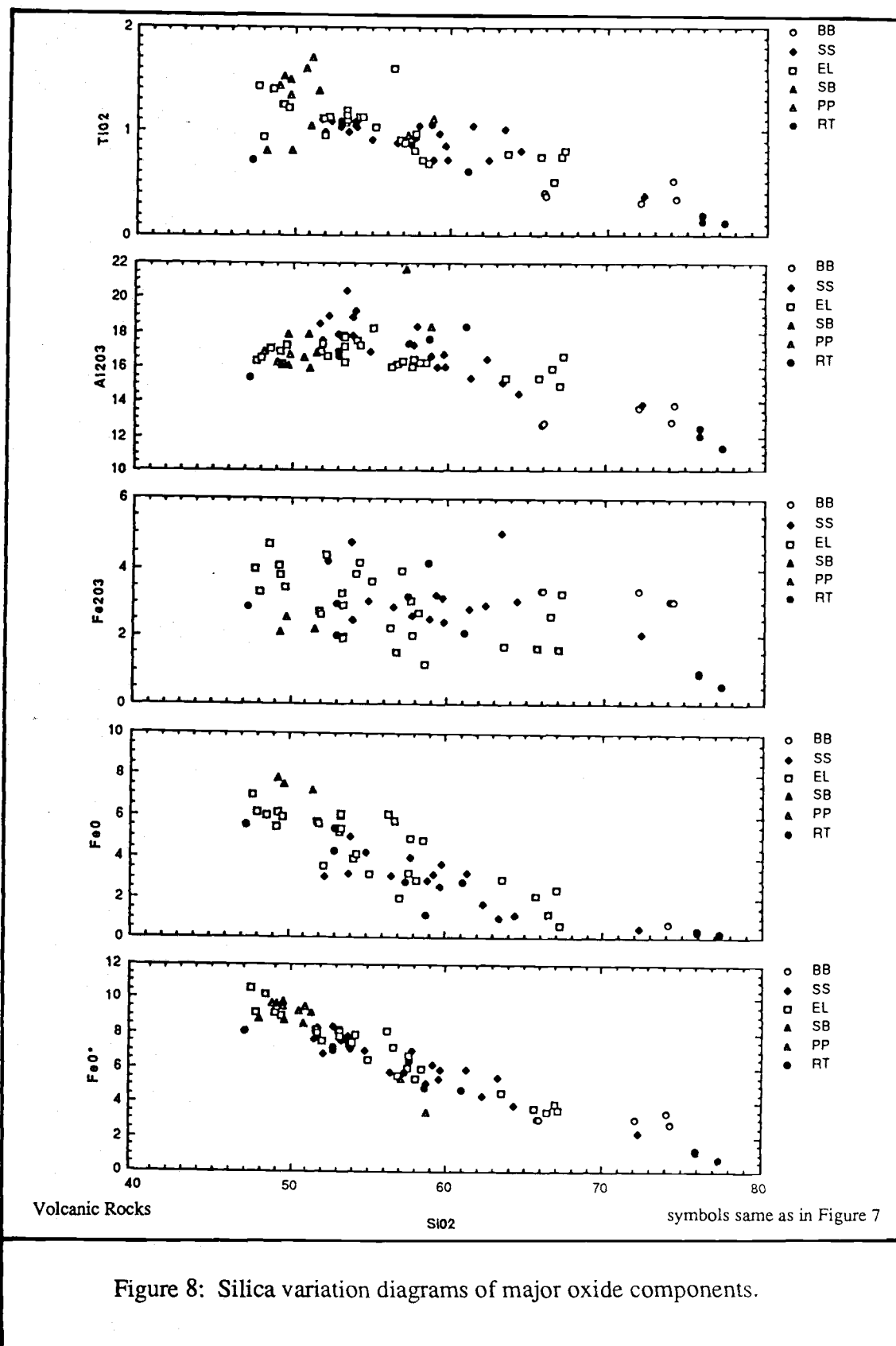
Southern basalts

The Southern basalts consist of horizontal flows of olivine basalt which form 5 to 10 meter thick benches with blocky to platy jointing. These rocks are unaltered and well-exposed, but are generally restricted in areal extent to terraces south of Rocky Top at an elevation of less than 1000 meters (3200 ft). The southern basalts are most likely Pleistocene in age and are considered correlative with the Santiam basalts as described by Thayer (1934, 1936, and 1937) and White (1980a, 1980b), and the Pigeon Prairie lavas reported by Rollins (1976). This correlation is based on their unaltered character, distinct chemical composition, and restricted occurrence to a geomorphologically young surface.

Olivine phenocrysts constitute around 10 percent of the finely crystalline rock, and ranges from one to two millimeters in diameter. Plagioclase feldspar is sometimes found as a phenocryst phase, but is commonly restricted to the hyalopilitic groundmass where it constitutes 30 percent of the rock.

CHEMICAL CHARACTERISTICS

The volcanic rocks of the study area display systematic trends with respect to major elements when plotted on silica variation diagrams as illustrated in Figure 8. These plots show that major oxide concentrations for TiO_2 , FeO^* , FeO , MgO , and CaO decrease whereas Na_2O , and K_2O increase with increasing SiO_2 . The remaining oxides Al_2O_3 , and Fe_2O_3 are relatively constant and decrease only at the highest concentrations of SiO_2 . A calc-alkaline magma affinity is exhibited by these variation diagrams. The ternary AFM diagram depicted in Figure 9 shows that these volcanic rocks also plot within the calc-alkaline field as defined by Irvine and Baragar (1971).



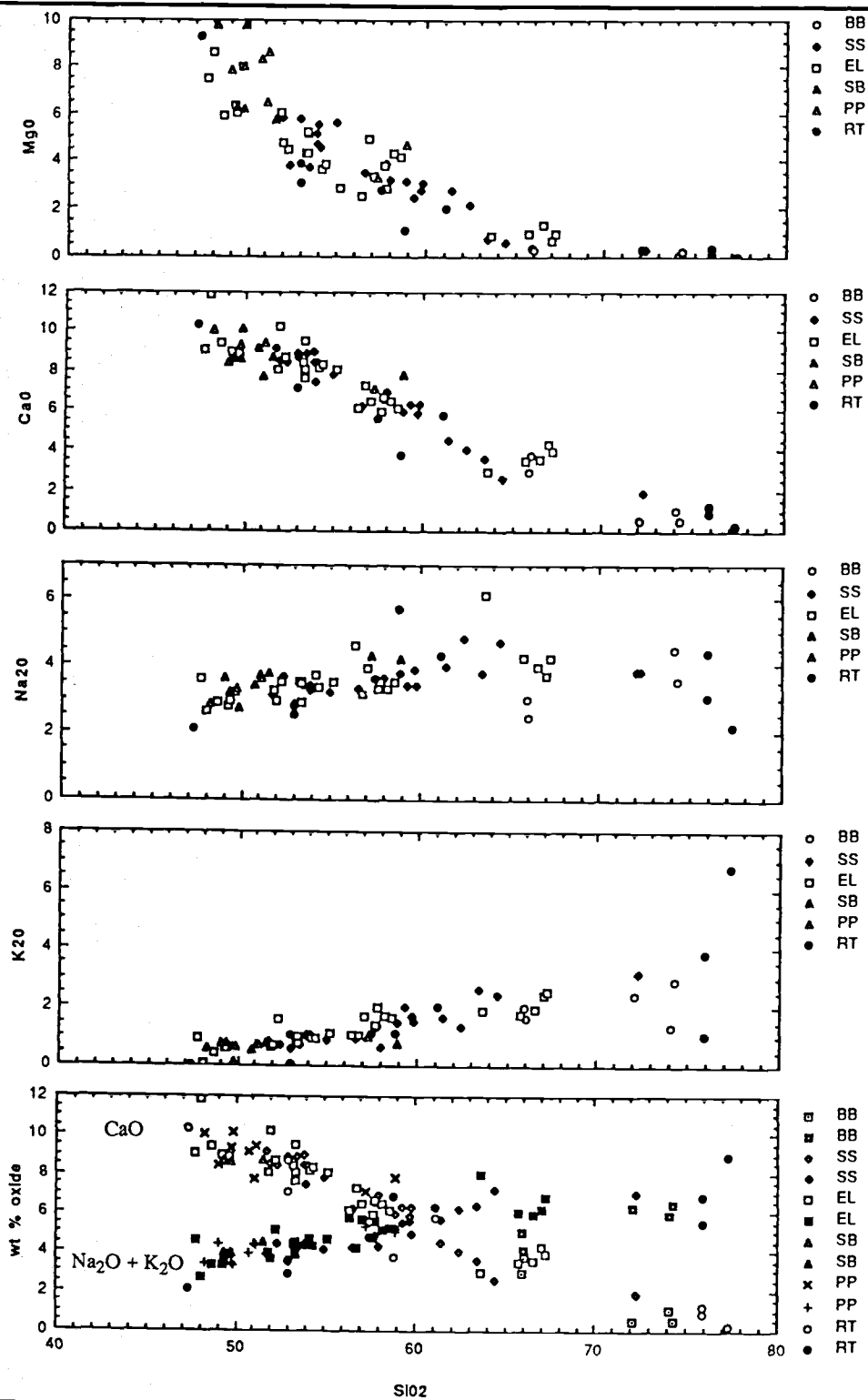
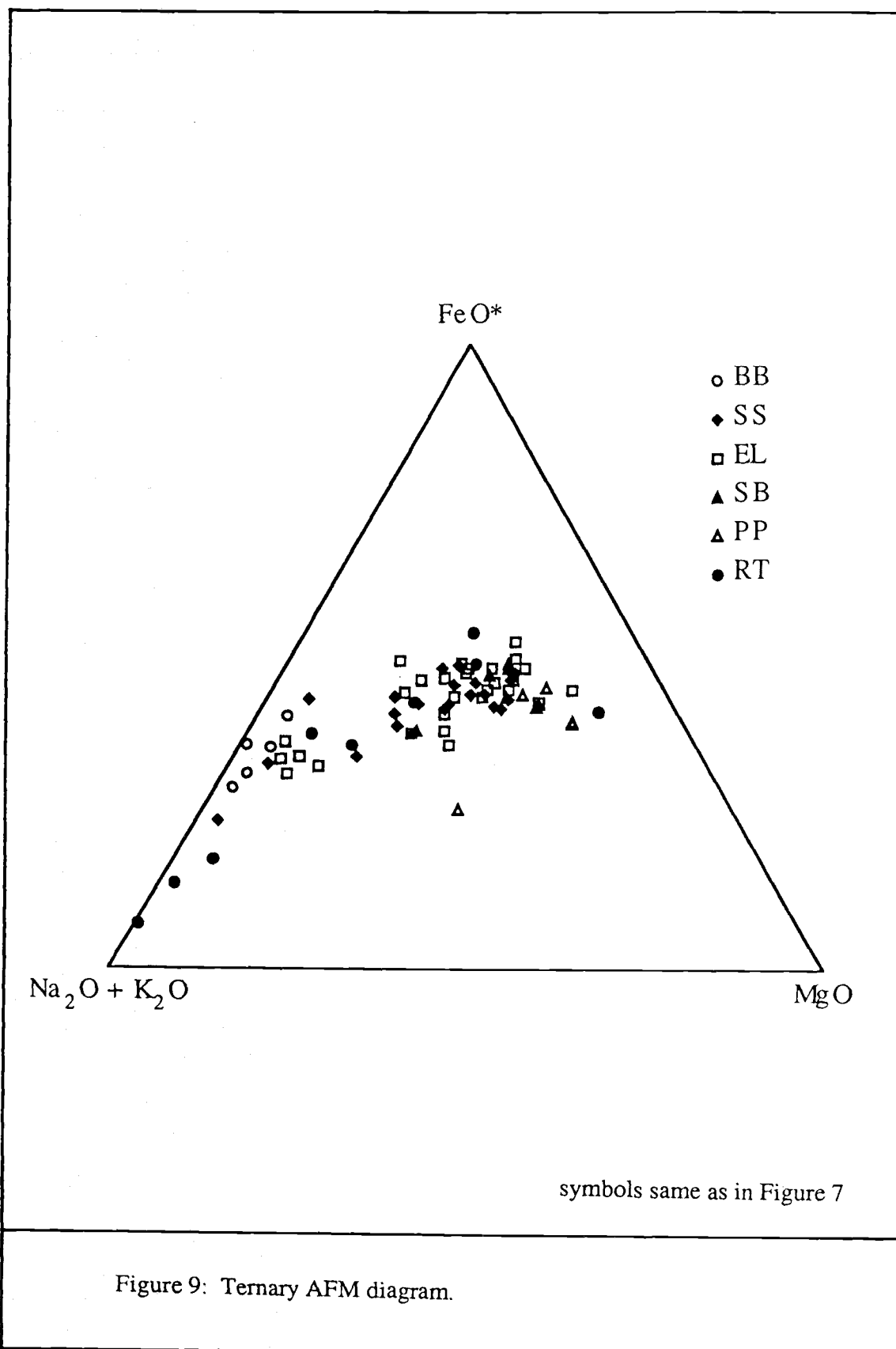


Figure 8: continued

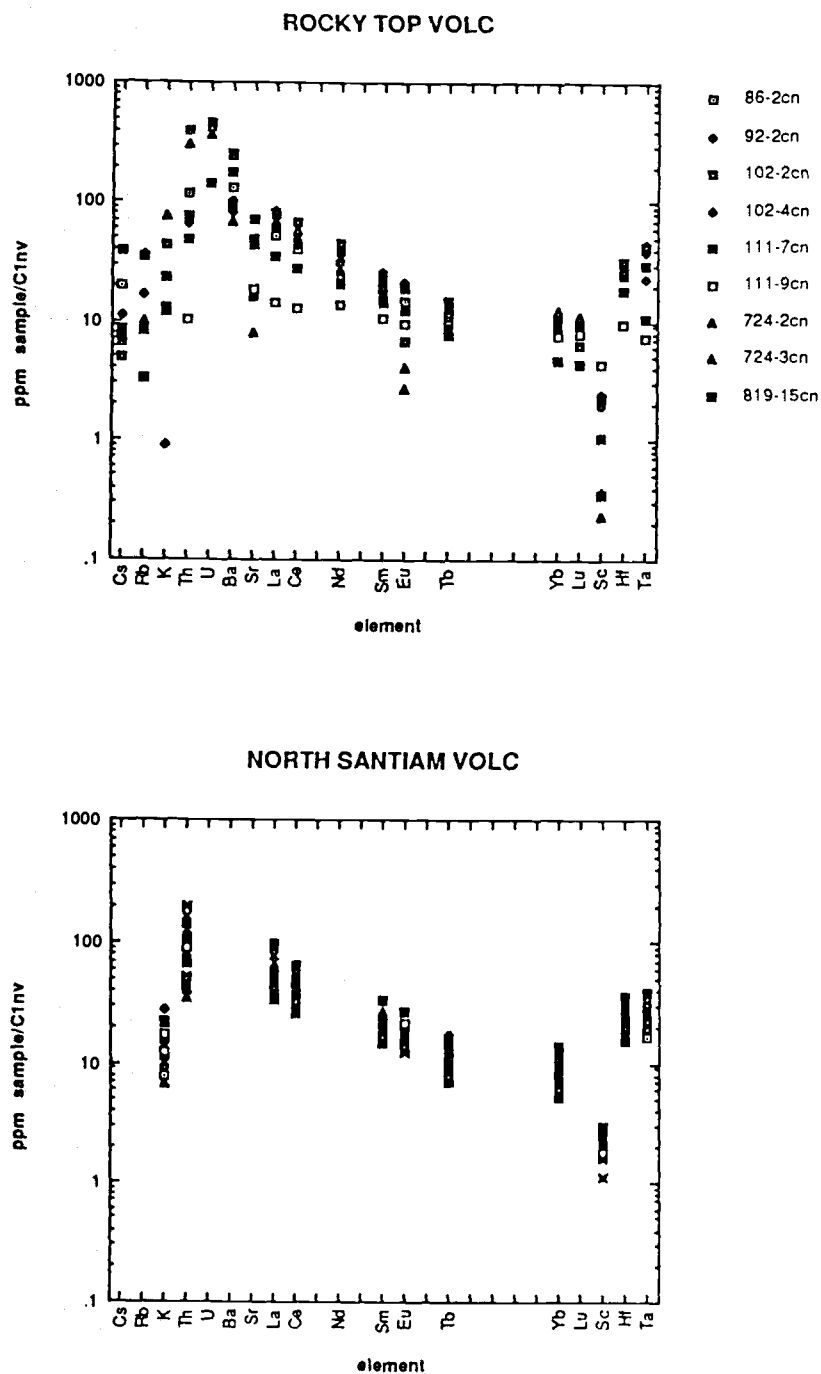


A chondrite normalized trace element plot for representative samples of volcanic rocks within the Rocky Top area is shown in Figure 10. All the rocks display moderate light rare-earth element enrichment, with the exception of a sample from the Southern basalts which are only slightly enriched with respect to light rare-earth elements. The range in Eu values can be attributed to feldspar fractionation of plagioclase and the wide range in SiO₂ composition of these rocks. Similarly, the range in Sc can be attributed to the fractionation of pyroxene, hornblende, or Fe-Ti oxides. The variations in the trends for Cs, Rb, K, Th, U, Ba, and Sr can be accounted for by the wide range of SiO₂ in these rocks.

The trace element proportions for Th, Hf, and Ta are plotted in Figure 11 on a discrimination diagram proposed by Wood (1980). As expected, all the samples from the Rocky Top area plot within the boundary for destructive plate-margin basalts and differentiates. All samples, except one (Qsb, 111-9) fall within the calc-alkaline field. The single anomalous sample is representative of the Southern basalts and plots in the primitive arc tholeiites field.

DISCUSSION

The late Oligocene to late Miocene volcanic rocks exposed within the Rocky Top area form an impressive 3000 meter thick record of Western Cascade calc-alkaline volcanism. These rocks range in composition and character from basaltic lava flows to rhyolitic tuffs. All of these units have locally undergone moderate to intense hydrothermal alteration. In contrast, the Pliocene to Pleistocene volcanic rocks represented by the Northern and Southern basalts are chemically distinct, unaltered, and found as intracanyon flows into the older rocks. Because of these relationships, it is inferred that these basalts were erupted after hydrothermal mineralization ceased, and



North Santiam data from Pollock, 1985

Figure 10: Chondrite-normalized trace element plots for volcanic rocks.

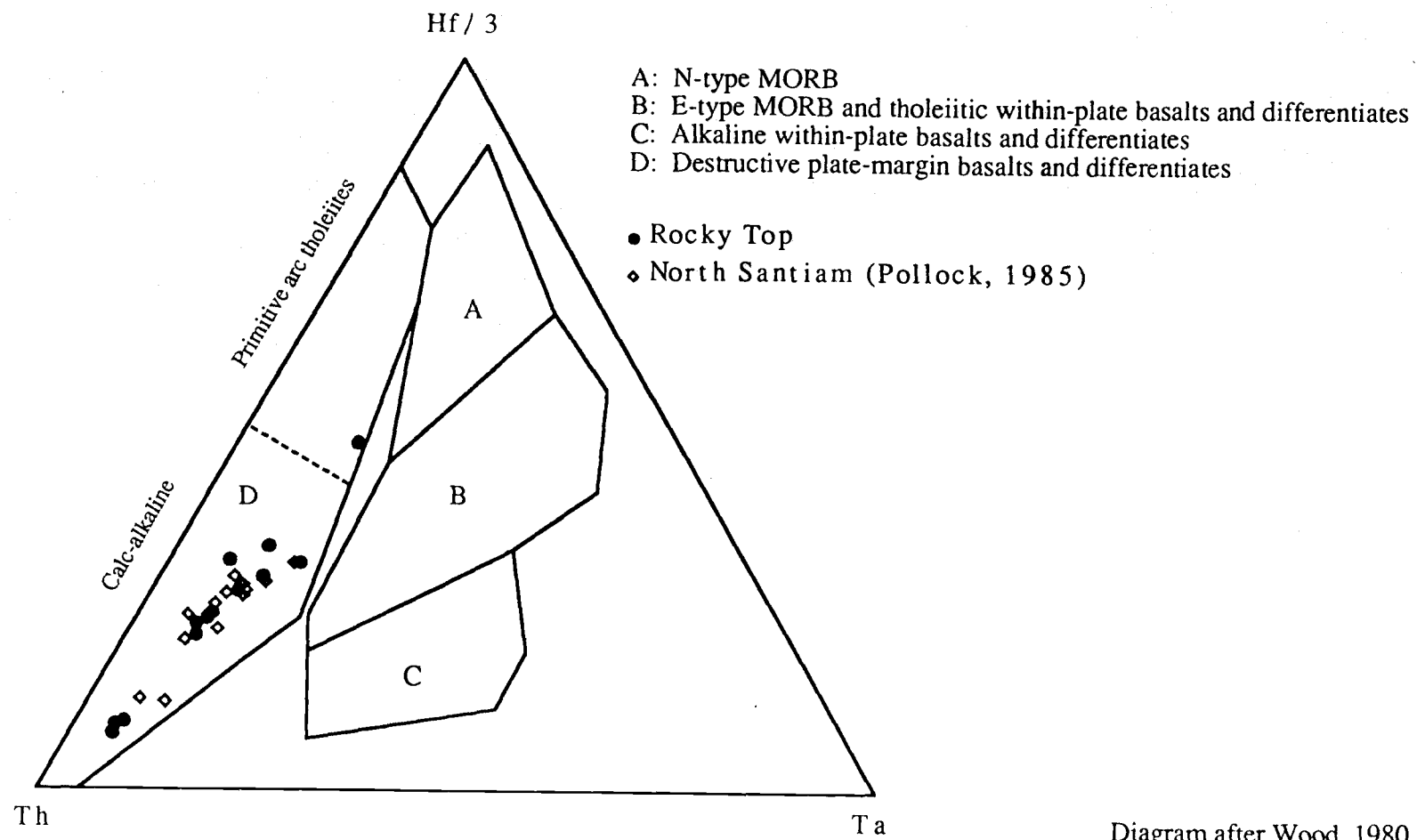


Figure 11: Th-Hf-Ta discrimination diagram for volcanic rocks.

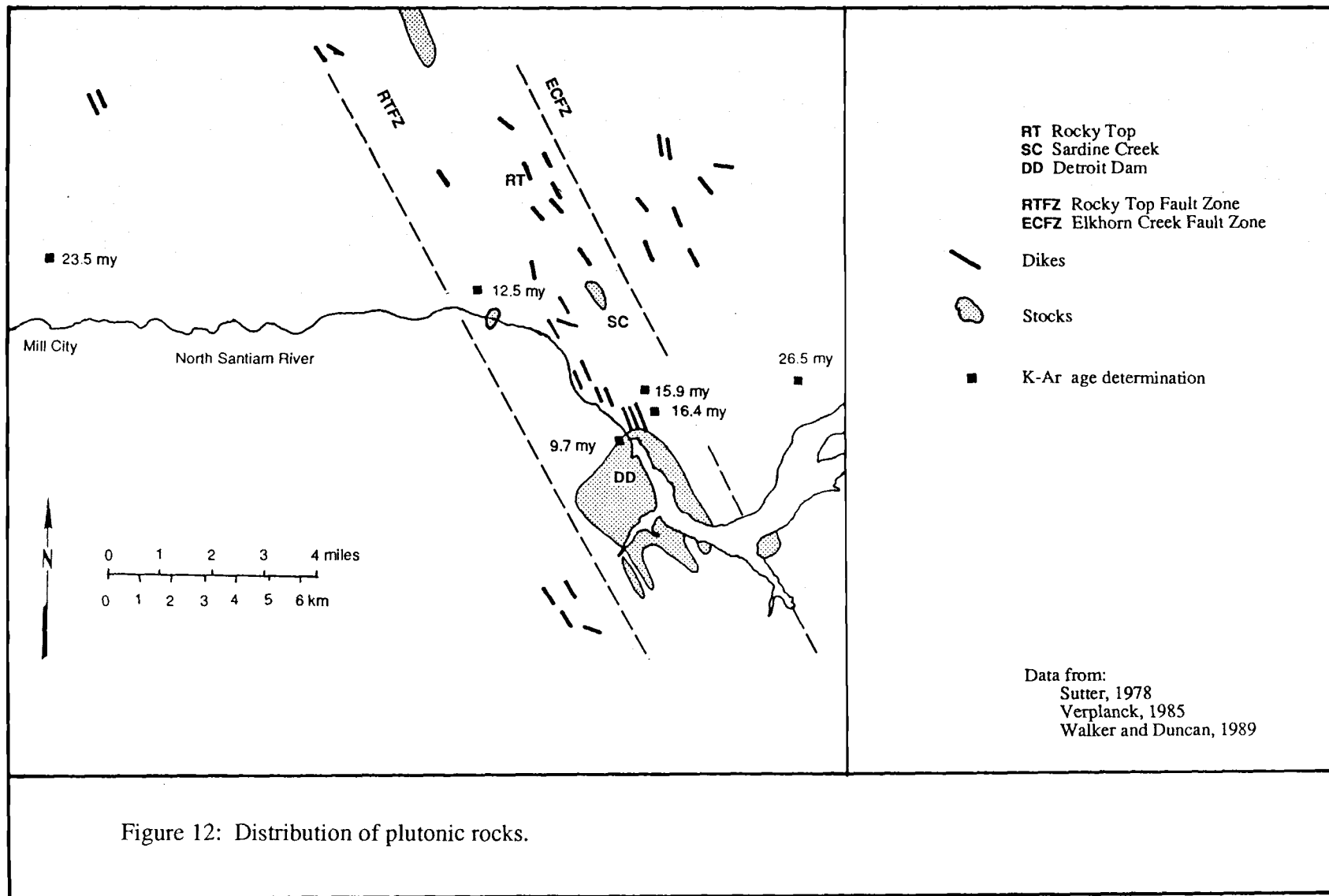
after the Rocky Top area had been incised at least 200 meters relative to the source of the Northern basalts.

PLUTONIC ROCKS

Plutonic rocks of intermediate composition intrude the Tertiary volcanic rocks of the Western Cascades (Fig. 3) and are intermittently clustered along a NNE-trend which extends from Shellrock Mountain on the Columbia River to Sampson Creek near the Oregon-California border (Buddington and Callaghan, 1936). These intrusive rocks were emplaced as small monolithologic dikes, plugs, and sills, and as larger composite stocks which broadly exhibit a south to north increase in size and complexity. Elongate intrusions generally strike northwest and many are associated with hydrothermal mineralization (Callaghan and Buddington, 1938). The intrusions in the Western Cascades of Oregon range from 7 to 22 million years in age for magmatic mineral and whole rock K-Ar age determinations, whereas associated ages for hydrothermal minerals are generally one to two million years younger (Power and others, 1981).

The largest intrusive complex in the vicinity of Rocky Top is the Detroit Stock as shown in Figure 12. It is a pluton of intermediate composition having at least five stages of intrusion into volcanic rocks at least as young as early Miocene age. Walker and Duncan (1989) report a whole-rock K-Ar age determination of 9.9 ± 0.2 million years on a sample from the Detroit Stock. Cross-cutting relationships exposed near Detroit Dam at Cumley Creek (Sec 7 T10S R5E) reveal the relative ages between five intrusive stages. Oldest to youngest, these are: (1) pyroxene quartz diorite, (2) hornblende quartz diorite, (3) diorite, (4) hornblende granodiorite, and (5) tonalite (Curless and others, 1990).

A five kilometer wide zone of dikes extends northwest from the Detroit Stock through Rocky Top (Fig. 12). Intrusive rocks within the adjacent Sardine Creek and Rocky Top areas have mineralogical, textural, and chemical features similar to the spatially and temporally related Detroit Stock. Two plutonic rock units are mapped



within the Rocky Top area, and are classified as quartz diorite and granodiorite according to the IUGS classification system as detailed in Figure 13 (Streckeisen, 1976). Their distribution is illustrated on Plate 1. Characteristic features and modal proportions of representative samples of quartz diorite and granodiorite are presented in Table 2.

DESCRIPTION OF PLUTONIC UNITS

Quartz diorite

Quartz diorite is the most abundant plutonic rock type in the Rocky Top area. It is exposed as dikes up to 10 meters wide and, although their distribution is widespread, the majority are limited to a northwest-trending central zone between Rocky Top and Sardine Creek. There are over 17 pyroxene quartz diorite dikes mapped within the Rocky Top area. They are confined to units older than the andesite sequence of Rocky Top (Tart), have near vertical dips, and generally strike between N40° to 50°W. Their emplacement was strongly controlled by pre-existing structures, and the dikes have sharp to slightly brecciated contacts with narrow chilled, and locally vesiculated margins. Fresh samples from the dikes are generally medium gray in color. However, many dikes are altered or weathered to various shades of gray-greens, as a result of secondary chlorite and epidote, or iron stained tans from the oxidation of disseminated pyrite.

Quartz diorite exposed at Rocky Top is holocrystalline, and porphyritic to equigranular in texture. Most crystals average about one millimeter in size, although phenocrysts of plagioclase feldspar, and lesser pyroxene may reach five millimeters in length.

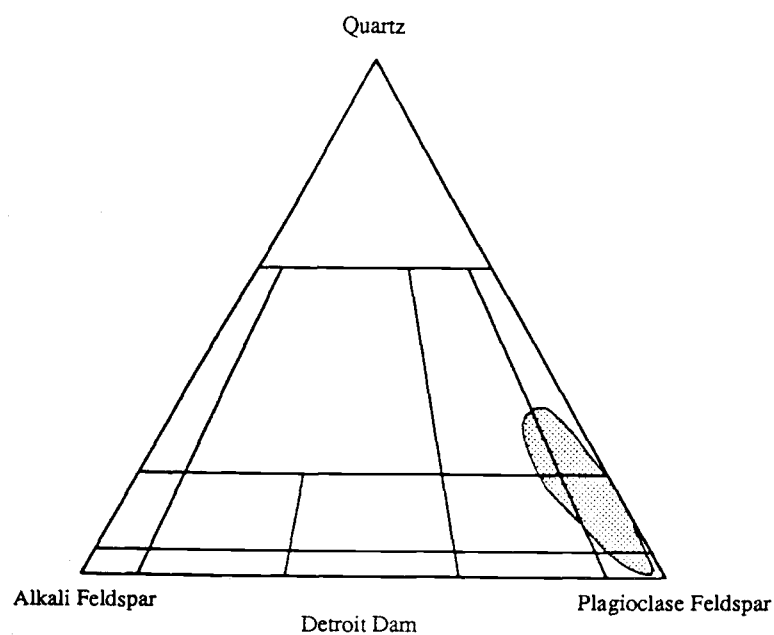
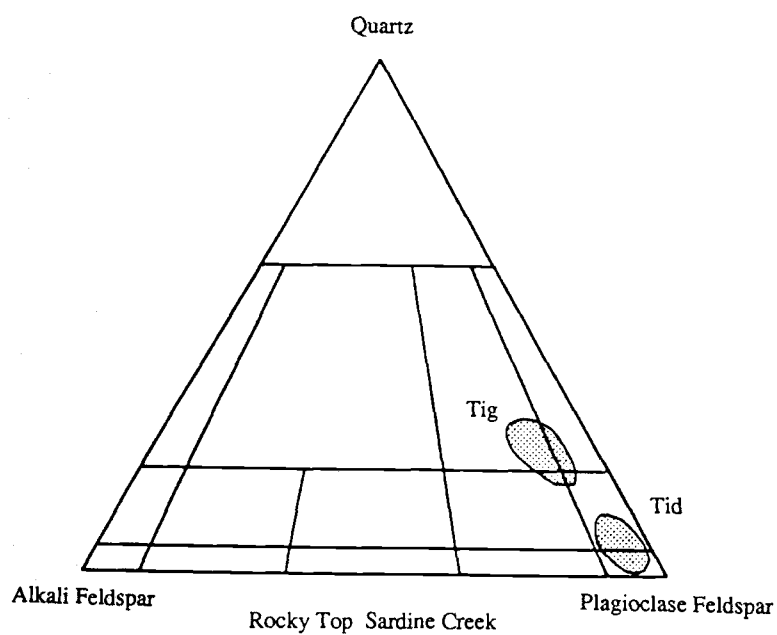


Diagram after Streckeisen, 1976

Figure 13: IUGS classification of intrusive rocks based on modal mineralogy.

TABLE 2: General character and modal mineralogy of plutonic rock units exposed at Rocky Top.

	Quartz Diorite	Granodiorite
Highest stratigraphic occurrence	Upper Elk Lake Sequence	Upper Sardine Sequence
Geometry	NW-trending dikes NW-elongate stock	NW-elongate stocks NW-trending dikes
Wall-rock contact	Sharp with narrow chill margins	Local intrusive breccias
Texture	Equigranular Porphyritic	Porphyritic
Characteristic mineralogy (vol %)		
Quartz	1-7	15-22
K-Feldspar	1-3	5-8
Plag-Feldspar	55-70	50-60
Pyroxene	20-30	
Hornblende		10-20
Opakes	5	2
Trace minerals	0.1	1
major-oxides (wt %)		
TiO ₂	0.8 ± 0.06	0.5 ± 0.02
Al ₂ O ₃	>16	<15.3

Plagioclase feldspar is the most abundant mineral phase in the quartz diorites. It ranges from 55 to 70 percent by volume, and is proportioned between the groundmass and phenocrysts in a ratio of about 2:1. The majority of the phenocrysts are euhedral and exhibit strong zoning with compositions varying between cores of An₆₀ to rims of An₄₀. Carlsbad and albite twins are common and a combination of the twins was used to determine core to rim compositions. Lath-shaped microlites are euhedral to subhedral in shape, range up to 0.25 millimeters in length, and are often twinned.

Euhedral to subhedral phenocrysts and subhedral groundmass crystals of blocky clinopyroxene represent 20 to 30 percent by volume of the quartz diorite. Phenocrysts range up to five millimeters, whereas the granular groundmass crystals average 0.5 millimeters in diameter.

Magnetite accounts for approximately five percent by volume. It ranges in shape from subhedral crystals to anhedral blebs. It is disseminated in the groundmass and rarely exceeds 0.05 millimeters in diameter. The remaining minerals that make up the quartz diorite consist of quartz (1-7%), potassium feldspar (1-3%), and apatite (0.1%).

Quartz diorite dikes are associated with zones of faults, and fractures. In addition, minor brecciation of the enclosing rock types is also common. These highly permeable zones served as a conduit for later hydrothermal fluids which altered both the dikes and surrounding volcanic rocks. Hydrothermal alteration of the dikes ranges from weak to intense. Plagioclase feldspar is replaced by sericite, albite, or epidote plus carbonate. Pyroxene is altered chiefly to chlorite, iron oxides, and rarely epidote.

Granodiorite

Intrusions of hornblende granodiorite composition form limited exposures of irregularly shaped, northwest-striking elongate dikes, and small stocks with locally

well-developed intrusion breccias. These rocks crop out in the Sardine Creek watershed at altitudes around 485 meters (1600 ft) in sections 25 and 36 (T9S R4E).

Rocks mapped as granodiorite are chiefly light colored, and porphyritic in texture. Fresh samples are generally light gray, and weathered samples range from light browns to gray. In addition, hydrothermal alteration changes the color from shades of light gray to increasing shades of green dependant upon the abundance of secondary chlorite and epidote.

In hand sample the rock appears porphyritic with medium-sized phenocrysts of plagioclase feldspar and hornblende set in a groundmass of quartz, plagioclase, and potassium feldspar. Petrographic examination reveals a holocrystalline porphyritic rock with euhedral to subhedral phenocrysts of plagioclase feldspar and hornblende. The finely crystalline granular groundmass consists of quartz, plagioclase, and potassium feldspar.

Plagioclase feldspar is the most abundant mineral phase and makes up 50 to 60 percent by volume of the granodiorite. Phenocrysts (25-35% of plagioclase in Tig) are euhedral to subhedral and range from two to five millimeters in length. Normal zoning is developed across carlsbad and albite twins which range from An50 to An35 in composition. Microlites of lath-shaped plagioclase feldspar make up about 25 percent by volume of the groundmass, where they range from 0.5 to less than 0.1 millimeters in length.

Euhedral to subhedral hornblende constitutes 10 to 20 percent by volume of the rock. It is present as phenocrysts which range from two to four millimeters in length, and is often partially replaced by chlorite.

The remaining mineral phases are confined to the groundmass. They are anhedral, less than 0.5 millimeters in diameter, and consist of quartz (15-22%), potassium feldspar (5-8%), magnetite (2%), and apatite (1%).

CHEMICAL CHARACTERISTICS

Plutonic rocks from the Rocky Top, Sardine Creek, and Detroit Dam areas, as well as those from North Santiam (Olson, 1978), display systematic trends with respect to major elements when plotted on silica variation diagrams as illustrated in Figure 14. These plots show that major oxide concentrations for TiO_2 , Al_2O_3 , Fe_2O_3 , FeO , FeO^* , MgO , and CaO decrease, whereas K_2O increases with increasing SiO_2 . The remaining oxide Na_2O maintains a relatively constant value. Pyroxene quartz diorite and hornblende granodiorite from Rocky Top to Detroit Dam can be distinguished from each other based on the abundance of SiO_2 , TiO_2 , and Al_2O_3 . Quartz diorite has a concentration of SiO_2 between 56 to 62, TiO_2 around 0.8 ± 0.06 and Al_2O_3 greater than 16 percent by weight. In contrast, granodiorite has a concentration of SiO_2 between 66.5 to 68.5, TiO_2 around 0.5 ± 0.02 and Al_2O_3 less than 15.3 percent by weight.

Chondrite-normalized trace element plots for representative samples of plutonic rocks throughout the Rocky Top area are shown in Figure 15. All the rocks display moderate light rare-earth element enrichment. The trace elements from Rocky Top, Sardine Creek, and Detroit Dam have essentially the same values, and lack a pronounced Eu anomaly. The rocks from the Detroit Dam have a somewhat larger range of trace elements which can be attributed to the range of SiO_2 in five intrusive stages compared to just two at Rocky Top and Sardine Creek. The Eu values can be attributed to feldspar fractionation of plagioclase over the range in SiO_2 composition of these rocks. Similarly, the decrease in Sc with differentiation to higher SiO_2 can be attributed to the fractionation of pyroxene, hornblende, or Fe-Ti oxides.

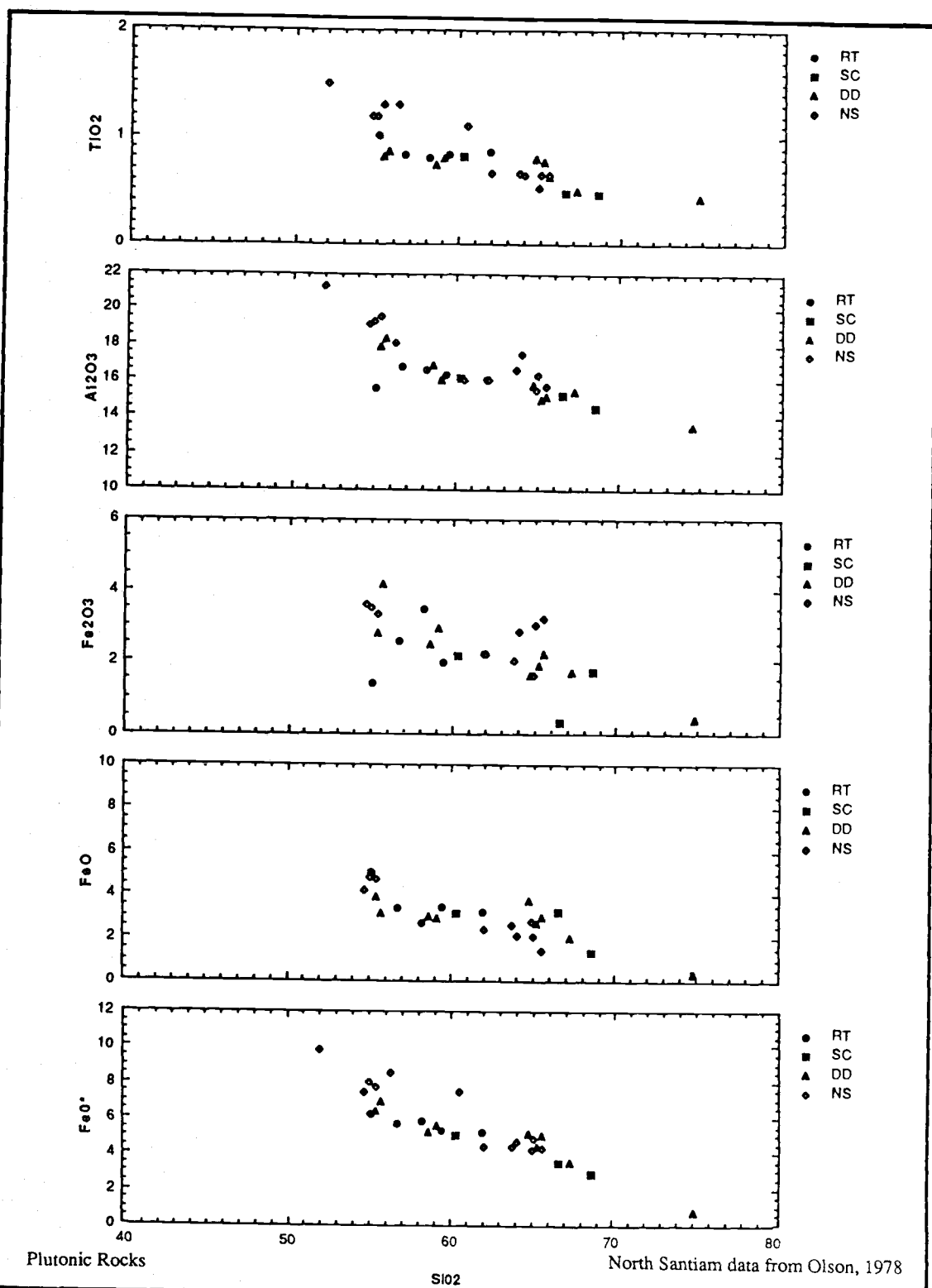


Figure 14: Silica variation diagrams of major oxide components for plutonic rocks.

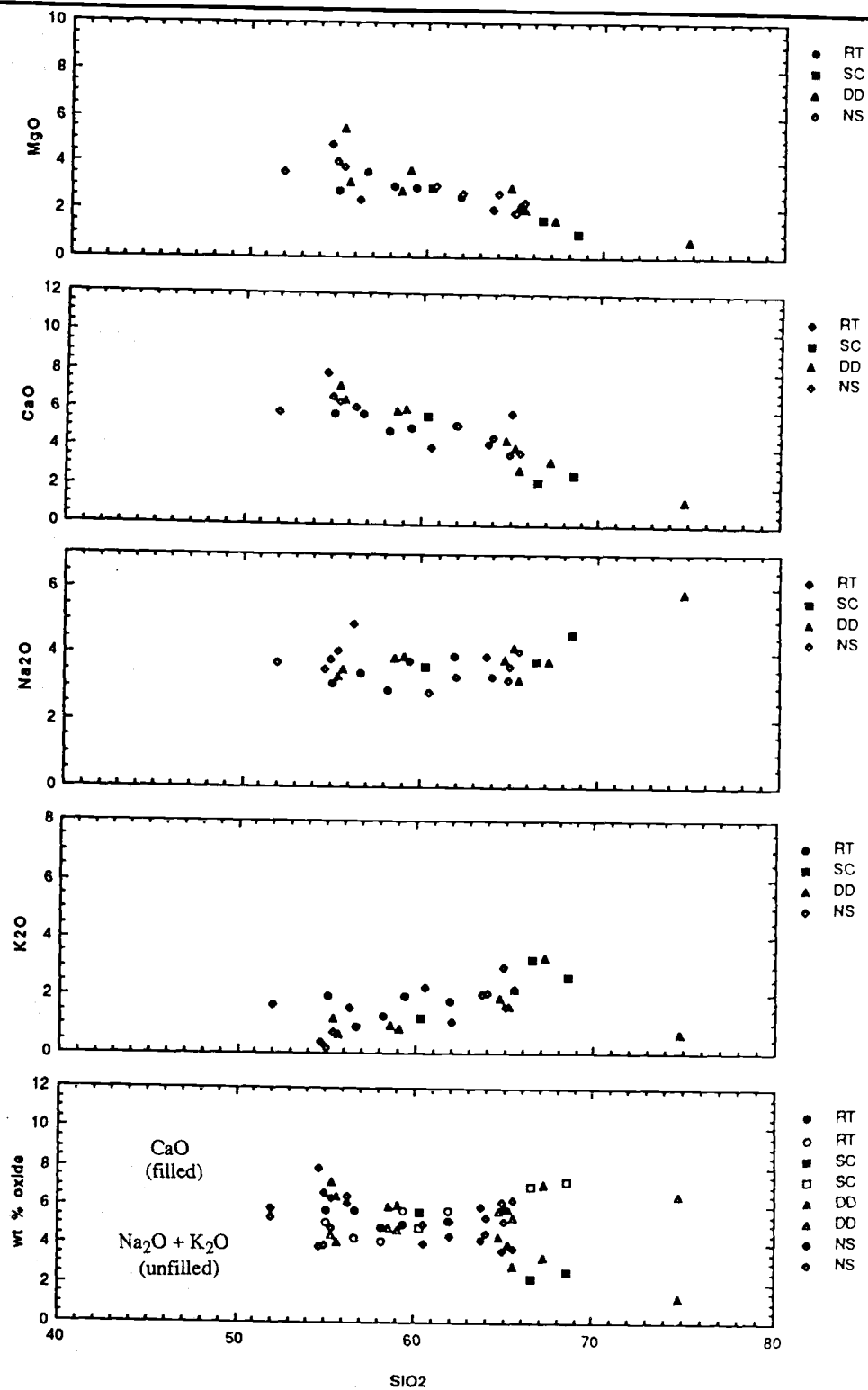


Figure 14: continued

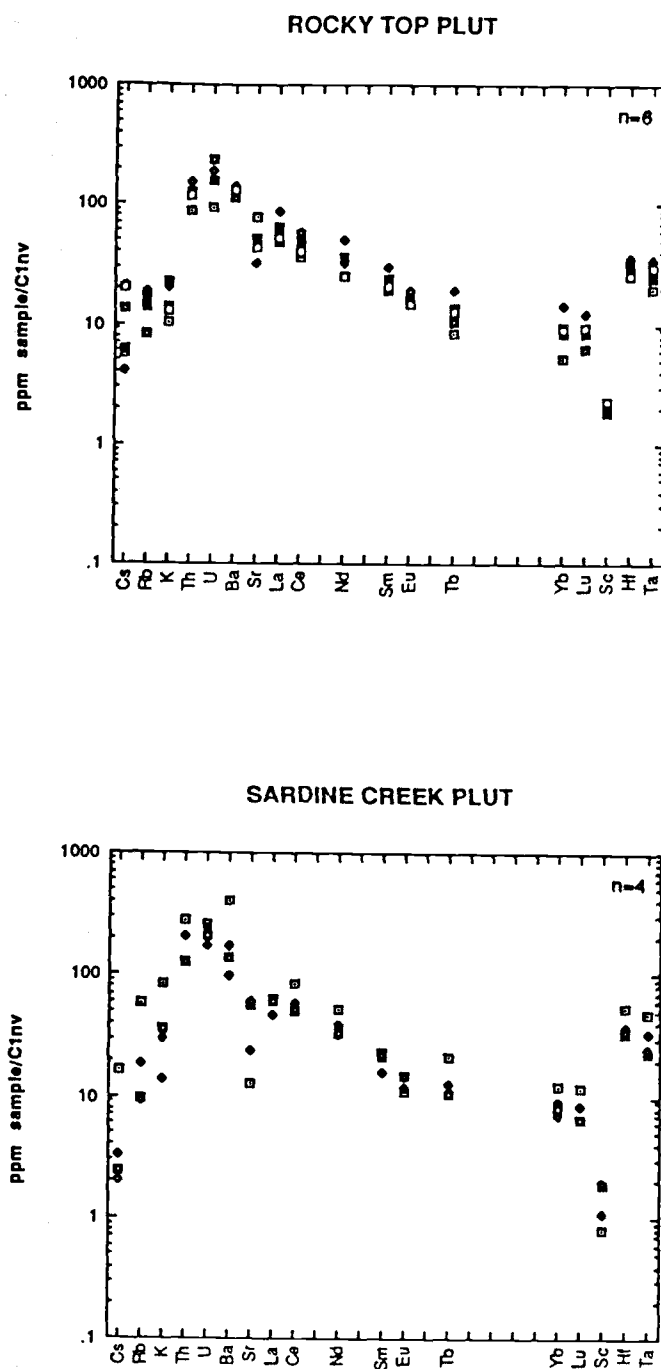
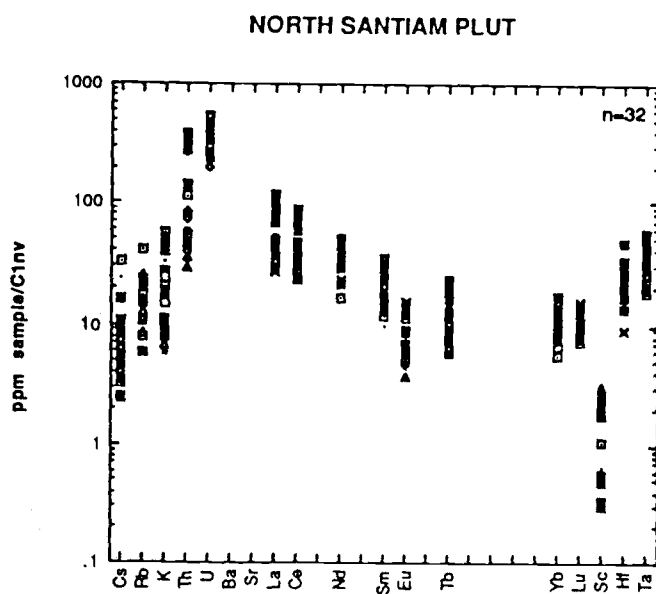
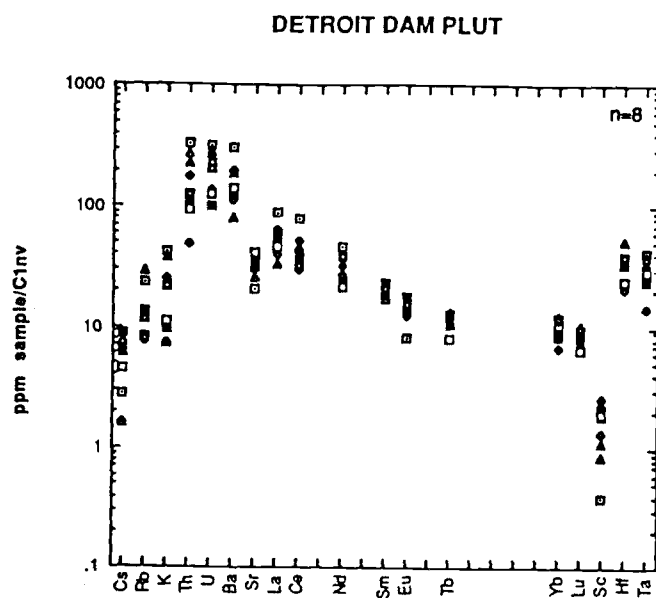


Figure 15: Chondrite-normalized trace element plots for plutonic rocks.



North Santiam data from Pollock, 1985

Figure 15: continued

DISCUSSION

The majority of intrusive rocks exposed in the Rocky Top area are sharp-walled dikes having shapes and distribution that are chiefly controlled by northwest-striking faults and fractures. Although the plutonic rocks are widespread within the area, their distribution and orientation display a definite spatial pattern. More than 90 percent crop out within the northwest-trending central zone. Dikes of pyroxene quartz diorite intrude middle Miocene (Tuel) and older volcanic units, whereas those of hornblende granodiorite can only be demonstrated to intrude rocks of early Miocene age (Tus). However, the hornblende granodiorite intrusions within the Rocky Top area are inferred to be younger than quartz diorite dikes based on the cross-cutting relationships exposed at the nearby Detroit Stock (Curless and others, 1990).

Stratigraphic reconstruction from Sardine Creek to Rocky Top, combined with fluid inclusion data, suggests that the intrusions of hornblende granodiorite composition were emplaced at a minimum depth of roughly 1000 meters (3520 ft), whereas the older quartz diorites were emplaced at shallower levels. If volcanic activity was associated with the intrusions, the unit most similar, with respect to timing and composition, is the andesite sequence of Rocky Top (Tart).

Plutonic rocks within the Rocky Top area are spatially and temporally associated with hydrothermal mineralization. The intrusions are inferred to range in age from roughly 10 to 14 million years old based on whole-rock K-Ar age determinations of 9.9 ± 0.2 million years from the Detroit Stock (Walker and Duncan, 1989); and 12.5 ± 0.2 million years from the Sardine sequence (Verplanck, 1985), which is intruded by quartz diorite and granodiorite. These dates most likely represent hybrid ages between plutonism and volcanism, respectively, combined with the age of hydrothermal mineralization. The 12 million year date from Verplanck (1985) records an age between

Sardine volcanism (>22 my) and hydrothermal mineralization (<12 m.y.) associated with the plutonic rocks. The emplacement of intrusive rocks is the last recognizable magmatic event to occur in the area that clearly pre-dates hydrothermal mineralization. If intrusive activity preceded hydrothermal alteration by one to two million years (Power and others, 1981), then a maximum age of 14 million years should be considered for the plutonic rocks. On the other hand, the 10 million year date from the Detroit Stock (Walker and Duncan, 1989) should be considered a minimum age for the plutonic rocks because of closely associated hydrothermal alteration (Curless and others, 1989, 1990).

SURFICIAL DEPOSITS

A large part of the Rocky Top area is covered by a relatively thin layer of unconsolidated surficial deposits that effectively obscure many bedrock outcrops and contact relationships. These deposits range in age from Pleistocene to recent, and are divided into four map units, which consist of: (1) terrace deposits, (2) glacial drift, (3) colluvium, and (4) alluvium. Apparent offset of surficial deposits by faults was not observed.

DESCRIPTION OF SURFICIAL DEPOSITS

Terrace deposits

Terrace deposits are present immediately south of Rocky Top at elevations of roughly 500 to 1000 meters (1600-3200 ft) and generally 200 to 600 meters (600-2000 ft) above the present channel of the North Santiam River. They are poorly exposed and typically confined to the shallowly dipping slopes associated with the broad valley stages of the North Santiam River as described by Thayer (1934, 1939). In the best exposures, terrace sediments usually consist of a basal gravel and lag concentrate which grades irregularly upward into sand and silt. These deposits range up to five meters in thickness, and are highly dissected by annual and perennial streams. Locally, the terrace deposits may include older colluvium, alluvium, and glacial drift.

Glacial drift

Glacial deposits in the Rocky Top area consist of variably sorted unstratified till, and moderately sorted, stratified deposits of outwash. These deposits can be divided into younger and older groups based on the extent of weathering, clast source area, and

relationship to present topographic features. Younger glacial deposits with clasts of a local origin are relatively well-exposed, generally limited to elevations greater than 1200 meters (4000 ft), and are commonly associated with several north-facing cirques in the headwaters of Elkhorn Creek. In contrast, older glacial deposits are poorly exposed, contain exotic clasts, and are limited to the tops of previously described terraces. The older glacial deposits are not easily distinguished from other surficial deposits associated with these terraces, and are therefore mapped as part of the terrace deposit unit.

Colluvium

Colluvium consists of locally derived deposits of unconsolidated and poorly sorted talus and mixed soil and rock. Recent accumulations are mapped at the base of the western escarpment (sections 16 and 21, T9S R4E) and south of Rocky Top, where they overlie the oldest terrace deposits. Other minor deposits of talus are present at the base of cliffs in the Elkhorn Creek watershed.

Alluvium

Recent stream sediments consist of unconsolidated and variably sorted sand and gravel. Locally, these deposits may include minor well-sorted material related to recent glaciation. Alluvial deposits range widely in apparent development from a thin veneer in Sardine and Elkhorn Creeks to an extensive network of sand and gravel bars along sections of the North Santiam River.

DISCUSSION

The downcutting of the North Santiam River to its present level was a relatively long process which undoubtedly was interrupted by periods of lateral erosion or

sediment accumulation. One of the oldest terrace benches at Rocky Top is capped by the unaltered Southern basalts. These basalts are chemically and mineralogically similar to the Pigeon Prairie lavas of Rollins (1976), which form intracanyon flows and crop out on a perched terrace about 15 km upstream from Rocky Top. Priest (1989, 1990) reports a 0.5 ± 0.05 million year K-Ar age determination from an intracanyon flow near Pigeon Prairie. Assuming a range in age from 1.6 to 0.5 million years for the Southern basalts, then the North Santiam River has thus been incised roughly 600 meters (2000 ft) to its present level at a rate of between 35 to 120 centimeters per 1000 years.

Sherrod (1986) reports incision rates up to 33 centimeters per 1000 years.

Downcutting, and preservation of older surficial deposits, most likely occurred in response to the uplift of the Western Cascades relative to the High Cascades, which in the region surrounding Rocky Top started about five million years ago (Priest and others, 1983).

STRUCTURAL GEOLOGY

The structural development of the Western Cascades in the region surrounding Rocky Top is well-documented but poorly constrained. This can be attributed to the complicated and irregular distribution of most volcanic units, as well as to problems generated by insufficient exposure and the effects of hydrothermal alteration.

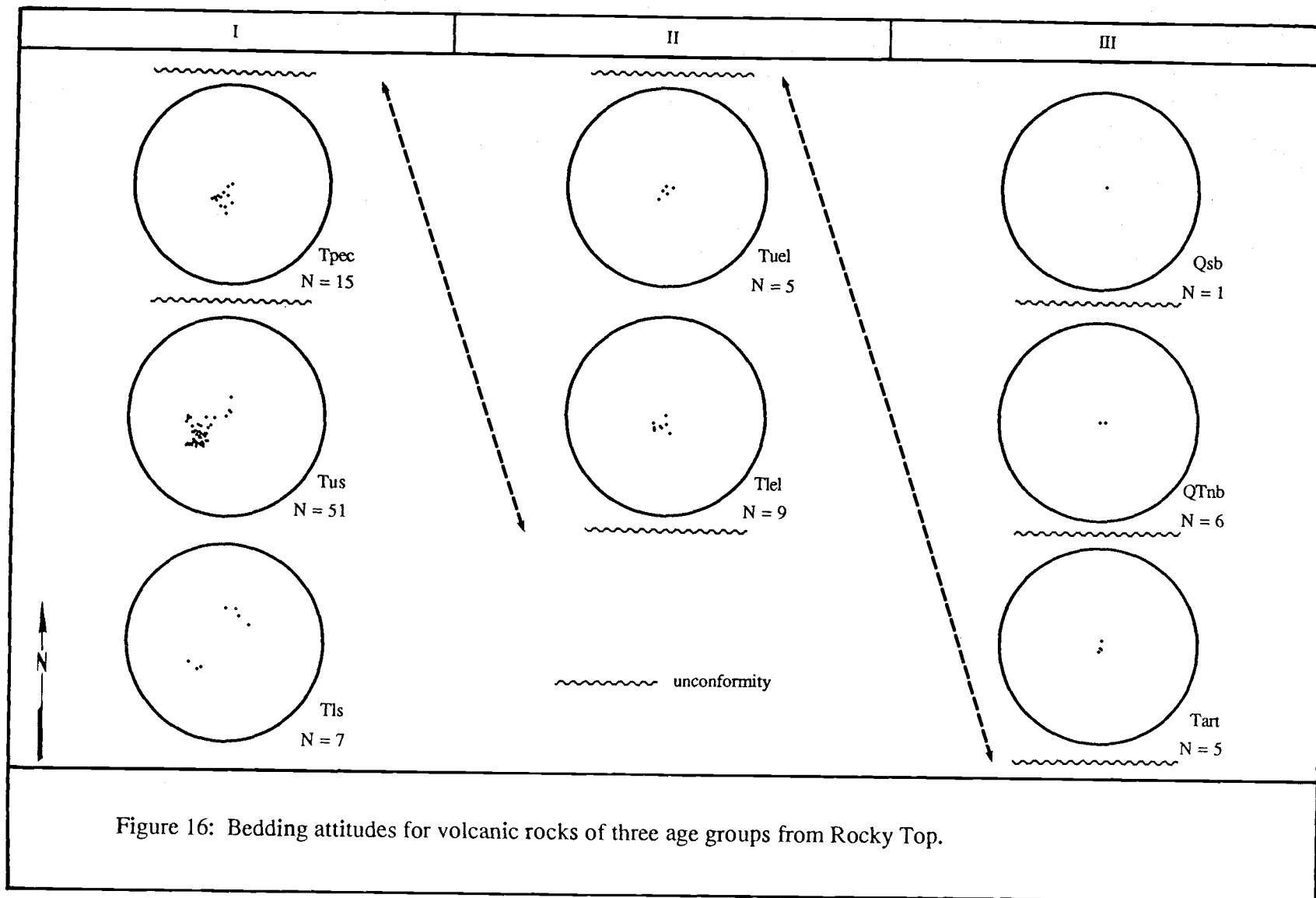
The generally poor exposure, created by numerous unconsolidated surficial deposits and abundant vegetation, makes it difficult to correlate rock units over any large area. Likewise, the lack of regionally extensive units leads to difficulties in understanding regional stratigraphic relationships, which in turn complicates structural interpretations.

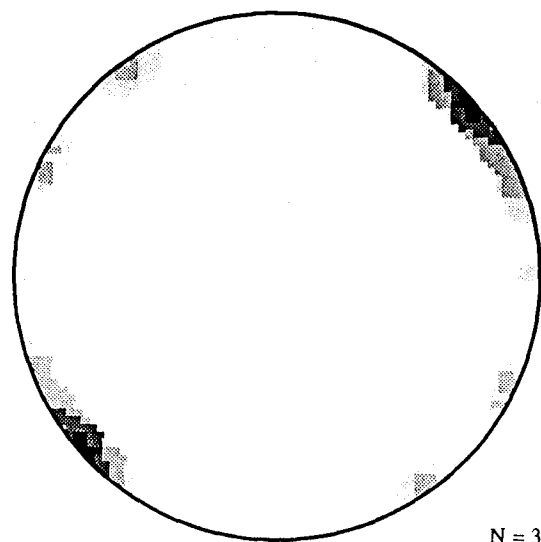
Additional problems emerge in areas where faults and fractures served as pathways for hydrothermal fluids. Hydrothermal alteration is capable of modifying the original texture, mineralogy, and radiometric age of the surrounding country rocks to such an extent that it is difficult to establish the structural sequence of events in an area.

With these limits in mind, structural data for the Rocky Top area are summarized in Figures 16 and 17. The Rocky Top area is dominated by northwest-striking, generally northeast-dipping strata, and by steeply dipping, northwest-striking faults and dikes. In addition, five important angular unconformities are present in the volcanic section which help place constraints on the structural history of the area.

BEDDING ATTITUDES AND UNCONFORMITIES

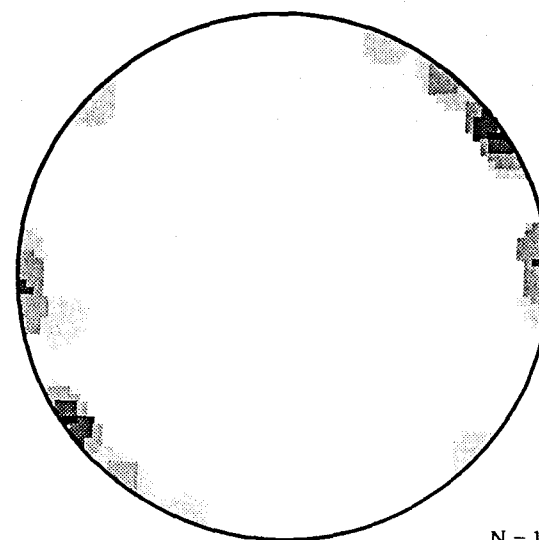
The Rocky Top area contains in excess of 1200 vertical meters (3900 ft) of volcanic rocks which range from late Oligocene to Pleistocene in age. These rocks are





N = 38

Faults (%)



N = 17

Dikes (%)

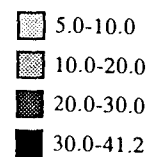


Figure 17: Contoured poles to planes for faults and dikes at Rocky Top.

divided into three age groups separated by angular unconformities (Fig. 16) that may be recognized in the field.

Bedding attitudes from the three age groups of volcanic rocks within the Rocky Top area are summarized in Figure 16. These lower-hemisphere equal area projections display the data for poles to bedding planes. A shallowing of dips with respect to age can be demonstrated as follows: Group I rocks generally strike N40° to 60°W and dip up to 40°NE. Group II rocks strike from N10° to 40°W and have dips from 15°NE to horizontal. Group III rocks all have roughly horizontal attitudes.

There are at least five separate unconformities between volcanic units in the Rocky Top area as summarized in Figure 16 and on Plate 1. All provide relative age constraints on the timing of deformation, intrusion, hydrothermal mineralization, and uplift. The youngest unconformity overlain by volcanic rocks is found at the base of the Southern basalts, which form intracanyon flows on a terrace within the study area. The next oldest unconformity is found at the base of the Northern basalts. This unconformity records the first significant post-mineralization incision in the area. This interpretation is based on the observation that the next oldest volcanic unit, the hydrothermally altered andesite sequence of Rocky Top (Tart), is the highest ridge capping unit in the area. The remaining unconformities are found within the Miocene section. They record the end of emplacement of plutonic rocks, and hydrothermal mineralization, as well as progressive tilting within the section.

FAULTS AND DIKE ORIENTATIONS

The most prominent structural features in the Rocky Top area are northwest-trending faults. However, a subordinate set of contemporaneous northeast-trending faults are present. Northwest-trending faults have been reported throughout the entire

Western Cascades (Callaghan and Buddington, 1936). The faults within the Rocky Top area, according to map unit offsets, have only small amounts of dip-slip displacement, up to 24 meters (80 ft). Strike-slip displacement cannot be determined with certainty. Fault planes are generally steep to vertical (Fig. 17), and slickensides occur in all orientations.

The Rocky Top area is cut by two northwest-trending fault zones which are separated by an area in which the volcanic rocks of the Sardine sequence have been tilted in excess of 40°. These high-angle faults separate the Rocky Top area into thirds, which are designated the southwest, central, and northeast structural areas. Bedding attitudes in each of these areas change consistently within the Sardine sequence as illustrated in Plate 1. The southwest fault zone is informally named the Rocky Top Fault Zone, whereas the northeast fault zone is informally named Elkhorn Creek Fault Zone.

The Rocky Top Fault Zone localized Miocene intrusions and channeled associated hydrothermal fluids. This fault zone cuts the upper member of the Sardine sequence and is intruded by quartz diorite, which was subsequently mineralized. Post-mineralization fault movement has been minor, and the fault zone apparently does not offset Pleistocene terrace deposits. Curlless and others (1990) have suggested that this fault zone continues southeast toward the Detroit Dam area, based on the presence of a pronounced lineament, exposures of northwest-trending faults, and distribution of intrusive rocks. In addition, a pronounced northwest trend in depleted $\delta^{18}\text{O}$ (after Taylor, 1971) is shown in Figure 18. This isotopic anomaly suggests that the Rocky Top and Elkhorn Creek Fault Zones extend toward the Detroit Dam area and were responsible for the localization of hydrothermal mineralization.

The Elkhorn Creek Fault Zone separates the central and northeast areas. This fault zone has a similar strike, dip, and association with nearby intrusions and local

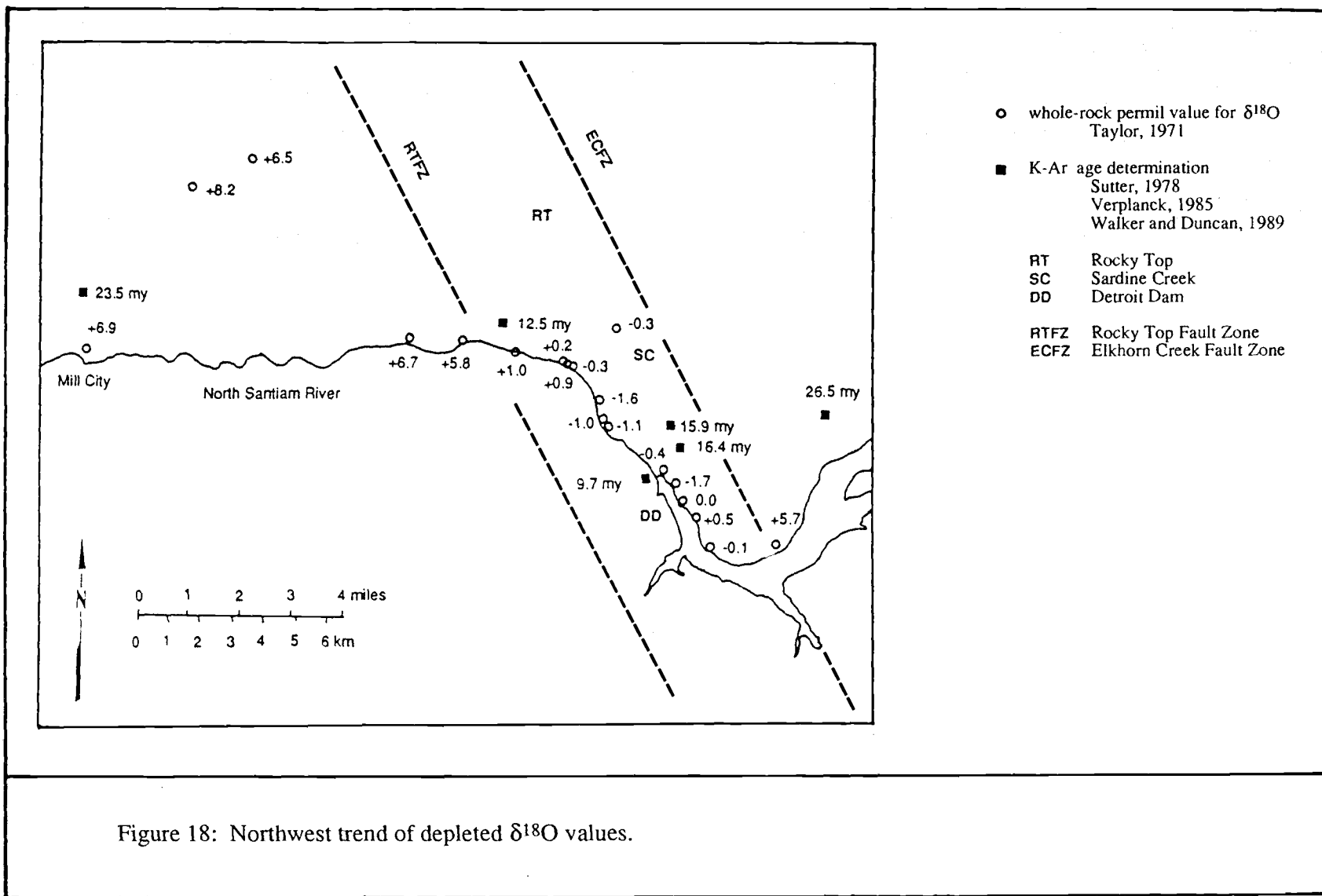


Figure 18: Northwest trend of depleted $\delta^{18}\text{O}$ values.

hydrothermal mineralization as the Rocky Top Fault Zone. An important difference, however, is that the Elkhorn Creek Fault Zone cuts rocks as young as the upper member of the Elk Lake sequence.

The minimum vertical offset across the Elkhorn Creek Fault Zone is roughly 24 meters (80 ft) as inferred from the outcrops located in sections 13 and 24 (T9S R4E). Displacement along this fault zone took place before and after the deposition of the Elk Lake sequence. Because the oldest lava flows of the Northern basalts are not offset where they cross the projected trace of one of the main Elkhorn Creek faults, movement along this zone had stopped by Pliocene time.

Both the Rocky Top and Elkhorn Creek Fault Zones can be traced more than 15 kilometers northwest from Rocky Top through Elkhorn Ridge to Sweet Springs Mountain and Panther Rock, and probably 40 kilometers farther northwest toward the town of Mt. Angel.

Quartz diorite and granodiorite dikes of probable late Miocene age intrude volcanic rocks as young as the upper Elk Lake sequence. They range in width from one to 10 meters, and have steep to vertical dips. The strikes and dips of the dikes are contoured on the lower-hemisphere equal area projection in Figure 17. Nearly all the dikes strike between northwest and north-south, and about one-half have a N40° to 50°W strike. The average strike is similar to those of the major fault zones running through the area.

UPLIFT

Various workers have argued that the deep incision of modern streams is the best evidence for uplift of the Western Cascades (Sherrod, 1986; Priest, 1989,1990; Taylor, 1989, 1990). The largest rivers in the Western Cascades are the westward flowing North Santiam and McKenzie Rivers. Both drainages have around one kilometer of

relief in their eastern sections, which decreases to zero at the Willamette Valley (Priest, 1989, 1990). Downcutting most likely occurred in response to the uplift of the Western Cascades relative to the High Cascades, which in the region surrounding Rocky Top started about five million years ago (Priest and others, 1983).

Rocky Top (elev. 1529 m, 5014 ft) is the highest point in the Rocky Top area and is capped with horizontal and weakly altered andesites (Tart). The lowest point in the area is occupied by the North Santiam River (elev. 305 m, 1000 ft). Total relief within the Rocky Top area thus exceeds 1200 meters (3900 ft). The flat-lying andesite sequence of Rocky Top represents the youngest volcanic unit that caps the highest ridge in the Rocky Top area. There is no significant sign of erosion between flows, nor intracanyon relationships in this sequence. These rocks are somewhat younger than the intrusive rocks in the area. An important inference is that the andesite sequence of Rocky Top is older than five million years in age. This is based on the fact that the youngest ridge-capping volcanic rocks in the Western Cascades range in age from 4.5 ± 0.3 million years (Verplanck, 1985) to 5.13 ± 0.01 (Priest and others, 1988), and younger volcanic rocks are found as intracanyon flows (Priest, 1989, 1990). The two stratigraphically younger volcanic units in the Rocky Top area, the Northern and Southern basalts, are found as intracanyon flows.

Terrace deposits, which record the progressive downcutting by the North Santiam River, are present immediately south of Rocky Top at elevations of roughly 500 to 1000 meters (1600-3200 ft) and generally 200 to 600 meters (600-2000 ft) above the present stream channel. One of the oldest terrace benches at Rocky Top is capped by the unaltered Southern basalts. These basalts are chemically and mineralogically similar to the 0.5 ± 0.1 (Priest, 1989, 1990) million year old Pigeon Prairie lavas of Rollins (1976), which form intracanyon flows about 15 km upstream from Rocky Top. If the Southern basalts thus range from 1.6 to 0.5 million years in age, then the North Santiam

River has incised its last 600 meters (2000 ft) at a rate of between 35 to 120 centimeters per 1000 years. Sherrod (1986) reports incision rates up to 33 centimeters per 1000 years in the Kitson Ridge area (Oakridge Quadrangle) of the Western Cascades, approximately 100 kilometers south of Rocky Top.

DISCUSSION

The tectonic history of the Rocky Top area is complex because of the superposition of several events, including regional deformation, faulting, emplacement of plutonic rocks, and hydrothermal activity. The oldest rocks exposed in the area have been tilted up to 40° , and are separated from younger rocks by an angular unconformity. Major northwest-striking faults acted as structural boundaries which accommodated displacement between blocks. Deformation was largely complete by the time that the non-deformed, ridge-capping andesite sequence of Rocky Top was emplaced.

Bedding attitudes from the Rocky Top area show that the structure of this region is more complex than previously described (Thayer, 1934, 1936, 1939; Peck and others, 1964). The Rocky Top area is located within a zone of folds defined by Thayer (1934, 1936, 1939). However, no evidence exists for compressional folds with northeast trends in the thesis area. Northeast-trending folds are not supported by the data for bedding attitudes. Also, if the northwest strikes and northeast to southwest dips in Group I volcanic rocks are fold related, then the fold axes trends about $N40^\circ W$ and plunge shallowly. This is orthogonal to the northeast-trend of folds in the region discussed by Thayer (1934, 1936, 1939) and Peck and others (1964).

The age of the structures can be inferred from the stratigraphic relationships observed from the flanks of Rocky Top. Although tilting in the region may have begun prior to the onset of Sardine volcanism, it is apparent that the lava flows of the upper

member of the Sardine sequence have been deformed to some extent by the northwest-striking faults. These and older volcanic strata were involved in faulting and tilting prior to the deposition of the less deformed pyroclastic sequence of Elkhorn Creek. In contrast, the relatively flat-lying flows of the andesite sequence of Rocky Top overlie older units across an angular unconformity, and show no evidence of having been significantly faulted or folded. Therefore, faulting and tilting of the volcanic rocks most likely started before the early Miocene and ended around the late Miocene.

Nakamura (1977) showed that changes in the principal stress directions can be inferred from dike orientations and structural relationships. The orientation of dikes in the Rocky Top area indicates intrusion into tensional fractures oriented in a northwest-southeast direction; or intrusion along steeply-dipping NW and NNE-trending faults with predominantly strike-slip motion. According to Sherrod and Pickthorn (1989), dikes with similar orientations were emplaced in the Western Cascades about 18 to 12 million years ago.

There is no evidence that the Willamette Valley has undergone enough subsidence or incision during the last five million years to cause one kilometer of downcutting by streams within the Western Cascades (Priest, 1989, 1990). The entrenchment of streams in the Western Cascades cannot be explained by lowering of a base level represented by the sea, because the sea has been absent from the mouths of Western Cascade streams since early Miocene time (Priest, 1989, 1990). The Rocky Top area was thus uplifted at some time after hydrothermal mineralization ceased (10-12 my). The relationships between ridge-capping, and intracanyon volcanic rocks suggest that the North Santiam river started to entrench during the Pliocene. Distribution of surficial deposits shows that downcutting continued to roughly 600 meters (2000 ft) above the present North Santiam channel during the Pleistocene after which the channel was

incised to its present level. Most of the uplift in the Rocky Top area has thus occurred within the last two million years.

Although the interpretation presented above differs from the work of Thayer (1934, 1936, 1939), and Peck and others (1964); the timing of fault movements, tilting, and uplift within the Rocky Top area appears to be similar to the structural relationships in the Hoover Ridge area near Detroit as described by Priest and others (1987).

HYDROTHERMAL MINERALIZATION

Previous studies of the distribution and character of hydrothermal mineralization in the Western Cascades are largely confined to historically productive mining districts; hydrothermal mineralization in adjacent non-productive areas remains largely undocumented. Zones of hydrothermal alteration and metallization within the Rocky Top area represent lateral and vertical extensions of hydrothermal mineralization associated with the Detroit Stock (Curless and others, 1990). Although hydrothermal mineralization is weakly developed in most areas at Rocky Top, it is locally intense near structures and shows a distinct temporal and spatial relationship to intrusions of intermediate composition. The Rocky Top area is not located within an historic mining district, although it does contain some distinctive characteristics of other districts in the Western Cascades.

HYDROTHERMAL ALTERATION

Following the nomenclature of Meyer and Hemley (1967) hydrothermal alteration assemblages defined in the vicinity of Rocky Top are propylitic, potassic, sericitic, and argillic. The general pattern of hydrothermal alteration is characterized by an early widespread propylitic zone with a potassic component missing. Later overprinting by structurally controlled sericitic and argillic alteration are present locally. Altered areas are generally confined between, and distributed along, the northwest-striking Rocky Top and Elkhorn Creek Fault Zones.

The main secondary mineral assemblages of hydrothermal alteration in the vicinity of the Rocky top area are listed in Table 3. These alteration assemblages are described as a cumulative of all rock types, and reflect the presence of gradational boundaries and

TABLE 3: Mineralogy of pervasive hydrothermal alteration assemblages.

Pervasive alteration	Feldspar sites	Mafic sites	Fe-Ti oxide sites	Groundmass	Characteristic assemblage
Propylitic	[feldspar] \pm albite epidote \pm calcite sericite	[Px, Hb, Ol] chlorite (epidote)	hematite \pm pyrite (rutile)	chlorite \pm epidote calcite \pm quartz \pm pyrite (rutile)	chlorite-epidote calcite \pm pyrite
Potassic	(K-feldspar)	HT biotite \pm magnetite [Px, Hb]	magnetite \pm pyrite (\pm chalcopyrite)	HT biotite \pm magnetite (K-feldspar) \pm Py (Cp)	HT biotite (K-feldspar) \pm Mt \pm Py \pm (Cp)
Sericitic mod.-str.	sericite [plagioclase] \pm calcite	sericite [chlorite] pyrite	pyrite \pm rutile \pm hematite	quartz sericite \pm Py \pm calcite (\pm chlorite \pm rutile)	quartz-sericite \pm Py (\pm chlorite \pm rutile)
intense		no relict texture		quartz sericite \pm Py (\pm rutile)	quartz-sericite \pm Py (\pm rutile)
Argillic mod.-str.	[plagioclase] clay minerals quartz	[chlorite] clay minerals	\pm pyrite	clay minerals quartz \pm sericite \pm Py (\pm rutile)	clay minerals quartz \pm Py (\pm rutile)
intense		no relict texture		clay minerals (\pm quartz \pm Py)	clay minerals (\pm quartz \pm Py)

() minor phase

[] relict phase

compositional complexities in intensely mineralized areas. Note that the alteration mineralogy within each assemblage is influenced by the primary composition of the host rock. Each assemblage may contain minerals reflecting incomplete establishment of equilibrium, or of the subtle overprinting by younger events. All assemblages are likely to reflect the combined effects of shallow burial of the volcanic pile, intrusion of plutonic rocks, subsequent hydrothermal mineralization, and chemical weathering.

Propylitic alteration is weakly pervasive throughout most rocks in the area and intensifies with proximity to faults, fractures, and intrusions. The assemblage is characterized by a secondary mineral assemblage of epidote + chlorite + quartz + sericite \pm calcite \pm albite \pm hematite \pm magnetite \pm pyrite, that is not texturally destructive. In hand specimen, propylitically altered rocks are various shades of pistachio to olive green, depending on the absolute and relative amounts of epidote and chlorite. Epidote and calcite replace the cores of normally zoned plagioclase phenocrysts, and sodic rims are selectively replaced by sericite. Hornblende and pyroxene are partially replaced by chlorite and magnetite. Propylitically altered rocks are also characterized by parallel-walled veinlets containing calcite, epidote, or quartz. Where propylitic alteration is most intense, pyrite is present as disseminated crystals, aggregates, or isolated clots. Pyrite-bearing rocks average less than one percent by volume of the sulfides, and occasionally may contain up to five percent by volume sulfide with intense propylitic alteration.

Potassic alteration is present three kilometers southeast of the Rocky Top area at the Detroit Stock, where several samples contain incipient veinlets and diffuse replacement zones of hydrothermal biotite (Curless and others, 1989, 1990). The potassic assemblage at the Detroit Stock is characterized by hydrothermally added biotite + magnetite \pm potassium feldspar \pm pyrite \pm chalcopyrite. Primary hornblende and pyroxene are pseudomorphed by clots and aggregates of secondary biotite. Individual potassium silicate selvages associated with quartz-magnetite veinlets may be as wide as

two centimeters, but locally coalesce to form zones of pervasive wall-rock alteration. Magnetite is the dominant opaque mineral; it is present as disseminated crystals in the groundmass and also as intergrowths with secondary biotite as well as in quartz veinlets. Pyrite, and to a lesser extent chalcopyrite, are also present in veinlets and as widespread disseminations. Potassic alteration grades outward into weak propylitic alteration, with hornblende phenocrysts surrounded by reaction rims of chlorite and magnetite, and weak sericitic alteration of plagioclase phenocrysts. Pervasive potassic alteration of the Detroit Stock can be observed in the vicinity of Cumley Creek (Sec 7 T10S, R5E), although late-stage sericitic and argillic alteration have somewhat overprinted the early hydrothermal minerals with sericitization of secondary K-feldspar and chloritization of secondary biotite.

The sericitic assemblage is characterized by quartz + sericite \pm pyrite \pm chlorite \pm rutile. The degree of sericitic alteration ranges from incipient, in which trace amounts of sericite replace feldspars, to intense, where the rock is completely replaced by quartz + sericite \pm pyrite and the original texture of the rock is destroyed. In hand specimens, sericitically altered rocks are pale gray-green to bleached tan-brown in color.

Petrographically, these rocks contain feldspar partially to completely replaced by sericite, with mild to strong silicification of the groundmass. Pyrite is considerably more abundant in sericitically altered rocks than in those affected by propylitization. Whereas propylitically altered rocks average about one percent by volume pyrite, rocks which have been sericitically altered commonly contain two to five percent by volume and locally up to 10 volume percent sulfide. Pyrite is the principal opaque mineral, and in areas of strong sericitic alteration the only Fe-Ti oxide is trace amounts of rutile; magnetite is completely destroyed. The distribution of sericitic alteration is locally controlled by fractures and the margins of dikes. The outer limits of sericitic alteration fade transitionally into the zone of older propylitic alteration.

Advanced argillic alteration is characterized by the replacement of plagioclase feldspar and mafic minerals by quartz, sericite, and clay minerals. Intense argillically altered rocks are almost entirely replaced by clay minerals. Argillic alteration is structurally controlled, variable in intensity, and overprints all earlier assemblages. It is both mineralogically and texturally destructive. Hand specimens representative of this alteration type are characterized by a bleached tan-white color. Pyrite is present in some of the argillically altered rocks, where it replaces primary mafic minerals as single crystals or aggregates that are scattered through the groundmass. Minor amounts of hypogene (?) barite are occasionally associated with this assemblage as veinlets up to five millimeters in width.

Cross-cutting and overprinting relationships between hydrothermal mineral assemblages can be documented by tracing weakly altered flows of the upper Sardine into, and commonly across, zones of strong alteration. Bulk rock analyses show chemical trends which reflect minor to major chemical and mineralogic changes in the same unit over tens of meters. Comparison of fresh and assorted alteration mineral assemblages are revealed in Figure 19. Chemical analyses of representative hydrothermally altered rocks are presented in Appendix 5. Petrographically, the amount of early-stage epidote and calcite replacing plagioclase feldspars generally increase with the intensity of hydrothermal alteration. Increasing intensity of alteration is seen as a gradual sericitization of plagioclase feldspar that culminates in clots of sericite with abundant secondary quartz, as well as pyrite replacing magnetite.

VEIN MINERALOGY AND TEXTURES

The assemblage of sulfide and gangue minerals in the Rocky Top area is relatively simple. Sulfide minerals consist of pyrite, galena, sphalerite, and chalcopyrite, with

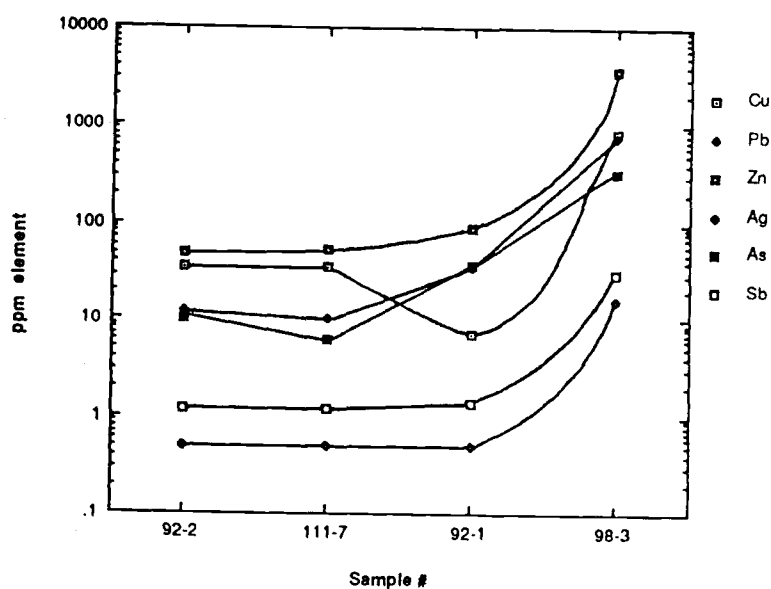
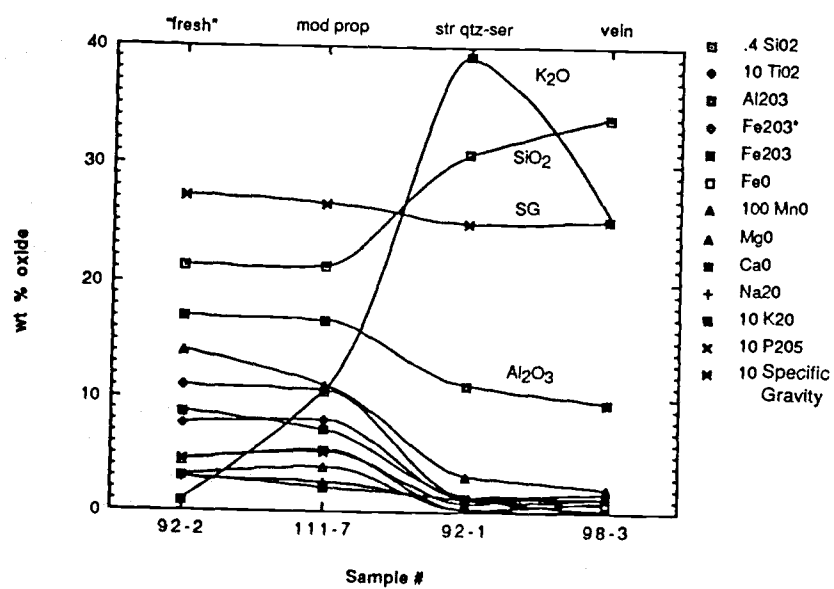


Figure 19: Chemical changes with respect to alteration assemblage.

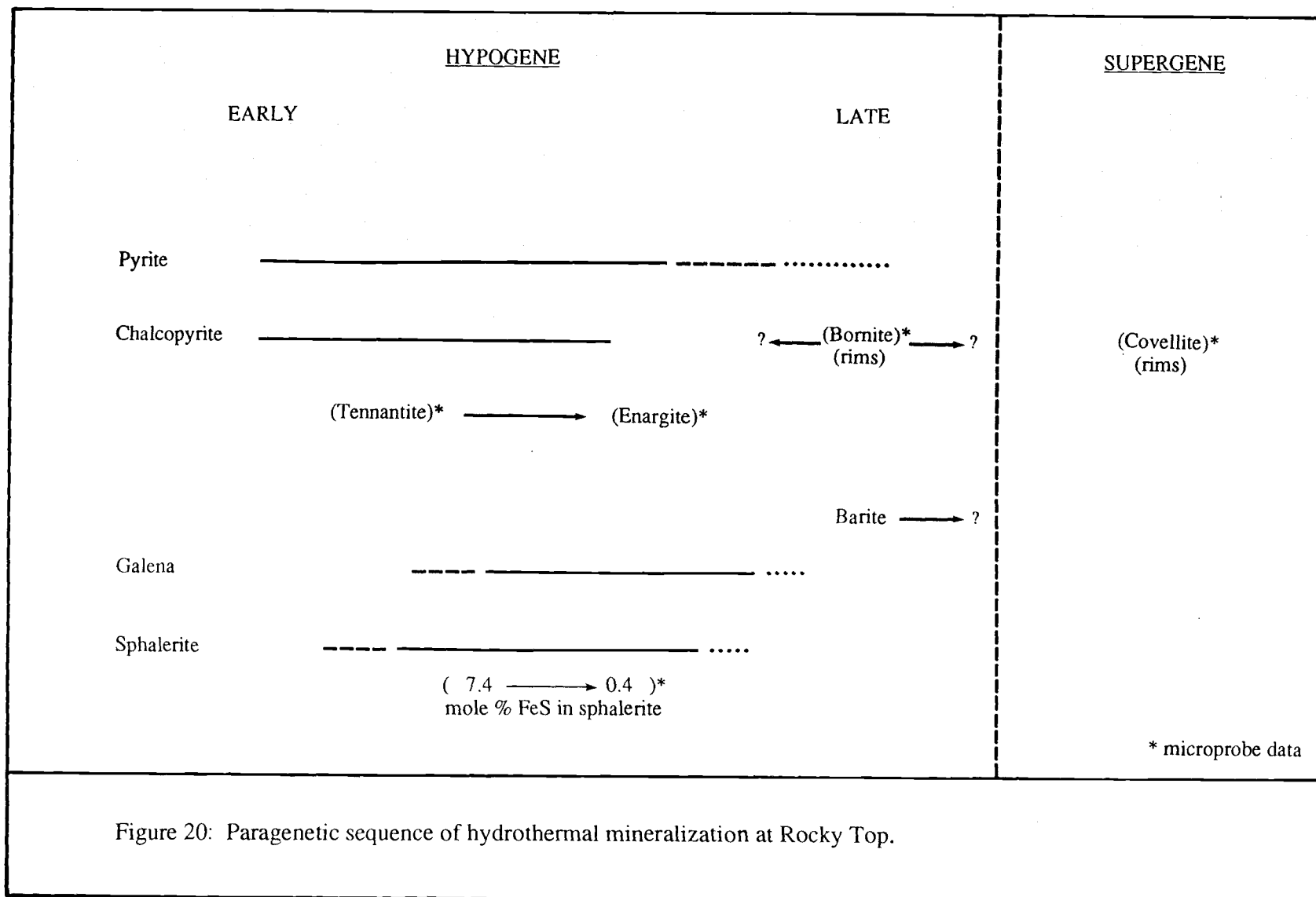
trace amounts of tennantite, enargite, bornite, and covellite. Quartz is the dominant gangue mineral with subordinate amounts of carbonate and barite.

The most well-developed vein mineralization is associated with a broad zone of quartz-sericite alteration near the center of section 15 (T9S, R4E). Although the veins are texturally complex and variable in appearance from one location to the next, they are nonetheless composed of three basic textural elements. These dominant elements are: (1) angular rock fragments which range from equant to tabular in shape, and range from less than one millimeter to several centimeters in size; (2) massive vein material which cements rock fragments; and (3) vuggy veinlets which are generally less than one centimeter in width and range from megascopic tabular open space fillings to microscopic stringers.

The abundances of vein minerals are considerably variable. In most locations, the veins consist primarily of quartz and fragments of wall-rock which contain much less than one percent by volume sulfide minerals. Locally, however, the veins may contain more than 10 percent sulfides, or small veinlets at other localities may consist entirely of barite. Veins may exhibit sharp contacts with the wall rock with no visible sign of a selvage, or selvages of sericite, quartz, and minor pyrite of variable thickness, which may be completely overprinted by later stage sericitic or argillic alteration.

Sulfide minerals are present as open-space fillings of fractures as well as disseminations within the surrounding wall rocks. The paragenesis of sulfur-bearing minerals are presented in Figure 20.

Pyrite is the most abundant sulfide in mineralized zones of the Rocky Top area. Pyrite may be found in quartz veins, or as disseminations with either quartz-sericite or propylitic alteration assemblages. It may also be found as aggregates or cubes up to two millimeters in size or as oxidized limonitic casts of jarosite \pm goethite \pm (hematite).



Sphalerite, galena, and subordinate chalcopyrite are locally abundant in minor amounts in small veins and as disseminations. These minerals are associated with well-developed sericitic alteration in the center of sections 13 and 15 (T9S R4E). Sphalerite occurs as dark red-brown to black crystals, which range up to five millimeters in diameter. It is the only sulfide at Rocky Top that exhibits any noteworthy compositional variation. Iron contents range from 7.4 (early) to 0.4 (late) mole percent FeS. These values represent the compositions of progressively younger sphalerite deposited during hypogene mineralization.

Analyses of 16 sulfide minerals were performed on grain mounts using the Cameca microprobe at Oregon State University. The results are presented in Appendix 6. Thirteen elements per run were detected by wavelength dispersive spectrometers under the following operating conditions: filament voltage = 15 kV; sample current = 20 nA; and beam diameter \approx 2 μ m. Counting time was ten seconds per point for the elements S, Zn, Fe, Cu, As, Ag, (Al, Si, Mg, Na, and K); and 20 seconds per point for Pb, and Au. Each point was corrected for background and matrix effects (ZAF).

SULFUR ISOTOPES

Sulfur isotope analyses were performed on seven mineral concentrates (2 pyrites, 2 sphalerites, 1 chalcopyrite, 1 galena, and 1 barite) separated by hand-picking from four samples collected in the Rocky Top area. Sulfide mineral concentrates were prepared for analyses of sulfur isotopic compositions by combustion with excess CuO to produce SO₂. Mass spectrometric determinations of the resulting sulfur dioxide gases were performed by Global Geochemistry of Los Angeles, California. Sulfur isotope compositions are listed in Appendix 6.

There is minor variation in the $\delta^{34}\text{S}$ values of the sulfides. Sulfide minerals range from +2.8 to -3.3 permil and average about -0.5 permil. Pyrite samples have $\delta^{34}\text{S}$ values of 1.0 and 2.8 permil, and sphalerite $\delta^{34}\text{S}$ values of -0.3 and 0.0 permil. Single analyses of $\delta^{34}\text{S}$ are for chalcopyrite 0.4 permil, and galena -3.3 permil. This relatively narrow range of $\delta^{34}\text{S}$ values near 0 permil is suggestive of a magmatic origin for the sulfur and is consistent with data obtained elsewhere from the Western Cascades (e.g. Power, 1984; Summers, 1990). Sulfur from barite has a composition of +6.7 permil. Assuming isotopic equilibrium was maintained temperatures have been estimated from $\delta^{34}\text{S}$ of coexisting sphalerite and galena that indicate sulfide deposition occurred at 200-220°C, using equations from Field and Fifarek (1985).

FLUID INCLUSIONS

Doubly polished chips between 0.2 to 0.4 millimeters thick were prepared from vein quartz samples, which bracket the depositional sequence of intergrown sulfides within a zone of sericitic alteration (samples 92-1 and 98-3 Section 15, T9S R4E). Three categories of fluid inclusions, up to 50 microns in size, were identified. All are simple two-phase liquid-vapor inclusions at room temperature and have been classified as type-I primary, pseudosecondary, and secondary, according to the criteria outlined by Roedder (1984). Relatively isolated inclusions are interpreted as primary, and those occurring in discontinuous intersecting planes are considered to be pseudosecondary in origin. Both types appear to consist of between 70 and 90 volume percent liquid, contain no daughter minerals, and homogenized to liquid upon heating. No traces of gas hydrates were observed during freezing. Both primary and pseudosecondary inclusions are considered to represent fluids trapped during the growth of the quartz crystals. Inclusions that developed in and along fractures in quartz are interpreted as

secondary. Several of these inclusions were examined, but measurements were not performed on the secondary inclusions that cut across the pseudosecondary inclusions because they were either very small ($< 5 \mu\text{m}$) or large ($> 50 \mu\text{m}$) and showed evidence of necking. Homogenization and freezing temperature measurements of 20 inclusions in quartz were determined twice using a Chaimeca heating and freezing stage. Replicate measurements of homogenization temperatures showed a reproducibility of $\pm 2^\circ\text{C}$ for temperatures under 300°C . The reproducibility of freezing runs was within $\pm 0.2^\circ\text{C}$. Heating rates were roughly 2°C per minute near the temperature of homogenization. Fluid inclusion data are presented in Appendix 7. In addition, homogenization temperature and salinity data are plotted in Figure 21.

Primary and pseudosecondary inclusions in quartz homogenized to liquid over a temperature range between 180 and 250°C (Fig. 21). This temperature range is consistent with previously described isotopic temperature estimates derived from sphalerite and galena. Secondary inclusions gave lower temperatures which clustered around 150°C . Salinity data are based on freezing point depression in the system H_2O - NaCl (Potter and others, 1978). Freezing temperatures range from -0.7 to -3.1°C , and correspond to salinities from 1.2 to 5.1 equivalent weight percent NaCl (Fig 21). The non-pressure corrected temperatures of homogenization reflect cooling of the low salinity hydrothermal fluid bracketing the time of sulfide deposition.

Only liquid-rich fluid inclusions were observed at Rocky Top. The absence of vapor-rich inclusions and lack of other evidence of boiling in the hydrothermal system allows the determination of a minimum estimate of depth and hydrostatic pressure at the time of hydrothermal mineralization. Using data presented by Haas (1971), maximum homogenization temperatures of 250°C and salinities ranging from five to 10 weight percent NaCl yield hydrostatic pressures ranging from 37.1 to 38.6 bars. This corresponds to depths below the water table of around 400 to 425 meters.

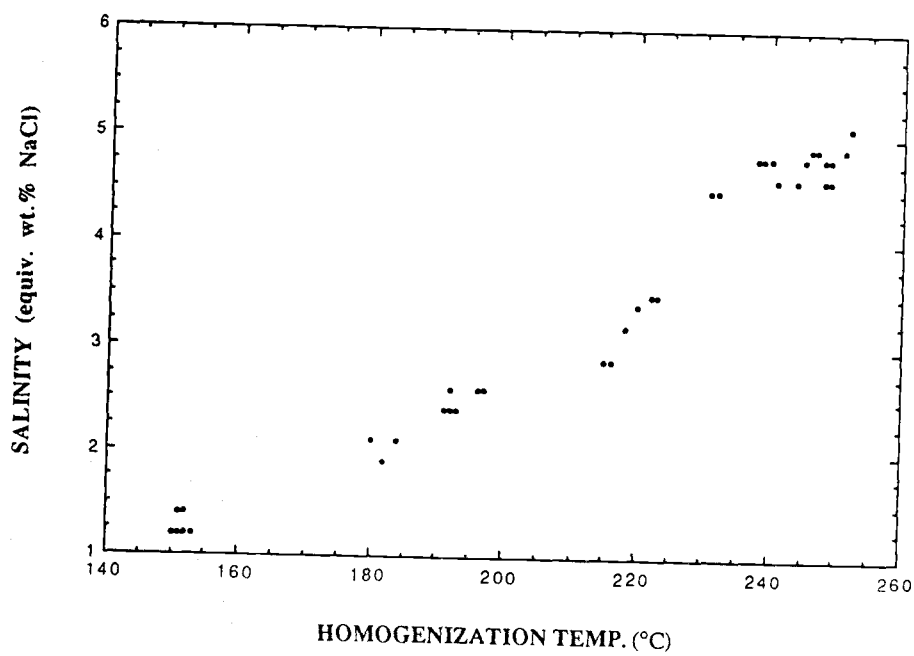
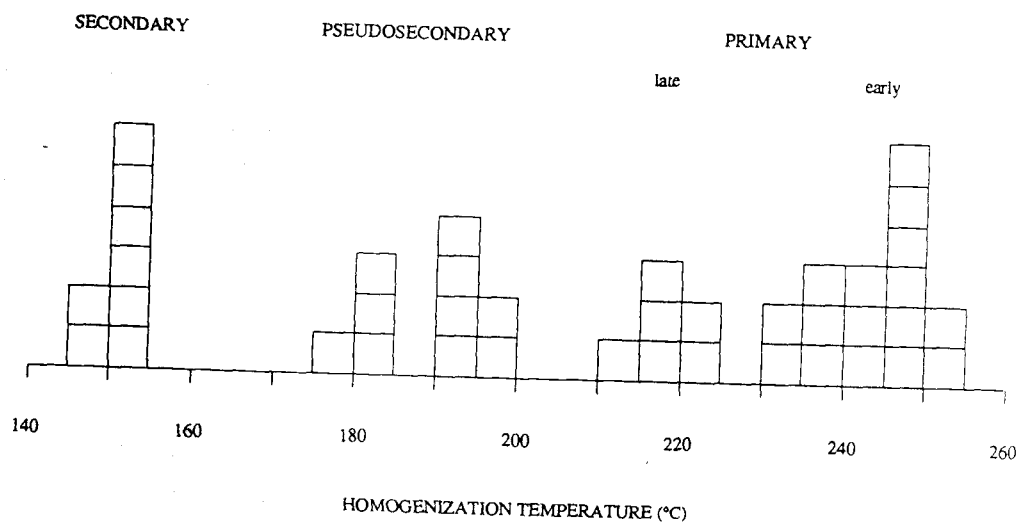


Figure 21: Homogenization temperatures and salinities of fluid inclusions.

TRACE METALS

A total of 84 rock-chip samples from the Detroit Stock, Sardine Creek, and Rocky Top areas were analyzed for Cu, Pb, Zn, and other trace metals. Concentrations range from below detection limit up to 830 ppm Cu, 1330 ppm Pb, 3570 ppm Zn, 16 ppm Ag, 16 ppb Au, and 75 ppm Mo. Threshold values were determined to be 60 ppm Cu, 30 ppm Pb, and 100 ppm Zn. Thresholds were determined from log-probability plots of metal concentrations versus cumulative frequency, as shown in Figure 22. The data were partitioned into background (bk) and mineralized (min) populations following procedures outlined by Sinclair (1976). The inflection point occurs within the central segment of the mixed population curve at a percentile that defines the proportion between of the mineralized and background populations. The curve was partitioned with each population plotting as a straight line. The threshold values were arbitrarily chosen to include one percent of the background population. In other words, samples with metal concentrations above the threshold would be expected to represent the mineralized population in 99 percent of the analyses. Checks were made on the partitioning procedure by calculating ideal combinations of the background and mineralized populations. If the check points matched with the real data curve, a plausible model for the data was obtained by partitioning.

Data for Cu, Pb, and Zn from Rocky Top, Sardine Creek, and Detroit Dam are plotted on ternary diagrams in Figure 23. The data are listed in Appendices 8 (RT), 9 (SC), and 10 (DD). The large symbols represent samples with concentrations above a threshold value for one or more metals. The data show that mineralized samples from Detroit Dam to Rocky Top are zoned with respect to Cu, Pb, and Zn. The relative proportions of these metals in mineralized samples depict a progressive change with increasing horizontal and vertical distance from Cu (Zn) at the Detroit Stock, through Zn

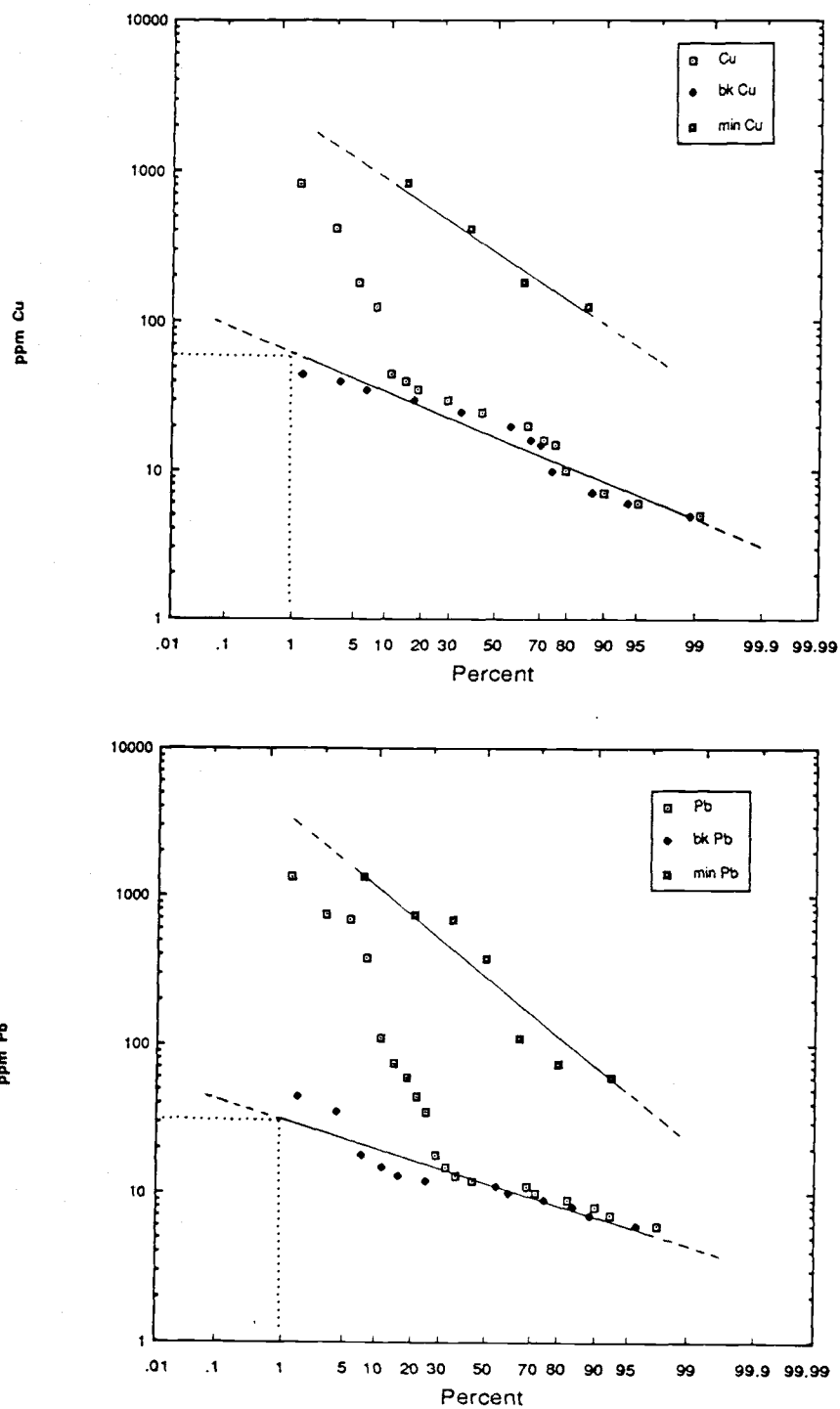


Figure 22: Log-probability plots for Cu, Pb, and Zn.

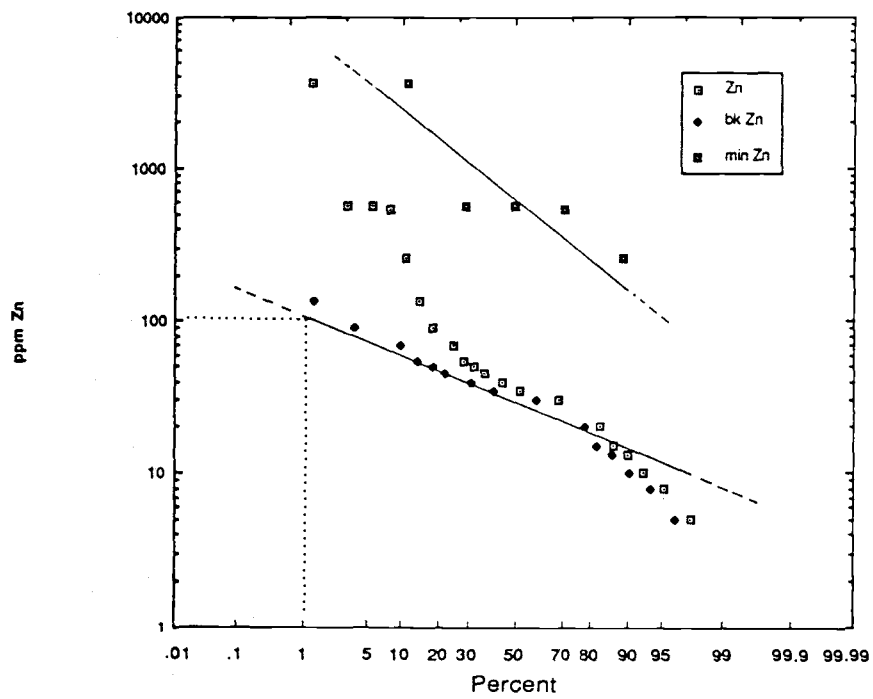


Figure 22: continued

A

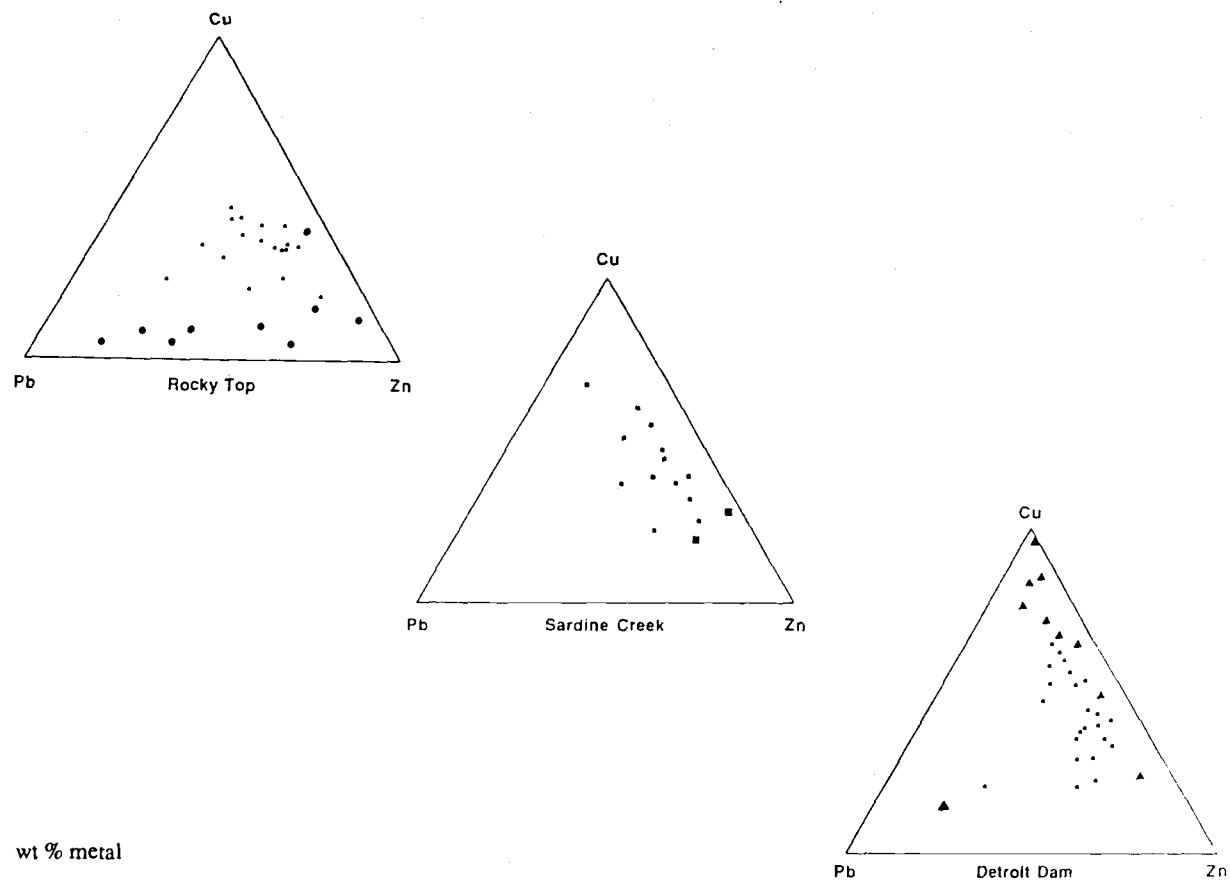
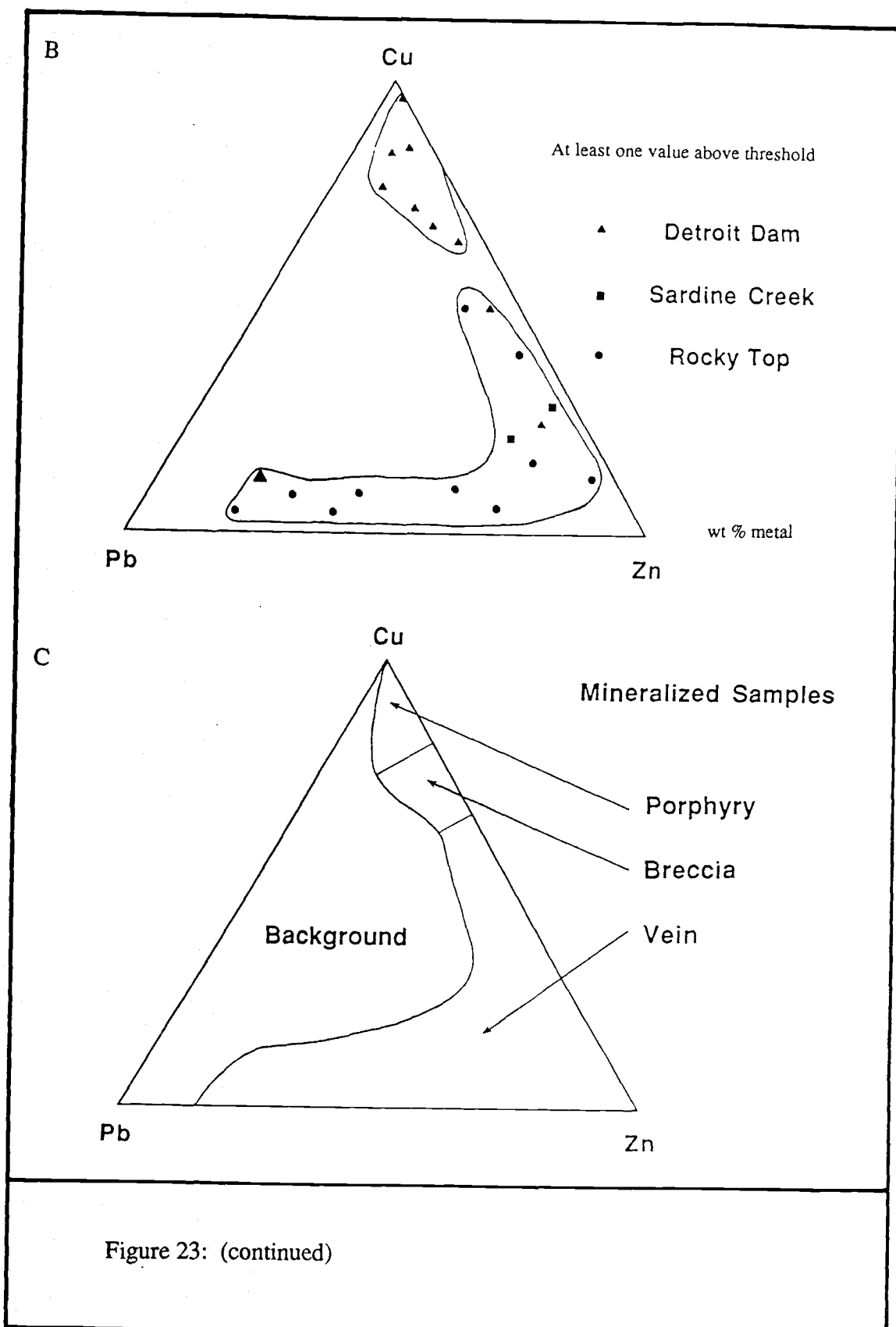


Figure 23: Ternary Cu-Pb-Zn diagrams.



(Cu) at Sardine Creek, to Pb (Zn) at Rocky Top. When compared with other data from the Western Cascades (Field and others, 1987) this trend can be interpreted as a progression from Cu-rich porphyry- and breccia-type mineralization at Detroit Dam to Pb-Zn vein-type mineralization at Rocky Top.

DISCUSSION

Hydrothermal mineralization exposed within the Rocky Top area is similar in mineralogic assemblage and zonation to that recently described for many of the mining districts of the Western Cascades. Hydrothermal alteration, other than mild propylitic, is localized in host rocks along and adjacent to fractures (faults and shears), and the margins of dikes. Late-stage sericitic (sericite-quartz) and argillic (clay-quartz) are structurally controlled, and overprint earlier propylitic and potassic alteration. The strongest propylitic and sericitic alteration is developed within and along the northwest-striking Rocky Top and Elkhorn Creek fault zones. This alteration grades laterally and vertically into visibly unaltered rock. Weak hydrothermal alteration can be documented geochemically by the enrichment or depletion of a range of elements in the host rocks immediately adjacent to these zones. Sometimes the effects of chemical modifications are self-evident. The enrichment of silica and potassium are reflected macroscopically in the quartz-sericite assemblage. Likewise, the addition of metals, particularly Fe, Cu, Pb, and Zn are normally related to the presence of pyrite, chalcopyrite, galena, and sphalerite. Subtle enrichments and depletions may, however, define the extent of alteration well beyond its visible boundaries (Fig. 19). Zones of weakly developed hydrothermal mineralization are common in the southeast corner of Rocky Top area. Alteration increases in intensity near structures where there is a distinct temporal and spatial relationship between hydrothermal mineralization and the presence of intrusive

rocks. The northwest-trending Rocky Top and Elkhorn Creek Fault Zones were responsible for the channelling of hydrothermal fluids. In addition, the distribution of alteration phases along these fault zones may reflect the position of unexposed granodiorite at depth.

A progressive decrease in temperature and salinity of fluid inclusions with increasing paragenetic time is revealed in Figure 21. The nearly linear relationship between homogenization temperatures and salinities of fluid inclusions from early to late stages indicates a history of progressive cooling and dilution of early hydrothermal fluids. Higher temperature and salinity fluids ($\approx 250^\circ\text{C}$, 5 equiv. wt. % NaCl) mixed with cooler, less saline waters, resulting in fluids of intermediate temperature and salinity ($215\text{--}230^\circ\text{C}$, 3–3.5 equiv. wt. % NaCl). Further cooling and dilution are recorded by secondary inclusions (150°C , ≈ 1 equiv. wt. % NaCl) which likely reflect the final stages of hydrothermal mineralization at Rocky Top. A small 38 to 40 bar pressure correction for the low salinity type I fluid inclusions, which have a maximum homogenization temperature of approximately 250°C , yield temperatures of formation of around 250 to no more than 260°C .

The approximate pH- $f\text{O}_2$ conditions under which mineralization appears to have formed are shown in Figure 24. A temperature of 250°C , $\log \Sigma\text{S} = -2$, $\log [\text{K}^+] = -1$, and $\log [\text{Ba}^{2+}] = -1$ were used for the calculations. Heavy solid lines represent stability fields for minerals in the system Fe-S-O. Thin solid lines are for Cu-bearing minerals. Heavy dashed lines correspond to the stability boundaries for aqueous sulfur species. Heavy dotted lines represent the boundaries between kaolinite, muscovite, and potassium feldspar. Thin dotted lines correspond to the mole percent FeS in sphalerite. The arrows depict the trend from early to late conditions of hydrothermal mineralization. The range in pH is inferred by the stability of sericite (muscovite) in equilibrium with excess quartz, and was derived using data from Bowers and others (1984). The

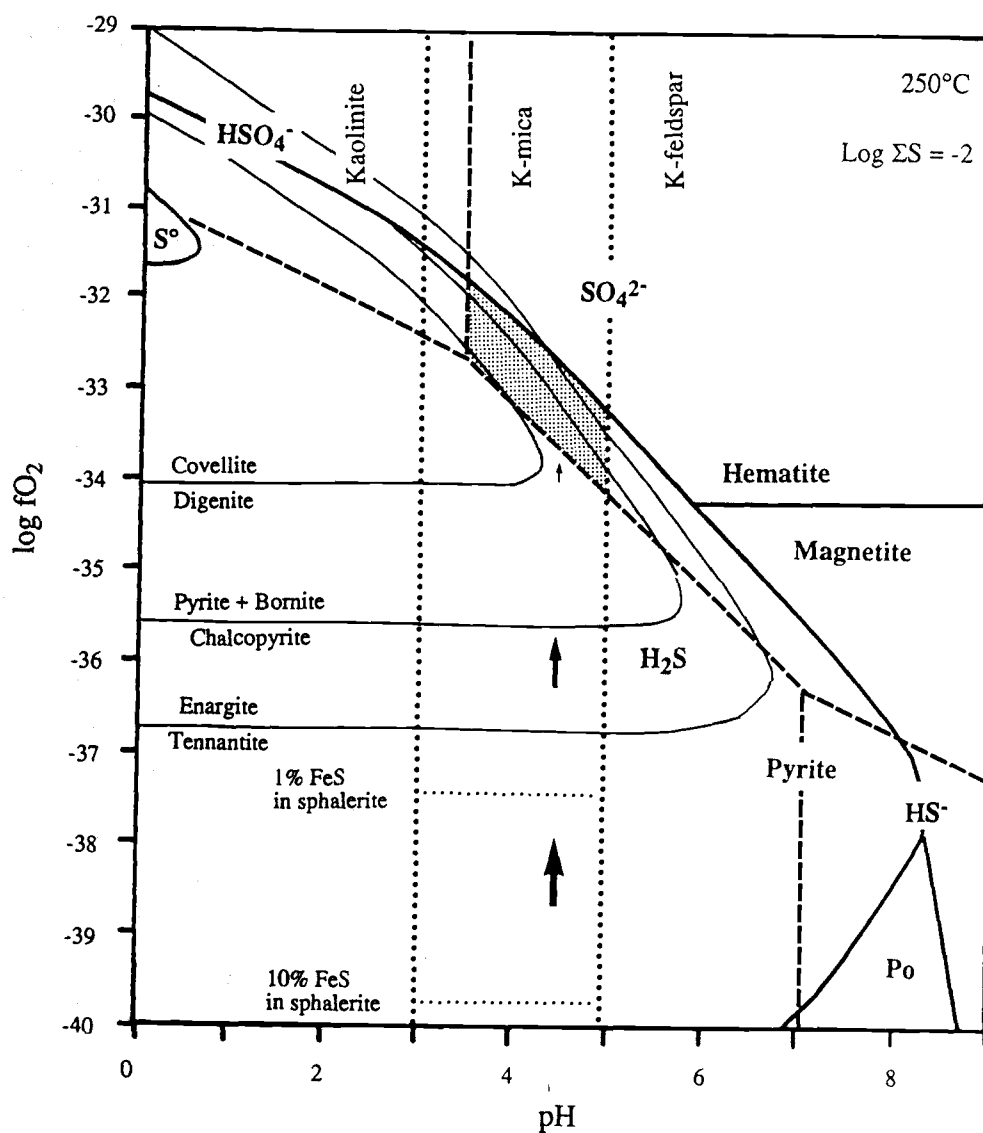


Figure 24: Log fO_2 -pH diagram at 250°C for the system Fe-S-O-Cu-Ba-K-Al-HCl-KCl.

stability range for barite in a one molar NaCl solution was determined using data from Holland and Malinin (1979). The shaded area (Fig. 24) represents the stability field for barite, pyrite, and sericite (muscovite). Equilibrium constants used for constraining reactions are from Helgeson (1969), and Robie and others (1978). Temperatures different from 250°C would result in shifting phase boundaries and contours, but for changes of $\pm 25^\circ\text{C}$ such shifts are small and do not affect the general observations and conclusions given below.

An increase in the fugacity of oxygen and sulfur with time is shown by the replacement of tennantite by enargite and the progressive decrease in iron content of sphalerite. This is also illustrated with the supergene rimming of chalcopyrite by bornite and covellite. The deposition of barite shows that the hydrothermal fluids progressed from H_2S to SO_4^{2-} dominated stability fields.

The equilibria isotopic relationship between sulfide and sulfate species is shown in Figure 25 for 250°C and $\delta^{34}\text{S}_{\Sigma\text{S}} = 0$ permil. The heavy solid line represents values for H_2S , whereas the thin solid line represent those for SO_4^{2-} . The arrows depict the trend from early to late conditions of hydrothermal mineralization. Assuming equilibrium conditions with respect to time between isotopic species in sphalerite and barite with H_2S and SO_4^{2-} , a temperature of 250°C, pH between 3.0 and 5.0, and accounting for the range of -0.26 to 0.01 permil for sphalerite, values of $\delta^{34}\text{S}_{\Sigma\text{S}}$ are restricted to around zero permil. Under these conditions, sulfur from both sulfides and sulfates at Rocky Top can be attributed to a magmatic source of around zero permil, assuming temperatures around 250°C, and an increase in $\log (\text{SO}_4^{2-}/\text{H}_2\text{S})$ from -2 to >0.

Recently the deposits in the Western Cascades have been viewed as a depth-related continuum of deposit types. The mineralization exposed at Rocky Top is characteristic of base-metal veins reflecting high-level deposits in the Western Cascades as described by Power (1984); Field and others (1987); and Summers (1990). Mineralized samples

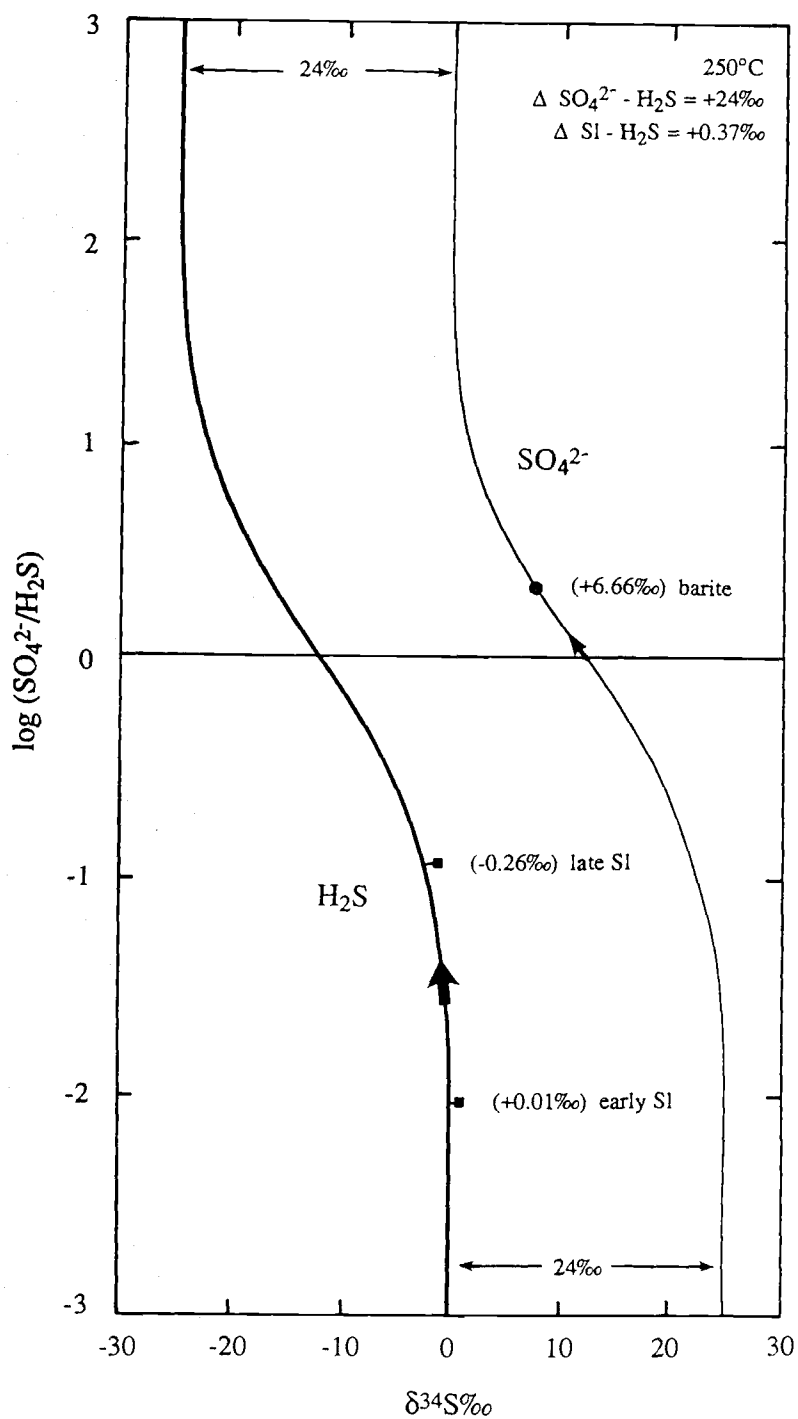


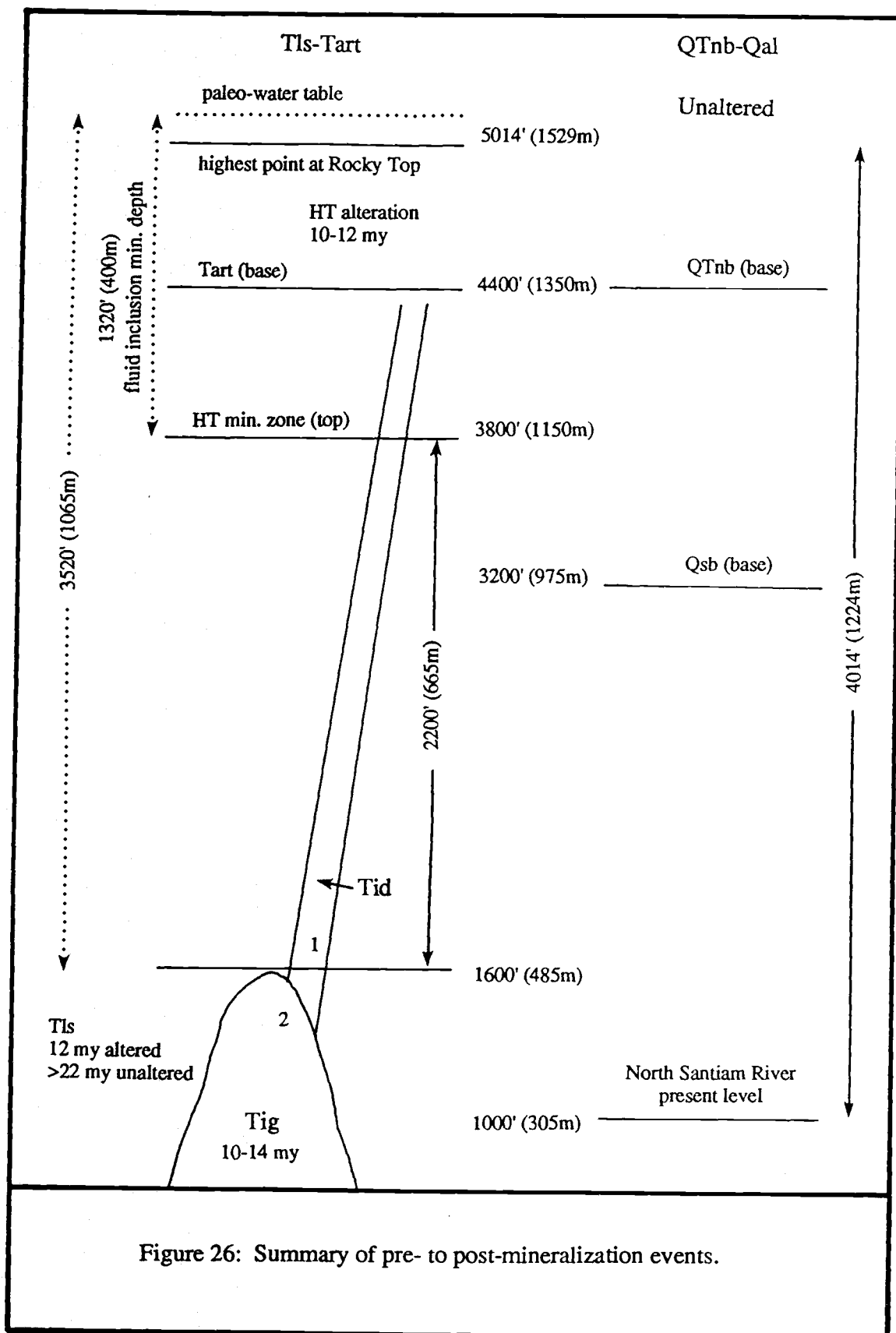
Figure 25: Isotopic relationship between sulfide and sulfate species.

display a trend from Cu-rich porphyry- and breccia-type mineralization at Detroit Dam to Pb-Zn vein-type mineralization at Rocky Top. This trend is interpreted to be related to the lateral and vertical distance from the Detroit Stock.

SUMMARY AND CONCLUSIONS

The geologic history of the Rocky Top area is complex because of the superposition of several events, including regional deformation, faulting, emplacement of plutonic rocks, and hydrothermal activity. A summary of these events is presented in Figure 26.

The late Oligocene to late Miocene volcanic rocks exposed within the Rocky Top area form a 3000 meter thick section which records of Western Cascade calc-alkaline volcanism. All of these units have locally undergone moderate to intense hydrothermal alteration. The oldest rocks have been tilted up to 40° , and are separated from younger rocks by an angular unconformity. Major northwest-trending faults represent structural boundaries which accommodated displacement between blocks. Although deformation in the region may have begun prior to the onset of Sardine volcanism, it is apparent that the lava flows of the upper member of the Sardine sequence (Tus) have been tilted up to 40° along northwest-striking faults and northwest-trending fold axes. These and older volcanic strata were involved in faulting and tilting prior to the deposition of the less deformed pyroclastic sequence of Elkhorn Creek (Tpec). In contrast, the relatively flat-lying flows of the andesite sequence of Rocky Top (Tart) overlie older units across an angular unconformity. Deformation was largely complete by the time that the ridge-capping andesite sequence of Rocky Top (Tart) was emplaced because the unit shows no evidence of having been significantly faulted or tilted. Therefore, faulting and tilting of the volcanic rocks most likely started before the early Miocene and ended around the middle to late Miocene. In addition, regional folding/tilting ended prior to the onset of hydrothermal mineralization because the intensely altered upper member of the Elk Lake sequence (Tuel) and all younger units have essentially horizontal attitudes. The Pliocene



to Pleistocene volcanic rocks (QTnb, and Qsb) are unaltered, and found as intracanyon flows into the older rocks.

Stratigraphic reconstruction from Sardine Creek to Rocky Top suggests that intrusions of hornblende granodiorite (Tig) were emplaced at a minimum depth of roughly 1000 meters (3520 ft), whereas older quartz diorites (Tid) were emplaced at shallower levels. The early pyroxene-bearing quartz diorite dikes (Tid) were probably not directly responsible for hydrothermal mineralization, as revealed by their narrow chilled margins which suggest that they were probably only a minor heat source. These early dikes, however, were responsible for much of ground preparation in the form of fracturing, which increased permeability in the enclosing volcanic rocks. The relatively larger bodies of younger hornblende-bearing granodiorite (Tig) are a more conceivable source for hydrothermal mineralization. They were emplaced at deeper levels, and not only provided a heat engine, but many have contributed fluids to the hydrothermal system. Compositional traits and spatial distribution of the plutonic rocks at Rocky Top suggest that they are related to the Detroit Stock. The intrusions are inferred to range in age from roughly 10 to 14 million years old based on whole-rock K-Ar age determinations of 9.9 ± 0.2 million years from the Detroit Stock (Walker and Duncan, 1989); and 12.5 ± 0.2 million years from the Sardine sequence (TIs) (Verplanck, 1985), the latter date is interpreted as an alteration age. If intrusive activity preceded hydrothermal alteration by one to two million years, then a maximum age of 14 million years should be considered for the plutonic rocks. The 10 million year date from the Detroit Stock should be considered a minimum age because of closely associated hydrothermal alteration.

Most of the stocks in the Western Cascades are exposed in deep canyons, whereas the mining districts of paleo-hydrothermal systems are near the mountain tops. Investigation of the interrelationships between mineralization and associated plutonic

rocks combined with volcanic stratigraphy, structure, and topography suggest that Rocky Top may be one of the youngest and highest level hydrothermal systems of the Western Cascades. Extensive hydrothermal alteration is associated with structures and intrusions along a northwest-trending corridor extending from the Detroit Stock to Rocky Top. Propylitic alteration is widespread throughout the area and intensifies with proximity to northwest-trending fractures. Potassic alteration is limited to the Detroit Stock where several samples contain incipient veinlets and diffuse replacement zones of hydrothermal biotite. Late-stage sericitic and argillic alteration are structurally controlled, and overprint earlier propylitic and potassic alteration. Fluid inclusions at Rocky Top have low salinities, and temperatures of homogenization that range between 180 and 250°C. Sulfur isotopes range from +2.8 to -3.3 permil for sulfides and +6.7 permil for barite. Sulfur from both sulfides and sulfates can be attributed to a magmatic source of around zero permil, assuming temperatures around 250°C, and an increase in $\log (\text{SO}_4^{2-}/\text{H}_2\text{S})$ from negative two to greater than zero. Mineralized samples from Detroit Dam to Rocky Top are zoned with respect to Cu, Pb, and Zn. The samples display a trend from Cu-rich porphyry- and breccia-type mineralization at Detroit Dam to Pb-Zn vein-type mineralization at Rocky Top. The trend is interpreted to be related to a lateral and vertical distance from the Detroit Stock.

Because the unaltered Northern and Southern basalts are found as intracanyon flows into hydrothermally altered rocks, it follows that the Rocky Top area was uplifted at some time after hydrothermal mineralization ceased (10-12 my). The relationships between ridge-capping, and intracanyon volcanic rocks suggest that the North Santiam River started to entrench during the Pliocene. Distribution of surficial deposits show that downcutting continued to roughly 600 meters (2000 ft) above the present North Santiam channel during the Pleistocene after which the channel was incised to its present

level. Most of the uplift in the Rocky Top area has thus occurred within the last two million years.

Recently the deposits in the Western Cascades have been viewed as a depth-related continuum of deposit types. The hydrothermal mineralization exposed at Rocky Top is characteristic of base-metal veins reflecting high-level deposits in the Western Cascades as described by Power (1984); Field and others (1987); and Summers (1990). Most of the Western Cascades, including the Rocky Top area, has sustained recent uplift and extensive erosion. The depth of oxidation in these deposits is relatively shallow, and it is not uncommon to find fresh sulfides exposed at the surface. Although hydrothermal mineralization within the Rocky Top area has many features in common with nearby mining districts of the Western Cascades, the absence of well-developed breccia pipes, through-going veins, and zones of intense pervasive alteration are consistent with the lack of extensive exploration and previous mining activity in this area.

BIBLIOGRAPHY

- Allen, J.E., 1966, The Cascade Range volcano-tectonic depression of Oregon, *in* Lunar Geological Field Conference, Bend, Oregon, August 1965, Transactions: Oregon Department of Geology and Mineral Industries, in cooperation with Oregon Division of Planning and Development, p. 21-23.
- Anders, E., and Ebihara, M., 1982, Solar system abundances of the elements: *Geochemica et Cosmochemica Acta*, v. 46, p. 2363-2380.
- Bates, R.B., Beck, M.E., Jr., and Burmester, R.F., 1981, Tectonic rotations in the Cascade range of southern Washington: *Geology*, v. 9, p. 184-189.
- Bowers, T.S., Jackson, K.J., and Helgeson, H.C., 1984, Equilibria activity diagrams: for coexisting minerals and aqueous solutions at pressures and temperatures to 5 kb and 600°C: Springer-Verlag, New York, 397 p.
- Buddington, A.F., and Callaghan, E., 1936, Dioritic intrusive rocks and contact metasomatism in the Cascade region of Oregon: *American Journal of Science*, v. 31, p. 421-449.
- Callaghan, E., 1933, Some features of the volcanic sequence in the Cascade Range in Oregon: American Geophysical Union 14th Annual Meeting, Transactions, p. 243-249.
- Callaghan, E., and Buddington, A. F., 1938, Metalliferous mineral deposits of the Cascade Range in Oregon: U.S. Geological Survey Bulletin 893, 141 p.
- Cummings, M.L., Pollock, J.M., Thompson, G.D., and Bull, M.K., 1989, Stratigraphic development and hydrothermal activity in the central Western Cascades, Oregon, *in* Muffler, L.P.J., Blackwell, D.D., and Weaver, C.S., eds., U.S. Geological Survey Open-File Report 89-178, p. 490-520.
- Cummings, M.L., Pollock, J.M., Thompson, G.D., and Bull, M.K., 1990, Stratigraphic development and hydrothermal activity in the central Western Cascades, Oregon: *Journal of Geophysical Research*, v. 95, no. B12, p. 19601-19610.
- Curless, J.M., Field, C.W., and Vaughan, M.W., 1989, Hydrothermal mineralization in the vicinity of Rocky Top, Western Cascades, Oregon: *GSA Abstracts with Programs*, v. 21, no. 5, p. 71.
- Curless, J.M., Vaughan, M.W., and Field, C.W., 1990, Plutonism and hydrothermal mineralization associated with the Detroit Stock, Western Cascades, Oregon: *GSA Abstracts with Programs*, v. 22, no. 3, p. 16.
- Field, C.W., and Fifarek, R.H., 1985, Light stable-isotope systematics in the epithermal environment, *in* Berger, B.R., and Bethke, P.M., eds., *Geology and geochemistry of epithermal systems: Society of Economic Geologists, Reviews in Economic Geology*, v. 2, p. 99-128.

- Field, C.W., and Power, S.G., 1985, Metallization in the Western Cascades, Oregon and Southern Washington: GSA Abstracts with Programs, v. 17, no. 4, p. 218.
- Field, C.W., Power, S.G., and Curless, J.M., 1987, Magmatism and mineralisation in the Western Cascades of Oregon and Washington, U.S.A., *in* Proceedings of the Pacific Rim Congress 87 on the geology, structure, mineralisation, and economics of the Pacific Rim: Australasian Institute of mining and Metallurgy, p. 811-816.
- Haas, J.L., Jr., 1971, The Effect of Salinity on the Maximum Thermal Gradient of a Hydrothermal System at Hydrostatic Pressure: *Economic Geology*, v. 66, p.940-946.
- Helgeson, H.C., 1969, Thermodynamics of hydrothermal systems at elevated temperatures and pressures: *American Journal of Science*, v. 267, p. 729-804.
- Holland, H.D., and Malinin, S.D., 1979, The solubility and occurrence of non-ore minerals, *in* Barnes, H.L., ed., *Geochemistry of hydrothermal ore deposits II*: John Wiley and Sons, New York, p. 461-508.
- Hughes, S.S., and Taylor, E.M., 1986, Geochemistry, petrogenesis, and tectonic implications of central High Cascade mafic platform lavas: *Geological Society of America Bulletin*, v. 97, p. 1024-1036.
- Irvine, T.N., and Baragar, W.R.A., 1971, A guide to the chemical classification of the common volcanic rocks: *Canadian Journal of Earth Sciences*, v. 8, no. 5, p. 523-548.
- Laul, J.C., 1979, Neutron activation analysis of geological materials: *Atomic Energy Review*, v. 17, p. 603-695.
- LeMaitre, R.W., 1984, A Proposal by the IUGS Subcommittee on the Systematics of Igneous Rocks for a chemical classification of volcanic rocks based on the total alkali silica (TAS) diagram: *Australian Journal of Earth Science*, v. 31, p. 243-255.
- Lux, D.R., 1981, Geochronology, geochemistry, and petrogenesis of basaltic rocks from the Western Cascades, Oregon: Columbus, Ohio, Ohio State University doctoral dissertation, 171 p.
- Magill, J., and Cox, A., 1980, Tectonic rotation of the Oregon Western Cascades: Oregon Department of Geology and Mineral Industries Special Paper 10, 67 p.
- McBirney, A.R., and White, C.M., 1982, The Cascade province, *in* Thorpe, R.S., ed., *Andesites: orogenic andesite and related rocks*, John Wiley and Sons, New York, p. 115-135.
- McBirney, A.R., Sutter, J.F., Naslund, H.R., Sutton, K.G., and White, C.M., 1974, Episodic volcanism in the central Oregon Cascade Range: *Geology*, v. 2, no. 12, p. 585-589.

- Meyer, C., and Hemley, J.J., 1967, Wall rock alteration, *in* Barnes, H.L., ed., *Geochemistry of hydrothermal ore deposits*: Holt, Rinehart and Wilson, Inc., New York, p.166-235.
- Nakamura, K., 1977, Volcanoes as possible indicators of tectonic stress orientation - Principle and proposal: *Journal of Volcanology and Geothermal Resources*, v. 2, p. 1-16.
- Olson, J. P., 1978, Geology and mineralization of the North Santiam mining district, Marion County, Oregon: Corvallis, Oregon, Oregon State University master's thesis, 135 p.
- Peck, D. L., Griggs, A. B., Schlicker, H. G., Wells, F. G., and Dole, H. M., 1964, Geology of the central and northern parts of the Western Cascade Range in Oregon: U.S. Geological Survey Professional Paper 449, 56 p.
- Pollock, J. M., and Cummings, M. L., 1985, North Santiam mining area, Western Cascades- relations between alteration and volcanic stratigraphy: Discussion and field trip guide: *Oregon Geology*, v. 47, p. 139-145.
- Pollock, J.M., 1985, Geology and geochemistry of hydrothermal alteration, eastern portion of the North Santiam mining area: Portland, Oregon, Portland State University master's thesis, 100 p.
- Potter, R.W., Clynne, M.A., and Brown, D.L., 1978, Freezing point depression of aqueous sodium chloride solutions: *Economic Geology*, v. 73, p. 284-285.
- Power, S.G., 1984, The "tops" of porphyry copper deposits - mineralization and plutonism in the Western Cascades: Corvallis, Oregon, Oregon State University doctoral dissertation, 243 p.
- Power, S.G., Field, C.W., Armstrong, R.L., and Harakal, J.E., 1981, K-Ar ages of plutonism and mineralization, Western Cascades, Oregon and southern Washington: *Isochron/West*, no. 31, p. 27-29.
- Priest, G.R., 1989, Volcanic and tectonic evolution of the Cascade volcanic arc, 44°00" to 44°52'30" N, *in* Muffler, L.P.J., Blackwell, D.D., and Weaver, C.S., eds., U.S. Geological Survey Open-File Report 89-178, p. 430-489.
- Priest, G.R., 1990, Volcanic and tectonic evolution of the Cascade volcanic arc, central Oregon: *Journal of Geophysical Research*, v. 95, no. B12, p. 19583-19599.
- Priest, G.R., and Vogt, B.F., 1983, Geology and geothermal resources of the central Oregon Cascade Range, Oregon: Oregon Department of Geology and Mineral Industries Special Paper 15, 123 p.
- Priest, G.R., Black, G.L., Woller, N.M., and Taylor, E.M., 1988, Geologic map of the McKenzie Bridge quadrangle, Lane County, Oregon: Oregon Department of Geology and Mineral Industries Geological Map Series, GMS-48, scale 1:62,500.

- Priest, G.R., Woller, N. M., Black, G. L., and Evans, S. H., 1983, Overview of the geology of the central Oregon Cascade Range, *in* Priest, G. R., and Vogt, B. F., eds., *Geology and geothermal resources of the central Oregon Cascade Range*: Oregon Department of Geology and Mineral Industries Special Paper 15, p. 3-28.
- Priest, G.R., Woller, N.M., and Ferns, M.L., 1987, Geologic map of the Breitenbush River area, Linn and Marion Counties, Oregon: Oregon Department of Geology and Mineral Industries Geological Map Series, GMS-46, scale 1:62,500.
- Pungrassami, T., 1970, Geology of the western Detroit Reservoir area, Quartzville and Detroit quadrangles, Oregon: Corvallis, Oregon, Oregon State University master's thesis, 76 p.
- Robie, R.A., Hemingway, B.S., and Fisher, J.R., 1978, Thermodynamic properties of minerals and related substances at 298.15K and one bar (10^5 Pascals) pressure and at higher temperatures: U.S. Geological Survey Bulletin 1452, 456 p.
- Roedder, E., 1984, Fluid inclusions: Mineralogical Society of America, Reviews in Mineralogy, v. 12, 644 p.
- Rollins, A., 1976, Geology of the Bachelor Mountain area, Linn and Marion Counties, Oregon: Corvallis, Oregon, Oregon State University master's thesis, 83 p.
- Schmid, R., 1981, Descriptive nomenclature and classification of pyroclastic deposits and fragments: Recommendations of the IUGS Subcommittee on the Systematics of Igneous Rocks: *Geology*, v.9, p. 41-43.
- Sherrod, D.R., 1986, Geology, petrology, and volcanic history of a portion of the Cascade Range between latitudes 43° - 44° N, central Oregon, U.S.A.: Santa Barbara, California, University of California doctoral dissertation, 320 p.
- Sherrod, D.R., and Pickthorn, L.B.G., 1989, Some notes on the Neogene structural evolution of the Cascade Range in Oregon, *in* Muffler, L.P.J., Blackwell, D.D., and Weaver, C.S., eds., *U.S. Geological Survey Open-File Report 89-178*, p. 351-368.
- Sherrod, D.R., and Smith, J.G., 1989, Preliminary map showing Upper Eocene to Holocene volcanic and related rocks of the Cascade Range in Oregon: U.S. Geological Survey Open-File Report 89-14, scale 1:500,000.
- Sillitoe, R.H., 1973, The tops and bottoms of porphyry copper deposits: *Economic Geology*, v.68, p. 799-815.
- Simpson, R.W., and Cox, A., 1977, Paleomagnetic evidence for tectonic rotation of the Oregon Coast Range: *Geology*, v. 5, p. 585-589.
- Sinclair, A.J., 1976, Applications of probability graphs in mineral exploration: The Association of Exploration Geochemists, Special Volume No. 4, 95 p.

- Streckeisen, A.L., 1976, To each plutonic rock its proper name: *Earth Science Reviews*, v.12, p. 1-33.
- Summers, C.A., 1990, Base and precious metal deposits in the Western Cascades of Oregon and southern Washington: Mineralogy, fluid inclusions, and sulfur isotopes: Corvallis, Oregon, Oregon State University master's thesis, 144 p.
- Sutter, J. F., 1978, K/Ar ages of Cenozoic volcanic rocks from the Oregon Cascades west of 121° 30': *Isochron/West*, no. 21, p. 15-21.
- Taylor, E.M., 1968, Roadside geology, Santiam and McKenzie Pass Highways, Oregon, *in* Dole, H.M., ed., *Andesite Conference guidebook: Oregon Department of Geology and Mineral Industries Bulletin 62*, p. 3-33.
- Taylor, E.M., 1980, Volcanic and volcanoclastic rocks on the east flank of the central Cascade Range to the Deschutes River, Oregon, *in* Oles, K.F., Johnson, J.G., Niem, A.R., and Niem, W.A., eds., *Geologic field trips in western Oregon and southwestern Washington: Oregon Department of Geology and Mineral Industries Bulletin 101*, p. 1-7.
- Taylor, E.M., 1989, Volcanic history and tectonic development of the central High Cascade Range, Oregon, *in* Muffler, L.P.J., Blackwell, D.D., and Weaver, C.S., eds., *U.S. Geological Survey Open-File Report 89-178*, p. 369-394.
- Taylor, E.M., 1990, Volcanic history and tectonic development of the central High Cascade Range, Oregon: *Journal of Geophysical Research*, v. 95, no. B12, p. 19611-19622.
- Taylor, H.P., Jr., 1971, Oxygen isotope evidence for large-scale interaction between meteoric ground waters and Tertiary granodiorite intrusions, Western Cascade Range, Oregon: *Journal of Geophysical Research*, v. 76, no. 32, p. 7855-7874.
- Thayer, T. P., 1934, The general geology of the North Santiam River section of the Oregon Cascades: Pasadena, California, California Institute of Technology doctoral dissertation, 92 p.
- Thayer, T. P., 1936, Structure of the North Santiam River section of the Cascade Mountains in Oregon: *Journal of Geology*, v. 44, no. 6, p. 701-716.
- Thayer, T. P., 1937, Petrology of later Tertiary and Quaternary rocks of the north-central Cascade Mountains in Oregon, with notes on similar rocks in western Nevada: *Geological Society of America Bulletin*, v. 48, no. 11, p. 1611-1651.
- Thayer, T. P., 1939, Geology of the Salem Hills and the North Santiam River basin, Oregon: *Oregon Department of Geology and Mineral Industries Bulletin 15*, 40 p.
- Verplanck, E.P., 1985, Temporal variations in volume and geochemistry of volcanism in the Western Cascades, Oregon: Corvallis, Oregon, Oregon State University master's thesis, 115 p.

- Verplanck, E.P., and Duncan, R.A., 1987, Temporal variations in plate convergence and eruption rates in the Western Cascades, Oregon: *Tectonics*, v. 6, no. 2, p. 197-209.
- Walker, G.W., and Duncan, R.A., 1989, Geologic Map of the Salem 1°x 2° sheet, Oregon: U.S. Geological Survey, Miscellaneous Investigations Map I-1893, scale 1:250,000.
- White, C. M., 1980a, Geology of the Breitenbush Hot Springs quadrangle, Oregon: Oregon Department of Geology and Mineral Industries Special Paper 9, 26 p.
- White, C. M., 1980b, Geology and geochemistry of volcanic rocks in the Detroit area, Western Cascade Range, Oregon: Eugene, Oregon, University of Oregon doctoral dissertation, 178 p.
- Wood, D.A., 1980, The application of a Th-Hf-Ta diagram to problems of tectonomagmatic classification and to establishing the nature of crustal contamination of basaltic lavas of the British Tertiary Volcanic Province: *Earth and Planetary Science Letters*, v. 50, p. 11-30.

APPENDICES

APPENDIX 1: Locations of samples from Rocky Top

Sample #	Section ¹	LAT. (N)	LONG. (W)	LAT. (N)	LONG. (W)
73-1	13 Aadcb	44°.7966	122°.2590	44°47'48"	122°15'32"
73-2	13 Aadcb	44°.7968	122°.2591	44°47'48"	122°15'33"
86-1	14 Cbadd	44°.7885	122°.2913	44°47'19"	122°17'29"
86-2	14 Cacba	44°.7884	122°.2901	44°47'18"	122°17'24"
86-3	14 Cadbd	44°.7883	122°.2876	44°47'18"	122°17'15"
88-4	25 Bbbbd	44°.7694	122°.2753	44°46'10"	122°16'31"
92-1	15 Dbabd	44°.7886	122°.3024	44°47'19"	122°18'09"
92-2	15 Dbcdd	44°.7863	122°.3036	44°47'11"	122°18'13"
98-3	15 Dbabd	44°.7888	122°.3022	44°47'20"	122°18'08"
102-1	13 Dcacc	44°.7870	122°.2635	44°47'13"	122°15'49"
102-2	13 Acddd	44°.7925	122°.2621	44°47'33"	122°15'44"
102-3	23 Adadc	44°.7797	122°.2773	44°46'47"	122°16'38"
102-4	23 Adadc	44°.7797	122°.2773	44°46'47"	122°16'38"
111-2	15 Dabab	44°.7893	122°.2995	44°47'21"	122°17'58"
111-3	15 Daabb	44°.7898	122°.2987	44°47'23"	122°17'55"
111-5	15 Daadc	44°.7880	122°.2969	44°47'17"	122°17'49"
111-6	15 Daacd	44°.7880	122°.2975	44°47'17"	122°17'51"
111-7	15 Dbbdd	44°.7877	122°.3035	44°47'16"	122°18'13"
111-8	15 Dbcdb	44°.7867	122°.3042	44°47'12"	122°18'15"
111-9	23 Bddbb	44°.7773	122°.2879	44°46'38"	122°17'16"
724-2	24 Babbb	44°.7847	122°.2713	44°47'05"	122°16'17"
724-3	24 Babaa	44°.7848	122°.2692	44°47'05"	122°16'09"
812-1	13 Bcaad	44°.7954	122°.2717	44°47'43"	122°16'18"
819-15	24 Bbbab	44°.7846	122°.2744	44°47'05"	122°16'28"
821-3	24 Bbdab	44°.7831	122°.2725	44°46'59"	122°16'21"
821-5	24 Bcbac	44°.7808	122°.2744	44°46'51"	122°16'28"
826-3	23 Abbda	44°.7826	122°.2838	44°46'57"	122°17'02"
911-1	35 Abdcd	44°.7521	122°.2819	44°45'08"	122°16'55"
911-2	36 Bdbda	44°.7507	122°.2682	44°45'03"	122°16'06"
911-3	18 Cbbbc	44°.7918	122°.2560	44°47'30"	122°15'22"
911-4	14 Bbcde	44°.7940	122°.2944	44°47'38"	122°17'40"
911-5	15 Ddabc	44°.7851	122°.2985	44°47'06"	122°17'55"
MV-09	36 Aacab	44°.7536	122°.2594	44°45'13"	122°15'34"
MV-37	25 Acced	44°.7595	122°.2657	44°45'34"	122°15'57"
MV-45	25 Accdc	44°.7632	122°.2645	44°45'48"	122°15'52"

¹ All samples are from sections within T9S R4E (Willamette Meridian), except for sample 911-3 which is from section 18 of T9S R5E.

APPENDIX 2: Chemical analyses of volcanic rocks from Rocky Top

unit sample #	Tls 911-2	Tus 111-7	Tus 92-2	Tus 102-4	Tpec 102-2	Tlel 819-15	uncertainty
major-element oxides in weight percent ¹							
SiO ₂	53.24	52.92	52.98	58.77	75.88	61.09	
TiO ₂	0.92	1.06	1.09	1.06	0.19	0.61	
Al ₂ O ₃	19.82	16.61	16.88	17.64	12.04	18.31	
Fe ₂ O ₃	3.13	2.03	2.94	4.16	0.91	2.12	
FeO	3.14	5.38	4.32	1.13	0.31	2.83	
MnO	0.09	0.11	0.14	0.05	0.03	0.10	
MgO	4.46	3.85	3.03	1.13	0.17	2.03	
CaO	7.34	7.08	8.70	3.73	0.86	5.75	
Na ₂ O	4.00	2.51	2.75	5.70	3.05	4.27	
K ₂ O	0.78	1.05	0.08	1.15	3.80	2.03	
P ₂ O ₅	0.57	0.52	0.45	0.44	0.06	0.39	
LOI	3.03	5.23	4.03	3.35	0.67	1.70	
Total	100.52	98.35	97.39	98.31	97.97	101.23	
δ ²	2.73	2.66	2.73	2.53	2.44	2.65	
trace elements in parts per million ³							
Sc	17.5	17.0	18.9	14.9	2.7	8.0	± 3 %
Cr	66	111	136	44	92	60	± 10 %
Co	24.9	24.0	25.3	10.3	0.8	13.9	± 5 %
Ni	61	55	90	125		23	± 12 %
Rb	23	10		50	105	25	± 10 %
Sr	630	500	470	467	172	738	± 12 %
Cs	0.4	9.6	1.7	2.7	1.2	2.1	± 5 %
Ba	229	520	305	241	775	266	± 10 %
La	9.6	19.0	20.0	18.9	25.0	10.6	± 3 %
Ce	23.5	37.0	43.0	37.3	55.0	22.1	± 7 %
Nd	13.0	23.0	26.0	19.1	27.0	12.2	± 12 %
Sm	2.8	4.8	5.0	5.0	3.7	2.8	± 5 %
Eu	1.01	1.40	1.60	1.60	0.50	0.90	± 5 %
Tb	0.52	0.70	0.60	0.68	0.50	0.35	± 5 %
Yb	1.21	2.30	2.00	2.10	2.00	1.00	± 5 %
Lu	0.20	0.30	0.30	0.29	0.20	0.14	± 5 %
Hf	2.9	4.5	4.6	3.9	5.0	2.9	± 5 %
Ta	0.32	0.64	0.78	0.49	0.94	0.22	± 5 %
Th	1.6	3.0	2.6	3.0	16.0	1.9	± 5 %
U		1.5			5.0		± 7 %

¹ Major-element oxides by ICP-AES, FeO by titration, LOI by furnace by Chemex Labs, Sparks, NV

² density in g/cc

³ Trace-elements by INAA at the Radiation Center, Oregon State University procedure outlined by Laul (1979)

APPENDIX 2: (continued)

unit sample #	T1el 724-2	T1el 724-3	Tuel 911-3	Tart 86-1	Tart 86-2	QTnb 911-4	Qsb 111-9
major-element oxides in weight percent ¹							
SiO ₂	75.91	77.33	57.44		57.46	54.56	47.31
TiO ₂	0.13	0.12	0.88		0.86	1.09	0.71
Al ₂ O ₃	12.51	11.33	17.85		17.35	17.57	15.33
Fe ₂ O ₃	0.96	0.53	3.31		3.20	2.93	2.87
FeO	0.40	0.23	2.56		2.81	3.85	5.51
MnO	0.04	<0.01	0.09		0.11	0.14	0.22
MgO	0.40	0.03	3.56		2.75	3.84	9.28
CaO	1.29	0.24	7.10		5.56	7.48	10.29
Na ₂ O	4.37	2.15	3.52		3.58	2.97	2.09
K ₂ O	1.10	6.75	1.33		1.15	1.70	<0.01
P ₂ O ₅	0.15	0.13	0.50		0.30	0.60	0.25
LOI	2.03	0.55	1.93		2.89	3.20	2.64
Total	99.29	99.39	100.07		98.02	99.93	96.50
g ₂	2.36	2.47	2.72	2.60	2.59	2.72	2.88
trace elements in parts per million ³							
Sc	2.8	1.8	15.3	17.7	17.6	19.5	33.5
Cr	54	83	54	65	65	81	813
Co	1.3	0.3	19.9	17.4	19.0	23.8	46.2
Ni			47	120	40	62	215
Rb	30	108	33	31		42	
Sr	165	81	494	582	445	443	188
Cs	1.8	1.6	2.3	1.4	4.9	1.8	1.9
Ba	200	741	352	360	390	412	
La	24.2	26.5	15.4	15.0	16.0	20.3	4.5
Ce	45.6	47.2	35.8	31.0	33.0	45.6	10.4
Nd	15.8	19.6	16.4	18.0	15.0	24.3	8.4
Sm	3.4	4.5	3.5	4.0	4.1	4.9	2.1
Eu	0.20	0.30	1.13	1.20	1.10	1.34	0.70
Tb	0.41	0.55	0.54	0.50	0.60	0.70	0.44
Yb	2.20	2.60	1.52	1.80	1.90	2.04	1.60
Lu	0.31	0.35	0.24	0.27	0.30	0.29	0.25
Hf	3.9	4.3	3.8	4.0	4.1	4.5	1.5
Ta	0.84	0.93	0.42	0.48	0.56	0.54	0.15
Th	12.2	16.1	3.9	3.7	4.6	4.3	0.4
U	4.0	4.5	1.3	1.4		1.5	

¹ Major-element oxides by ICP-AES, FeO by titration, LOI by furnace, Chemex Labs, Sparks, NV² density in g/cc³ Trace-elements by INAA at the Radiation Center, Oregon State University procedure outlined by Laul (1979)

APPENDIX 3: Chemical analyses of plutonic rocks from Rocky Top

unit sample #	Tid 88-4	Tid 102-1	Tid 102-3	Tid 812-1	Tid SC-45	Tig SC-37	Tig SC-09
major-element oxides in weight percent ¹							
SiO ₂	56.68	61.91	58.20	59.36	60.28	66.50	68.51
TiO ₂	0.83	0.86	0.81	0.83	0.82	0.49	0.48
Al ₂ O ₃	16.75	16.04	16.57	16.23	16.05	15.23	14.45
Fe ₂ O ₃	2.56	2.19	3.46	1.97	2.13	0.30	1.72
FeO	3.35	3.22	2.70	3.47	3.14	3.18	1.34
MnO	0.10	0.09	0.06	0.09	0.09	0.10	0.06
MgO	3.55	2.55	2.95	2.92	2.92	1.54	0.96
CaO	5.77	5.18	4.80	5.02	5.62	2.28	2.59
Na ₂ O	3.41	3.91	2.87	3.76	3.61	3.78	4.61
K ₂ O	0.91	1.78	1.23	1.97	1.22	3.22	2.64
P ₂ O ₅	0.31	0.33	0.35	0.36	0.31	0.19	0.20
LOI	3.13	1.92	4.14	2.50	4.86	1.88	0.90
Total	97.68	100.30	98.41	98.83	101.36	99.01	98.59
δ ₂	2.66	2.66	2.55	2.58	2.70	2.68	2.57
trace elements in parts per million ³							
Sc		14.5	15.0	14.2	14.7	14.3	8.1
Cr	111	110	105	97	108	102	75
Co	21.0	15.0	28.0	17.0	17.4	17.1	5.9
Ni	46	28	41	35			
Rb	41	41	25	50	28	29	57
Sr	822	542	470	532	636	576	250
Cs	1.4	1.0	3.2	1.5	0.5	0.6	0.8
Ba	350	420	340	385	290	400	500
La	15.0	18.0	20.0	19.7	18.8	19.3	14.5
Ce	29.0	43.0	45.0	39.3	41.8	40.5	46.8
Nd	22.0	19.0	21.0	20.9	23.0	20.0	19.0
Sm	3.7	4.4	4.3	4.7	4.3	4.2	3.1
Eu	1.20	1.10	1.20	1.20	1.10	1.10	0.88
Tb	0.40	0.60	0.50	0.64	0.60	0.50	0.60
Yb	1.10	2.00	2.00	1.80	1.50	1.70	1.90
Lu	0.20	0.30	0.20	0.27	0.28	0.21	0.27
Hf	4.5	5.6	4.5	5.0	5.5	5.3	5.8
Ta	0.43	0.59	0.60	0.53	0.51	0.48	0.69
Th	3.5	6.0	5.1	4.7	5.0	5.0	8.0
U	1.0	2.0	2.5	1.7	1.8	2.2	2.5

¹ Major-element oxides by ICP-AES, FeO by titration, LOI by furnace by Chemex Labs, Sparks, NV² density in g/cc³ Trace-elements by INAA at the Radiation Center, Oregon State University procedure outlined by Laul (1979)

APPENDIX 4: Chemical analyses of plutonic rocks from Detroit Dam

unit sample #	(1) QD MV-17	(2) Hb QD MV-32	(3) D MV-13	(4) Hb GD MV-70	(5) Ton MV-31
major-element oxides in weight percent ¹					
SiO ₂	55.70	59.14	58.62	67.21	74.80
TiO ₂	0.86	0.80	0.75	0.51	0.43
Al ₂ O ₃	18.32	15.97	16.82	15.36	13.37
Fe ₂ O ₃	4.18	2.90	2.47	1.69	0.40
FeO	3.16	2.91	2.98	2.00	0.37
MnO	0.16	0.09	0.11	0.10	0.02
MgO	3.16	3.63	2.79	1.55	0.64
CaO	6.43	5.97	5.88	3.33	1.26
Na ₂ O	3.48	3.90	3.89	3.77	5.85
K ₂ O	0.65	0.84	0.98	3.30	0.66
P ₂ O ₅	0.30	0.29	0.29	0.22	0.13
LOI	4.05	4.10	1.93	1.60	3.74
Total	100.77	100.83	97.81	100.84	101.71
g ²	2.75	2.75	2.69	2.55	2.44
trace elements in parts per million ³					
Sc	19.9	16.8	14.7	8.5	6.5
Cr	54	155	91	29	103
Co	25.8	20.2	18.5	10.2	3.3
Ni	56	80	198		16
Rb	23	40	25	88	25
Sr	431	378	439	326	269
Cs	1.8	2.2	1.1	1.5	0.4
Ba	335	376	419	564	239
La	12.5	15.4	14.4	18.4	10.2
Ce	24.5	31.0	27.1	37.6	27.3
Nd	12.7	15.5	12.9	16.6	16.8
Sm	3.6	4.1	3.4	3.6	4.3
Eu	1.21	1.32	1.12	1.10	1.18
Tb	0.54	0.53	0.39	0.52	0.63
Yb	1.79	1.95	1.82	1.77	2.54
Lu	0.22	0.29	0.21	0.24	0.33
Hf	3.2	5.3	3.7	5.3	8.2
Ta	0.30	0.50	0.60	0.70	0.80
Th	1.9	4.3	3.7	9.1	11.0
U	1.5	1.1	1.4	3.1	2.6

¹ Major-element oxides by ICP-AES, FeO by titration, LOI by furnace by Chemex Labs, Sparks, NV² density in g/cc³ Trace-elements by INAA at the Radiation Center, Oregon State University procedure outlined by Laul (1979)

APPENDIX 5: Chemical analyses of altered rocks from Rocky Top

unit sample #	"fresh" 92-2	mod prop. 111-7	str qtz-ser 92-1	vein 98-3	argillic 911-5
major-element oxides in weight percent ¹					
SiO ₂	52.98	52.92	77.00	84.76	
TiO ₂	1.09	1.06	0.12	0.12	
Al ₂ O ₃	16.88	16.61	10.96	9.51	
Fe ₂ O ₃	2.94	2.03	1.08	0.63	
FeO	4.32	5.38	0.13	0.91	
MnO	0.14	0.11	0.03	0.02	
MgO	3.03	3.85	0.13	0.14	
CaO	8.70	7.08	1.10	0.04	
Na ₂ O	2.75	2.51	0.98	0.03	
K ₂ O	0.08	1.05	3.91	2.53	
P ₂ O ₅	0.45	0.52	0.07	0.12	
LOI	4.03	5.23	2.36	1.73	
Total	97.39	98.35	97.88	100.63	
δ^2	2.73	2.66	2.49	2.52	
trace elements in parts per million ³					
Sc	18.9	17.0	2.3	2.6	
Cr	136	111	97	256	
Co	25.3	24.0	1	3	
Ni	90	55			
Rb		10	107	70	
Sr	470	500	100		
Cs	1.7	9.6	2.5	1.7	
Ba	305	520	570	500	
La	20.0	19.0	30.0	30.0	
Ce	43.0	37.0	68.0	75.0	
Nd	26.0	23.0	20.0	34.0	
Sm	5.0	4.8	5.0	6.4	
Eu	1.60	1.40	0.40	0.20	
Tb	0.60	0.70	0.90	0.90	
Yb	2.00	2.30	2.70	3.10	
Lu	0.30	0.30	0.40	0.50	
Hf	4.6	4.5	4.3	4.1	
Ta	0.78	0.64	0.95	0.92	
Th	2.6	3.0	13.0	12.0	
U		1.5	4.5	4.5	

¹ Major-element oxides by ICP-AES, FeO by titration, LOI by furnace by Chemex Labs, Sparks, NV² density in g/cc³ Trace-elements by INAA at the Radiation Center, Oregon State University procedure outlined by Laul (1979)

APPENDIX 6: Sulfide mineral analyses

mineral sample #	Gn 98-3	Sl 98-3	Sl 94-1	Cp 94-1	Py 102-3	Py 911-5	Ba 911-5
$\delta^{34}\text{S} \text{ ‰}$	-3.33	+0.01	-0.26	+0.41	+1.02	+2.82	+6.66
wt %							
S	12.936	32.169	32.466	33.908	53.014		
Fe	0.000	3.932	0.212	29.386	45.169		
Cu	0.000	0.000	0.036	33.767	0.054		
Pb	85.516	0.000	0.000	0.000	0.000		
Zn	0.000	58.018	59.146	0.091	0.058		
As	0.055	0.270	0.004	0.020	0.000		
Au	0.000	0.000	0.015	0.014	0.000		
Ag	0.064	0.005	0.000	0.020	0.029		
Total	98.571	94.394	91.879	97.206	98.324		
mole %							
S	49.35	51.07	52.69	47.32	67.09		
Fe	0.00	3.58	0.20	23.54	32.82		
Cu	0.00	0.00	0.04	29.05	0.04		
Pb	50.48	0.00	0.00	0.00	0.00		
Zn	0.00	45.16	47.07	0.06	0.04		
As	0.09	0.18	0.00	0.01	0.00		
Au	0.00	0.00	0.00	0.00	0.00		
Ag	0.07	0.00	0.00	0.01	0.01		
mole % FeS in Sphalerite		7.4	0.4				

APPENDIX 6: (continued)

mineral sample #	Tn 94-1	En 94-1	En 94-1	Bn 94-1	Cv 94-1	Cp 94-1	Cp 98-3	Cp 98-3	Sl 98-3	Sl 94-1	Gn 94-1
wt %											
S	28.573	33.241	33.289	25.859	33.965	33.403	35.068	34.910	33.206	33.470	13.220
Fe	7.228	0.432	0.442	11.634	0.107	26.535	29.599	29.832	3.079	1.201	0.079
Cu	43.332	46.570	46.686	62.357	63.630	30.364	33.962	34.219	0.232	2.049	0.098
Pb	0.000	0.000	0.000	0.000	0.000	0.000	0.000	0.000	0.000	0.000	86.030
Zn	0.522	0.000	0.000	0.000	0.241	2.567	0.016	0.000	60.224	61.238	0.370
As	20.611	18.657	19.039	0.000	0.022	0.000	0.059	0.000	0.022	0.051	0.000
Au	0.000	0.000	0.000	0.000	0.000	0.019	0.000	0.000	0.000	0.000	0.000
Ag	0.000	0.000	0.000	0.000	0.000	0.000	0.000	0.000	0.000	0.000	0.044
Total	100.266	98.900	99.456	99.850	97.965	92.888	98.704	98.961	96.763	98.009	99.841
mole %											
S	41.70	47.36	47.23	36.43	46.28	48.68	48.02	47.73	51.36	51.12	49.27
Fe	6.06	0.35	0.36	9.41	0.08	22.20	23.27	23.42	2.73	1.05	0.17
Cu	39.00	40.91	40.85	54.16	53.46	27.28	28.67	28.85	0.22	1.93	0.23
Pb	0.00	0.00	0.00	0.00	0.00	0.00	0.00	0.00	0.00	0.00	49.61
Zn	0.37	0.00	0.00	0.00	0.16	1.83	0.01	0.00	45.67	45.86	0.68
As	12.87	11.37	11.56	0.00	0.01	0.00	0.03	0.00	0.01	0.03	0.00
Au	0.00	0.00	0.00	0.00	0.00	0.00	0.00	0.00	0.00	0.00	0.00
Ag	0.00	0.00	0.00	0.00	0.00	0.00	0.00	0.00	0.00	0.00	0.05
mole % FeS in Sphalerite									5.7	2.2	

APPENDIX 7: Fluid inclusion data

Sample #	Class ¹	Th (°C)	Tm (°C)	wt.% NaCl equiv.
98-3	S	150	-0.7	1.2
"	S	150	-0.7	1.2
"	S	151	-0.8	1.4
"	S	151	-0.7	1.2
"	PS	191	-1.4	2.4
"	PS	192	-1.5	2.6
"	PS	192	-1.4	2.4
"	PS	193	-1.4	2.4
"	P	231	-2.7	4.5
"	P	232	-2.7	4.5
"	P	238	-2.9	4.8
"	P	239	-2.9	4.8
"	P	240	-2.9	4.8
"	P	241	-2.8	4.6
"	P	244	-2.8	4.6
"	P	245	-2.9	4.8
"	P	246	-3.0	4.9
"	P	247	-3.0	4.9
"	P	248	-2.9	4.8
"	P	248	-2.8	4.6
"	P	249	-2.8	4.6
"	P	249	-2.9	4.8
"	P	251	-3.0	4.9
"	P	252	-3.1	5.1
92-1	S	152	-0.7	1.2
"	S	152	-0.8	1.4
"	S	153	-0.7	1.2
"	S	153	-0.7	1.2
"	PS	180	-1.2	2.1
"	PS	182	-1.1	1.9
"	PS	184	-1.2	2.1
"	PS	184	-1.2	2.1
"	PS	196	-1.5	2.6
"	PS	197	-1.5	2.6
"	P	215	-1.7	2.9
"	P	216	-1.7	2.9
"	P	218	-1.9	3.2
"	P	220	-2.0	3.4
"	P	222	-2.1	3.5
"	P	223	-2.1	3.5

¹S = Secondary, PS = Pseudosecondary, P = Primary
 Th = Temperature of homogenization (heating runs)
 Tm = Temperature of melting (freezing runs)

APPENDIX 8: Trace metal concentrations for samples from Rocky Top

Sample #	Cu ¹	Pb	Zn	Mo	Ag	Au ²	As
73-1	410	60	560	15	0.3	3	20
73-2	125	690	535	75	5.1	12	100
86-1	30	18	30	2	<0.3		
86-2	25	12	35	2	0.4		
86-3	25	13	30	<1	0.5		
88-4	25	12	20	<1	0.3		
92-1	7	35	90	<1	0.5		
92-2	35	12	50	<1	0.5		
98-3	830	750	3570	<1	16.3	5	
102-1	40	15	260	2	0.5		
102-2	10	6	35	<1	<0.3		
102-3	20	11	15	3	0.6		
102-4	7	7	8	1	<0.3		
111-2	30	12	45	1	<0.3		
111-3	20	9	30	<1	0.3		
111-5	30	12	30	<1	<0.3		
111-6	16	12	35	<1	0.3		
111-7	35	10	55	<1	0.5		
111-8	35	9	40	<1	<0.3		
111-9	15	7	10	<1	<0.3		
724-2	6	6	5	<1	<0.3		
724-3	5	10	5	2	<0.3		
812-1	30	13	45	<1	0.5		
819-15	45	10	35	<1	0.4		
821-3	10	45	40	<1	0.6		
821-5	6	8	13	<1	0.4		
826-3	10	110	70	<1	0.5		
911-1	11	4	35	<2	<0.3	3	
911-2	200	14	45	<2	<0.3	6	
911-3	40	16	30	<2	<0.3	3	
911-4	35	11	55	<2	<0.3	2	
911-5	<3	20	35	<2	<0.3	4	
RT-1 ³	25	75	135	4	0.3	15	45
RT-2	180	1330	565	20	<0.3	10	35
RT-3	25	380	90	20	0.3	16	4

¹ Cu, Pb, Zn, Mo, Ag, and As in ppm² Au in ppb³ RT-1, RT-2, and RT-3 were collected prior to this investigation

APPENDIX 9: Trace metal concentrations for samples from Sardine Creek

Sample #	Cu ¹	Pb	Zn	Mo	Ag
MV-4	45	13	45	<1	0.5
MV-5	45	15	8	<1	<0.3
MV-9	14	5	25	<1	<0.3
MV-13	14	3	19	1	<0.3
MV-15	6	7	14	<1	<0.3
MV-17	35	16	40	<1	<0.3
MV-28	40	5	100	1	<0.3
MV-29	10	4	6	<1	<0.3
MV-31	8	4	20	<1	<0.3
MV-32	20	5	18	<1	<0.3
MV-33	16	35	60	<1	<0.3
MV-34	25	9	35	1	0.3
MV-36	8	6	8	<1	<0.3
MV-37	25	5	12	<1	<0.3
MV-45	25	5	16	<1	<0.3
MV-70	30	25	100	<1	0.3

¹ Cu, Pb, Zn, Mo, and Ag in ppm

APPENDIX 10: Trace metal concentrations for samples from Detroit Dam

Sample #	Cu ¹	Pb	Zn	Mo	Ag	Au ²
DD-3	20	10	13	2	0.3	
DD-5	14	5	8	1	0.3	5
DD-8	2300	16	85	17	0.6	120
DD-12A	30	10	45	2	0.6	
DD-12M	11	6	14	2	0.5	
DD-14	110	6	14	1	0.4	2
DD-16A	35	12	60	1	0.5	
DD-16M	100	11	10	3	0.6	
DD-20	190	35	25	8	0.3	
DD-23	25	15	45	1	0.3	
DD-25	55	13	60	1	0.4	
DD-30	35	13	100	<1	1.1	
DD-37	175	14	85	2	0.8	4
DD-42	45	8	20	<1	0.6	
DD-43	20	4	12	1	0.4	
DD-45	12	11	30	2	0.3	
DD-48	35	8	25	2	0.3	
DD-52	115	15	30	<1	0.4	
DD-53	55	9	40	<1	0.4	
DD-57	12	15	30	<1	0.5	
DD-75	40	12	50	1	0.6	
DD-77	6	15	8	4	0.8	
DD-80	17	7	20	2	0.4	
DD-85	95	550	160	<1	2.3	6
DD-88	55	15	25	<1	0.4	
DD-91	55	10	20	2	0.5	
DD-100	85	12	80	1	0.3	
DD-101	15	7	18	2	0.3	<2
DD-116	60	11	30	2	0.5	
DD-117	25	7	25	2	0.3	
DD-118	18	14	30	1	0.4	
T8-4	55	10	70	1	<0.2	
T12-3	165	20	60	<1	<0.2	

¹ Cu, Pb, Zn, Mo, and Ag in ppm² Au in ppb

APPENDIX 11: List of abbreviations

BB	Breitenbush Formation (White, 1980b)
bk	background population
C1nv	C1 chondrite non-volatile (Anders and Ebihara, 1982)
Cp	chalcopyrite
D	diorite
DD	Detroit Dam
ECFZ	Elkhorn Creek Fault Zone
EL	Elk Lake Formation (White, 1980b)
GD	granodiorite
Hb	hornblende
HT	hydrothermal
K-feldspar	potassium feldspar
min	mineralized population
mod	moderate
Mt	magnetite
NS	North Santiam (Olson, 1978)
Ol	olivine
P	primary
Plag-feldspar	plagioclase feldspar
PP	Pigeon Prairie lavas (Rollins, 1976)
prop	propylitic
PS	pseudosecondary
Px	pyroxene
Py	pyrite
QD	quartz diorite
qtz-ser	quartz-sericite
RT	Rocky Top
RTFZ	Rocky Top Fault Zone
S	secondary
SB	Santiam Basalt (White, 1980b)
SC	Sardine Creek
Sl	sphalerite
SS	Sardine Formation (White, 1980b)
str	strong
Ton	tonalite
vol %	volume percent
wt %	weight percent